2023

Department of Mechanical and Aerospace Engineering

Assessing the technical, environmental, and economic performance of low global warming potential refrigerants

Author: Callum Tharme
Registration Number: 202267805

Supervisor: Dr Nick Kelly

A thesis submitted in partial fulfilment for the requirement of the degree:

Master of Science (MSc) Sustainable Engineering: Renewable Energy Systems & The Environment

2023

Copyright Declaration

Signed: Callum Tharme Date: 10.08.2023

Abstract

The demand for refrigeration systems is forecast to increase dramatically in the coming decades due to the technological development of low-income countries and the necessity for cooling in a warmer climate. Vapour compression cycles are one of the most popular means of moving heat from one environment to another, and current devices rely on refrigerant gases that can have a greenhouse effect hundreds to several thousands of times more potent than that of carbon dioxide.

With this in mind, further research is required to assess the potential options for low global warming potential replacements. This thesis conducted three analyses: technical, environmental, and economic, on the most popular current refrigerants available in a variety of applications. These applications were cryogenic cooling, fridge-freezers, air conditioning, air-source heat pumps, and ground-source heat pumps. The methodology of this project was to collect input parameters from literature and utilise software capable of simulating the vapour compression cycle on the applications above, in order to gather data that could be analysed and presented in this thesis. All of the results contained within this thesis pertain to the location of Glasgow, United Kingdom.

The key findings from this thesis were that, at present, the indirect emissions associated with the electrical consumption of the devices are the most significant environmental factor, accounting for between 80 – 90 % of annual emissions in the cryogenic and fridge-freezer case. This is due to the relatively high carbon intensity of the UK grid at present, although as this decreases due to increased penetration of renewable energy systems, the proportion of emissions from refrigerant leakage (direct emission) will become much more significant.

It is also found that, in general, natural refrigerants could operate at a greater coefficient of performance than hydrofluorocarbons, and so their electrical consumption was reduced. This was likely a function of the thermophysical properties of the natural gases, as they have a greater latent heat of vapourisation and greater critical temperatures.

The economic analysis was also closely related to the technical performance, as the major component of annualised costs was associated with the purchase of electricity. A reduction in operational costs ranging from 4.3 – 13.7 %, depending on the application, was seen in the natural refrigerant group in comparison to the HFC gases, thanks to increased efficiency.

Acknowledgements

I would like to thank the Department of Mechanical and Aerospace engineering staff for their help throughout the year in all taught modules, and in particular my supervisor Dr Nick Kelly for his guidance, input, and communication throughout the duration of this project.

I would also like to take this opportunity to thank my friends and family for their unwavering support throughout my postgraduate studies, and being an ever-present listening ear over the past year.

Contents

List of Figures

List of Tables

Terminology and Nomenclature

Abbreviation	Definition
AC	Air Conditioning
ASHP	Air-Source Heat Pump
ASHRAE	American Society of Heating, Refrigerating and Air-Conditioning Engineers
CFC	Chlorofluorocarbons
CH_4	Methane
CO_2	Carbon Dioxide
COP_C	Coefficient of Performance (Cooling)
COP_H	Coefficient of Performance (Heating)
GSHP	Ground-Source Heat Pump
GWP	Global Warming Potential
HCFC	Hydrochlorofluorocarbons
HFC	Hydrofluorocarbons
NH_3	Ammonia
UV	Ultraviolet

Unit	Type	Definition
£	Currency	Great British Pounds
$	Currency	US Dollar
Bar	Pressure	Bar
°C	Temperature	Degrees Celsius
K	Temperature	Degrees Kelvin
kg	Mass	Kilogram
kg/s	Flowrate	Kilogram per second
kW	Power	Kilowatt
kWh	Power	Kilowatt hour
MW	Power	Megawatt
$MtCO_2e$	Mass	Megatonne of CO_2 equivalent
ppm	Concentration	Parts Per Million
TWh	Energy	Terrawatt Hour

1. Introduction

1.1 Background

Refrigerants play a critical role in many aspects of the modern world ever since they were first used to aid the transportation of foods across continents in the late 19th century. These fluids have enabled populations to experience foreign cuisines and preserve harvested foods to be enjoyed year-round. Although the vapour compression cycle had been demonstrated for its refrigeration properties by American Jacob Perkins in 1834 as a means of producing ice, the devices weren't initially commercially successful (Balmer, 2011). In 1855, the Scot James Harrison submitted his patent for a refrigeration unit that used a combination of alcohol and ammonia (NH_3), which was subsequently used in breweries and meat factories across Australia and the United Kingdom (UK) (Britannica, 2020).

The use of refrigeration as a climate comfort technology was then developed in the early 1900s, when Willis Carrier invented the first electrical air conditioning (AC) system, using forced convection of water-filled coils (Varrasi, 2011). The demand for AC units didn't truly take off until after the Second World War when Americans began to spend money on more luxury items, and sales reached over one million units per year in 1956. At present, air conditioning is one of the leading uses for refrigerants and accounts for 10 *%* of global electricity demands. The United States, Japan and South Korea lead the way in household air conditioning systems, with uptakes at 91, 90, and 86 *%,* respectively, due to the hot, humid summers experienced in these locations. However, as industrialisation continues, particularly in India and China, it is thought that two-thirds of households worldwide will have some form of AC by 2050. This will increase the demand for cooling from 2,200 *TWh* to 6,200 *TWh*, based on current AC technologies (IEA, 2018). By comparison, only 5 *%* of households in the UK have AC, although, with recent heatwaves in 2019 and 2022, it is predicted that the demand will increase three-fold by 2050. Already there has been a 25 *%* increase in installed AC units since 2010 (Barry, 2022).

Heat pumps are another technology that makes use of refrigerants for both heating and cooling. Although in the early 1800s, many had proven the thermodynamic possibility of heat pumps, they weren't practically applied until 1877, when a heat pump was installed at the Bex salt mine in Switzerland (Zogg, 2008). The cities of Geneva and Zurich were the first proponents of heat pumps as a means of heating without excessive reliance on coal and biomass plants by utilising the large lakes and rivers in the surrounding areas during the second world war (Renz, 2020). In combination with the increased hydropower generation, these were the first examples of renewable heat generation. The heat pumps first installed in the 1930s, and 1940s were fully operational until the early 2000s, providing heating to the cities for up to 80 years before being replaced by more efficient modern devices. The scale of the installed systems ranged from 100 *kW* at the town hall to nearly 6 *MW* for the university district heating area.

In the UK, the use of heat pumps was less widespread, although, in 1946, heat drawn from the River Thames was used to heat the Festival Hall in London. The continued uptake and development of these systems was slower in the mid to late 20th century, in particular, due to the low oil price in the 1950s and 'dash-for-gas' in the 1980s. Despite this, refrigerants were beginning to be used extensively as home refrigerators and air conditioning (AC) units became more widespread throughout North America, Western Europe and Japan. Cars and computers also began to expand in the market, which increased the demand for cooling systems and refrigeration. Healthcare is also reliant on refrigerants to distribute temperature-sensitive medicines and vaccines from factories to hospitals and deliver aid to remote locations.

However, these cooling and heating systems require large amounts of refrigerants, such as chlorofluorocarbons (CFCs) and hydrochlorofluorocarbons (HCFCs), which can pose a threat to the ozone layer and contribute to global warming. CFCs were first created in the late 1800s as research was undertaken to replace the ammonia refrigerants used in the early systems mentioned above. It wasn't until 1930 that commercial production of CFCs began under the joint venture of General Motors and DuPont chemicals when they developed dichlorodifluoromethane, commercially known as 'Freon' (Wernke, 2014).

These chemicals were widely used not only in refrigerators, AC units, and cars but also in a large variety of aerosol products, as they had promising properties, such as being non-toxic and non-flammable. In 1985, a large hole was discovered in the ozone layer, the area of the atmosphere responsible for filtering DNA-damaging ultraviolet (UV) light. Further research led to the signing of the Montreal Protocol in 1987, which pledged a reduction in CFC production of 50 *%* by 2000; however, this was amended in 1990 to a complete elimination of production (Elkins, 1999).

1.2 Problem Definition

Refrigerants containing ozone-depleting chemicals have been eradicated in over 140 countries, and a range of compounds are used instead, typically formed of hydrofluorocarbons (HFCs). However, these refrigerants have a significant Global Warming Potential (GWP), several thousands of times more potent than carbon dioxide (CO_2). This creates a conundrum concerning cooling: by using these refrigeration methods, the demand for electricity increases, while the refrigerants contribute to global warming, leading to further demand for cooling. With regard to this problem, new alternatives to high GWP refrigerants have been explored, as well as revisiting old compounds that can reduce the environmental impact of these technologies. Although alternative fluids have been investigated, more detail is needed on their impact on cooling and heating efficiency, the economic cost of operating new devices, and the life cycle emissions of systems utilising these chemicals.

1.3 Aim

This thesis aims to investigate low global warming potential refrigerants and report on the impact on technical operations, environmental impact, and economics. It will then provide a comparison between these and conventional high GWP refrigerants for several different refrigerant systems.

1.4 Objectives

The key objectives of the project were as follows:

1. Conduct a literature review on refrigerants, their applications, and their context in wider society.
2. Describe the thermodynamics of the vapour-compression cycle.
3. Assess the current emissions associated with both refrigeration and heat pump applications.
4. Select the most appropriate alternative and conventional refrigerants for assessment in each system.
5. Model the vapour-compression cycle and report the technical performance of several systems.
6. Conduct an environmental and economic analysis of the systems.
7. Assess the overall performance of these alternatives compared to conventional refrigerants.

1.5 Methodology

This section briefly describes the overall methodology for this project. More detail on the approach taken with regard to the specific model can be found in *Chapter 3*.

The process diagram below (Figure 1.1) depicts the numerous stages involved in undertaking this project. After defining the aims and objectives, as seen above, the next phase was to conduct a literature review into the field of refrigeration and specifically high and low GWP refrigerants. This was also crucial in placing this project in the context of societal and engineering challenges, such as reducing the impact of these technologies on the planet. The current and previous groups of refrigerants are described, as well presentation of the low GWP refrigerants being researched.

After the selection of a range of refrigerants, and also the software to be utilised for this project, it was necessary to gather specific data and assumptions that were to be applied to the models. This involved gathering the typical operational temperature ranges of the refrigeration systems to be modelled, along with parameters such as compressor efficiency and specific refrigerant mass. Upon inputting this data into the software and collection of results, these were processed to present the analyses to satisfy the objectives above.

Finally, the results were validated through comparison to recent literature conducted on similar refrigerants, in order to assure the accuracy of the conclusions that are presented. The limitations of the model were also highlighted to provide a basis for potential future works.

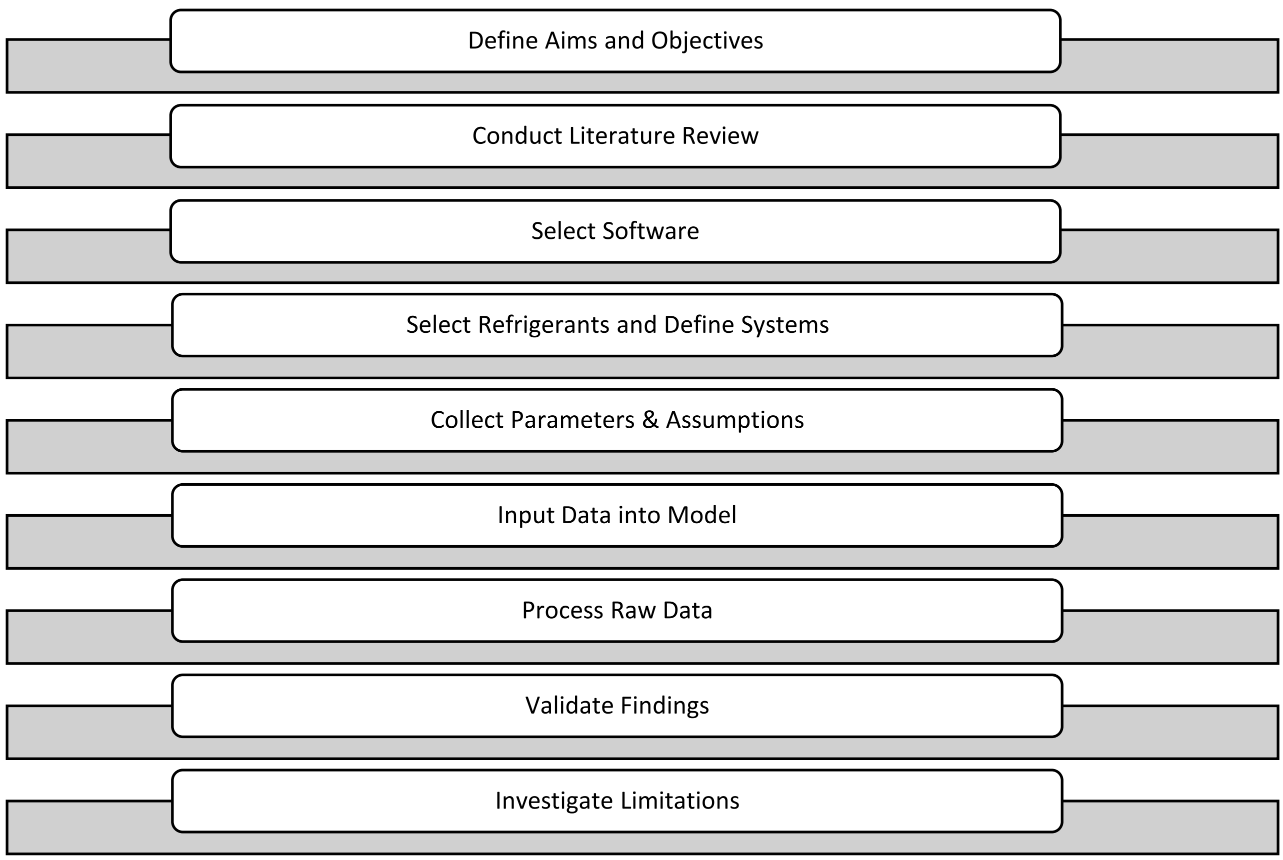

Figure 1.1: Process Diagram of Project Methodology

2. Literature Review

This literature review will cover the key research conducted for this project, particularly the types of refrigerants and the theory behind their operation within major applications, as well as the proposed alternatives to current fluids. However, before this is described in detail, the need for exploration in new refrigerants is put in the context of major socio-environmental events, such as climate change and the previous discovery of the ozone hole. This provides the background into the necessity of projects such as this, whilst highlighting the gap in current research to keep up with every changing legislation.

2.1 Climate Change and Ozone Depletion

It has been known for over 40 years that anthropogenic activities have led to changes in the environment. The term 'global warming' was first made popular in the 1980s; however, in recent years, the terms have begun to take a more urgent tone, such as 'crisis' or 'emergency', to portray the severity of the situation we now face. Many scientists and naturalists, such as David Attenborough, have called climate change the "biggest threat modern humans have ever faced" (UN, 2021). Indeed, it is now at the forefront of almost all major policy decisions in the Western world, and since the turn of the century, there have been several international agreements on climate change policy, most importantly in Montreal and Paris. These accords aim to reduce carbon dioxide emission to net zero by 2050 and in doing so, limit the rise in global mean temperature to at least below $2°C$, with the aim of $1.5°C$, since the pre-industrial era (UNCC, 2023). Many countries have also self-imposed their climate policies; for example, the US has the Clean Air Act (US Gov, 2021), whilst the EU proposed the European Climate Pact (EC, 2019), and the UK has its own Climate Change Act (UK Gov, 2008).

However, as many developing countries continue to industrialise, the demand for energy and electricity is only increasing, and so without access to clean energy generation, carbon emissions are forecast to increase. There is also evidence to suggest that emissions increase unidirectionally with the gross domestic product (GDP) (Azlina, 2014). Whilst emissions tend to peak early in a country's development before renewable and low-carbon technologies are implemented, this will likely take many decades to achieve, which won't aid ambitions to limit global warming. This follows the environmental Kuznets curve hypothesis, depicting the rise in environmental degradation as the per-capita income of a country increases before declining with greater technological development (Shahbaz et al., 2013). Although this relationship is not universally true, as case studies in Malaysia suggest (Azlina, 2014), and in a globalised economy, the trend has changed to an N-shape curve, as opposed to the classic inverse-U shape (Figure 2.1), there is evidence that industrialisation will negatively affect the ability to meet global emissions targets.

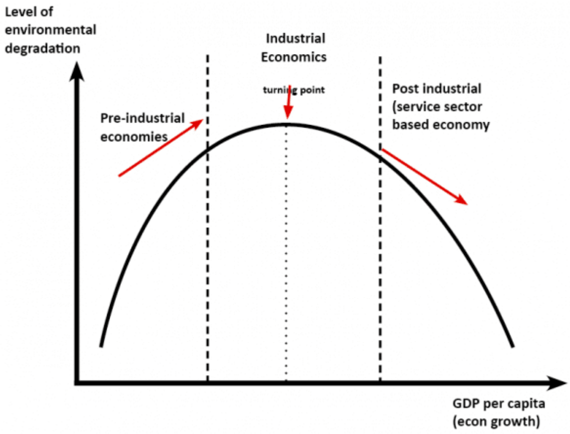

Figure 2.1: Environmental Kuznets Curve (Pettinger, 2019)

The concentration of CO_2 in the atmosphere has been increasing rapidly since the start of the industrial revolution in the late 19th century when coal became the major fuel resource. In the pre-industrial age, CO_2 levels were approximately 280 parts per million (ppm), and as of April 2023, it is now 421 ppm (NASA, 2023). These are levels not seen since the Pliocene era, approximately 3 million years ago, a time when global mean temperatures were 1.4 to 3.9 $°C$ warmer than today (Tierney et al., 2019). This represents an insight into the potential changes to global meteorological events over the next century, such as the increased frequency of floods, droughts, hurricanes, and the human impact that these may have.

Despite reduction targets from the aforementioned Paris accords, greenhouse gas emissions (including CO_2) have been steadily increasing, particularly due to the industrialisation of China and India, where coal still represents over 50 % of the energy mix, whilst fossil fuels as a whole satisfy nearly 90 % of energy demand (Danlami Musa et al., 2018). This has led to an increasingly strong greenhouse effect in the atmosphere, where infrared radiation is absorbed by intramolecular bonds within gases such as CO_2, methane (CH_4) and hydrofluorocarbons (HFCs). Although CO_2 contributes around 75 % of the greenhouse effect (Yoro, 2020), there are a variety of other gases which are much more potent in their effect. Emissions of methane (CH_4), nitrous oxide (N_2O), sulphur hexafluoride (SF_6) and hydrofluorocarbons (HFCs) are particularly harmful as they have several times the global warming potential (GWP) of CO_2. Some HFCs can be up to 10,000 times more potent than CO_2 over 100 years (Flerlage, 2021). This means that despite their relatively small emissions compared to CO_2, their impact is measurable. The GWP is a measure of the gas's ability to trap infrared radiation in the atmosphere, in reference to CO_2 (GWP = 1). As radiation is absorbed in the intramolecular bonds of these gases, they become more energetic, and so their temperature increases. Hydrofluorocarbons are used extensively in refrigeration systems and contributed around 2% of global emissions as of 2014 (IPCC, 2014). However, gases such as HFCs were implemented as a more attractive alternative to chlorine-containing compounds (CFCs), which had another detrimental effect on the atmosphere.

Ozone depletion is also a key consideration in the context of climate change and refrigerants. It was discovered that a large hole in the ozone layer was forming in 1985 when Jonathan Shanklin of the British Antarctic Survey published findings in the journal Nature. It had been found that a decade earlier, the thickness of the ozone layer had begun declining, and by the time the discovery was made, it was two-thirds of the previous thickness. Although through research in 1974, chlorinated gases such as CFCs were thought to deplete the ozone layer, it wasn't until Shanklin's discovery that it was proven. The hole was most distinct in the spring months and covered an area of 20 million square kilometres over the Antarctic. This portion of the atmosphere is only 3 *mm* thick, yet extremely important for the protection of life on Earth from UV radiation, which can damage DNA and cause cancers. Alongside this, the amount of CO_2 in the atmosphere would increase in an ozone-depleted world, as the plant life currently responsible for storing 7.6 billion tonnes of CO_2 per year would begin to die off. Chlorofluorocarbons (CFCs) were widespread within the refrigeration industry at this time, with 1 million tonnes per year being produced for air conditioning, home refrigerators, and aerosols; however, they were found to be severely deteriorating the ozone layer. Leakages in these systems allowed the gases to rise to the stratosphere (15 to 30 *km* above the Earth), where they can interact with the ozone layer. This occurs when the chlorine atoms are split from the CFC molecule by UV radiation and then react with the ozone molecule (O_3), splitting it into O_2 and ClO. It was due to the discovery of the ozone hole that policies were hastily put in place in 1987 to globally eliminate the use of CFCs by 2010. It is thought that without the Montreal Protocol (1987), the ozone layer would be reduced by 72 *%* by 2100, whilst the global temperatures would have risen by a further 2.5 *°C* on top of current estimates (Harvey, 2021). The American Environmental Protection Agency also predicted that the phase-elimination of CFCs is directly responsible for preventing 443 million cases of skin cancer and 63 million cataracts in those born before 2100 (EPA, 2020). Today, the use of CFCs is banned in 197 countries, and they have been widely replaced by hydrofluorocarbons (HFCs) as refrigerants, which have 400 times lower ozone depletion potential (ODP).

2.2 Energy Demand for Cooling and Refrigeration

Since the advent of refrigeration systems in the late-19th century and air conditioning in the 20th century, the energy demand associated with these technologies has increased rapidly. Cooling requirements are responsible for around 35 – 40 % of total energy demands worldwide and are necessary for a wide range of industries, such as food, medicine, computing, and steel. Domestic uses of cooling include air conditioning for buildings and car cooling systems, whilst office spaces contribute heavily to cooling requirements. It is forecast that by 2050 the world will consume more energy for cooling than for heating, in particular, due to the low-income tropical countries increasing demand for cold technologies, as can be seen in China where in the space of 12 years between 1995 and 2007, the uptake of domestic refrigerators increased from 7 % to 95 % (Cox, 2012). Trends such as this are likely to be repeated across southern Asia and Africa in the coming decades.

In Europe, the demand for cooling systems is expected to increase rapidly, in particular, due to the effects of global warming. More extensive and frequent heatwaves, such as that experienced in the summer of 2022, caused a spike in eBay searches for "air conditioning" of 415 %, highlighting the gathering of interest in European markets. As temperatures frequently reach the high 30 $°C$ more regularly, the number of AC units will only increase.

The AC industry is currently dominated by the US and Japan, where units are installed in the vast majority of homes as standard, creating a large demand for power during the summer months. At present, the US consumes more electricity for cooling alone than the continent of Africa does as a whole (Cox, 2012). This extremely large demand has led to blackouts across southern US states, as the grid capacity cannot cope with the large spike in electricity consumption, whilst the transmission network infrastructure is also put under stress at higher temperatures.

Building standards contribute to the increased need for cooling in countries such as the UK, as the construction materials, methods, and design are based on the typical maritime weather experienced by the region. Figure 2.2 presents the age composition of UK housing stock, showing the majority is dated pre-1965, whilst over 20 % were constructed before the first world war (Piddington, 2013). As these houses were built with cost and space in mind and little consideration for heating or cooling demands, they are poorly insulated and have significant leakage of airflow, meaning they let heat out during the winter; whilst allowing heat flow into the dwelling during warm summer months. Large windows were also a fashionable item during these periods, especially south facing, with little shade, to enjoy a view from the living areas; however, this allows significant solar gains during high summer, and so even if the outdoor air temperature is relatively mild, the buildings can quickly overheat. To combat these issues, building regulations have been updated to include thermal modelling of solar gains, glazed area, and ventilation of occupied zones (The Building Regulations, 2010). The assessment method for compliance is regulated by the Chartered Institution of Building Services Engineers (CIBSE) through 'TM59 Design methodology for the assessment of overheating risk in homes (2017)', which outlines the requirements based on key parameters such as occupancy pattern, orientation, layout, shading, and ventilation.

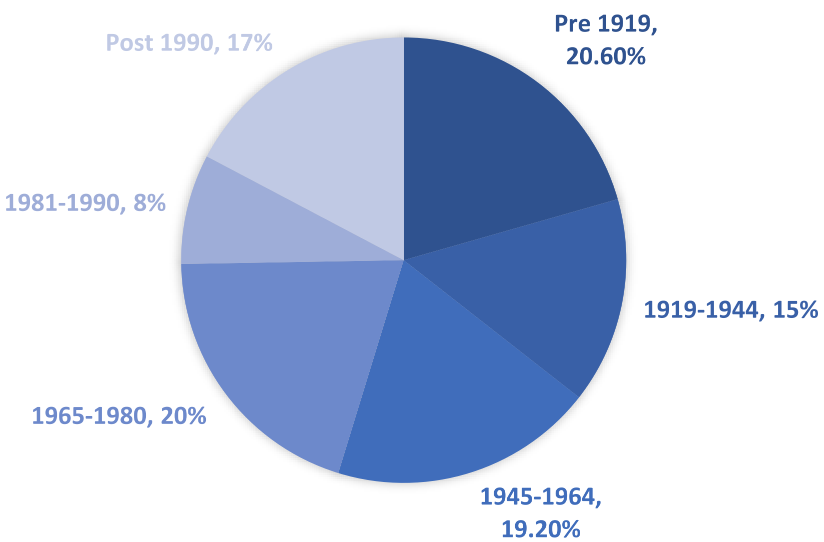

Figure 2.2: Construction date of UK housing stock, with the percentage of total [Data from (Piddington, 2013)]

Overheating in residential settings can have a range of negative impacts on occupant health, from stress to sleep deprivation and increased risk of mortality. It has been estimated that around 7,000 deaths may occur annually by 2050 due to overheating (UK Gov., 2018). This would greatly exceed the worst heatwave-related death toll to date; when in the summer of 2020, 2,556 people died (BMJ, 2022). Exacerbating the risk of overheating is the behaviour of occupants, particularly in the UK, where the natural inclination in hot weather is to open windows and spend lots of time outdoors. This is a contradiction to the areas of southern Europe and Asia, where the tendency is to use shutters to seal the interior away from hot, humid air whilst also preventing solar gains. These methods of passive cooling are widely used throughout the equator and tropical regions, where extended periods of high temperatures are experienced, and there is a lack of access to energy-intensive cooling methods. Recent literature has suggested that passive methods of cooling, including indoor vegetation, have the potential to reduce cooling demands by up to 35 % (Bhamare, 2019). This also represented an ambient temperature reduction of several degrees, improving thermal comfort significantly. However, these results varied depending on location and climate, so they may not be applicable in all settings.

Commercial refrigeration demands are also forecast to increase, in particular, due to the aforementioned development of low-income countries. Recent models suggest that the refrigeration requirements of OECD countries (38 of the richest countries on the globe) will increase by 61 % between 2013 and 2050, whereas non-OECD requirements will more than double in the same period (Sherman, 2022). Together this represents a further 667 TWh of energy annually, purely from commercial refrigeration. This growth is a consequence of an expanding Western lifestyle, such as supermarkets, hospitality, and chemical industries, into tropical countries, whilst the consumption from regions such as the US, UK, and EU continues to grow. The UK food and beverage industry has such a large cooling requirement that it is estimated that the associated ongoing emissions are approximately 14.1 *megatonnes* of CO_2 equivalent ($MtCO_{2,e}$) each year. Studies by Foster et al, suggest that 3.5 % of all UK greenhouse gas emissions are related to this industry and are predominantly due to the leakage of refrigerants into the atmosphere (83 %) (Foster et al., 2023). If the target set by the UK government of net zero emissions by 2050 is to be met, refrigeration in both commercial and domestic applications must be decarbonised; and alternative low GWP refrigerants are an area which could contribute greatly to this ambition.

2.3 Current Refrigerants

2.3.1 Nomenclature

Before detailing the different families of refrigerants, it is first necessary to explain the identification process used to systematically name the refrigerant compounds. The number system is defined under the guidance of the *American Society of Heating, Refrigerating and Air-Conditioning Engineers (ASHRAE) Standard 34: Designation and Safety Classification of Refrigerants* (ASHRAE, 2019). All the refrigerants' identifiers begin with 'R-', with the sequence of numbers following depending on the number of atoms and bonds in the gas. The first number is related to the number of unsaturated carbon-carbon bonds, with the second, third, and fourth numbers defined by the number of carbon, hydrogen, and fluorine atoms, respectively. The following equations describe the standard for identification:

$$Identifier: R - a\ b\ c\ d$$

$$a = no. of\ unsaturated\ carbon - carbon\ bonds\ (omit\ if\ zero)$$

$$b = no. of\ carbon\ atoms - 1\ (omit\ if\ zero)$$

$$c = no. of\ hydrogen\ atoms + 1$$

$$d = no. of\ fluorine\ atoms$$

Isomers of the same refrigerant are defined with lowercase letters after the number identifier, whilst blends with varying compositions of constituent compounds are shown with capital letters. Bracketed capitals (E) or (Z) are in relation to the conformation of the molecule (E = trans and Z = cis, respectively).

For example, trichlorofluoromethane (CCl_3F) has 0 carbon-carbon bonds, 1 carbon atom, 0 hydrogen atoms, and 1 fluorine atom; hence its formula is calculated as follows:

$$a = no. of\ unsaturated\ carbon - carbon\ bonds\ (omit\ if\ zero) = 0$$

$$b = no. of\ carbon\ atoms - 1\ (omit\ if\ zero) = 1 - 1 = 0$$

$$c = no. of\ hydrogen\ atoms + 1 = 0 + 1 = 1$$

$$d = no. of\ fluorine\ atoms = 1$$

Hence the assigned identifier is R-0011 or simply R-11.

2.3.2 Hazard Classification

The *ASHRAE Standard 34* also covers the safety of each refrigerant based on the gas' flammability and toxicity. A scale of 1 to 3 is used for flammability, whilst 'A' is used for non-toxic, and 'B' is used to denote higher toxicity. These groups can be summarised using the matrix below.

Table 2.1: ASHRAE Hazard Classification

Flammability	Non-toxic	High Toxicity
High	A3	B3
Low	A2	B2
	A2L	B2L
No flame	A1	B1

The testing conditions for flammability are 60 *°C* and 101.3 *kPa*, and three main parameters are: Lower Flammability Limit (LFL), Heat of Combustion, and Maximum Burning Velocity. The values used to define the classification are explained in Table 2.2 below.

Table 2.2: ASHRAE flammability limits

Parameter	*Unit*	*1*	*2L*	*2*	*3*
Flame Propagation	-	x	✓	✓	✓
Lower Flammability Limit	*(kg/m³)*	-	> 0.10	> 0.10	≤ 0.10
Heat of Combustion	*(kJ/kg)*	-	< 19,000	< 19,000	≤ 19,000
Burn Velocity	*(cm/s)*	-	≤ 10		

The group *'A2L'* was introduced to classify the alternative refrigerant Hydrofluro-olefins, to describe their lower flammability than group *A2* but still greater than *A1* gas'.

2.3.3 Chlorofluorocarbons and Hydrochlorofluorocarbons

The range of refrigerants currently and previously used has been dominated by the chemicals known as chlorinated and fluorinated gases. These were developed in the 1930s as safer alternatives to the first generation of refrigerants due to their non-toxic, non-flammable qualities. Accidents due to previous refrigerants being corrosive and destroying key components were frequent, so chlorofluorocarbons (CFCs) were developed as an effective replacement. As previously mentioned, the production was commercialised by the joint venture between General Motors and DuPont, as a working fluid for air conditioners. They have no natural sources and are generally produced by the halogen exchange of hydrogen fluoride (HF) with carbon tetrachloride (CCl_4) in the following reaction in the gaseous phase:

$$CCl_4 + HF \rightarrow CCl_3F + CCl_4 + CCl_2F_2$$

This reaction is done under high pressures and temperatures (435 *°C* and 70 *bar*), with a yield of 95 *%* with high ratios of CCl_4 to HF (Gouliaev et al., 1995). Metal fluoride catalysts can also be used to improve the speed of the reaction. This family of gases have excellent properties required for refrigeration cycles, such as a low boiling point, high volatility, and high critical point. They are also non-toxic and non-flammable whilst being colourless and odourless, and so are attractive for use in domestic appliances.

After the second world war, the consumer age began, and hundreds of thousands of refrigerators and air conditioning units were being sold worldwide, and demand for CFCs rose to nearly 1 million tonnes per year at the peak production in the 1980s (Oram, 2005). After the discovery of the ozone hole and research into the role that CFCs had in creating it, hydrochlorofluorocarbons (HCFCs) began to enter the market, as they had similar properties to CFCs, although due to the hydrogen atom, they breakdown more easily in the atmosphere (IPCC, 2021). The quicker decomposition means that when compared to CFCs, they have a smaller ozone depletion potential whilst also being less potent as a greenhouse gas. Table 2.3 highlights some commonly used compounds, along with their properties.

Table 2.3: Properties of select Chlorofluorocarbons and Hydrochlorofluorocarbons

ID	*Name*	*Type*	*Boiling Temp.*[1]	*Critical Temp.*[1]	*ODP*[2]	*GWP*[3]
#			(°C)	(°C)		(100 years)
R11	Trichlorofluoromethane	CFC	23.6	198	1	4,660
R12	Dichlorodifluoromethane	CFC	-29.8	123	1	10,200
R13	Chlorotrifluoromethane	CFC	-81.5	28.6	1	13,900
R21	Dichlorofluoromethane	HCFC	8.8	178.5	0.055	148
R22	Chlorodifluoromethane	HCFC	30.1	96	0.02	1,760
R23	Trifluoromethane	HCFC	-84.5	25.9	0	12,400

It can be seen that there is a range of physical and environmental properties in even this small sample of refrigerants. The reference chemicals for ODP and GWP are R11 and CO_2 respectively. The boiling point is a key parameter, as it must be low enough to allow the refrigerant to evaporate in the coils which are exposed to the ambient air. This means that gases with higher boiling points (such as R11, R21, and R22) are not suitable for uses where the cooling temperatures are lower than their boiling points. Although HCFCs have a greatly reduced ODP compared to their CFC predecessors, they still have a significant GWP; however, at the time of the Montreal Protocol in 1987, the ozone layer was the most critical environmental factor.

[1] P.J. Linstrom and W.G. Mallard, Eds., NIST Chemistry WebBook, NIST Standard Reference Database Number 69, National Institute of Standards and Technology, Gaithersburg MD, 20899, https://doi.org/10.18434/T4D303, (retrieved May 18, 2023).
[2] EPA. (2023). Ozone-Depleting Substances. Available at: https://www.epa.gov/ozone-layer-protection/ozone-depleting-substances
[3] IPCC, 2022: Climate Change 2022: Impacts, Adaptation, and Vulnerability. Contribution of Working Group II to the Sixth Assessment Report of the Intergovernmental Panel on Climate Change [H.-O. Pörtner, D.C. Roberts, M. Tignor, E.S. Poloczanska, K. Mintenbeck, A. Alegría, M. Craig, S. Langsdorf, S. Löschke, V. Möller, A. Okem, B. Rama (eds.)]. Cambridge University Press. Cambridge University Press, Cambridge, UK and New York, NY, USA, 3056 pp., doi:10.1017/9781009325844.

2.3.4 Hydrofluorocarbons

As alternatives were quickly sought to replace CFCs and prevent further damage to the ozone layer, it was found that the key ozone-depleting mechanism was dependent on the availability of chlorine in the stratosphere. To reduce the ODP of refrigeration systems, hydrofluorocarbons (HFCs) were introduced, as they have no impact on the ozone layer yet have similar physical properties to CFCs and HCFCs, making them suitable for a variety of applications. HFCs such as 1,1,1,2-Tetrafluoroethane (R134a) have become commonplace in air conditioners, insulations, and aerosols, and their replacement of CFCs has directly resulted in the recovery of the ozone hole, which has been shrinking since 2000 (NOAA, 2023). These gases are produced through similar mechanisms to the halogen exchange used in CFC synthesis, where the chlorine atom is displaced by fluorine, producing an HFC and hydrochloric acid. The table below (Table 2.4) shows that HFCs have no ozone-depleting potential, and although typically their GWP is lower than that of the previous generation of refrigerants, it is still much greater than CO_2.

Table 2.4: Properties of select Hydrofluorocarbons

ID	*Name*	*Type*	*Boiling Temp.*[1]	*Critical Temp.*[1]	*ODP*[2]	*GWP*[3]
#			(°C)	(°C)		(100 years)
R23	Trifluromethane	HFC	-84.45	25.9	0	14,800
R32	Difluoromethane	HFC	51.8	78.2	0	675
R41	Fluoromethane	HFC	-78.15	44.3	0	116
R134a	1,1,1,2-Tetrafluoroethane	HFC	-26.6	100.9	0	1,430
R125	Pentafluoroethane	HFC	-46.2	66.1	0	3,170

The atmospheric lifetime of HFCs is typically shorter than that of CFCs, with most estimated to last for 10 to 29 years, whereas some CFCs are expected to remain for nearly 100 years. This significantly reduces their global warming potential in comparison to the predecessor refrigerants. However, studies have shown that some HFCs can last for several hundred years, and the lifetime is dependent on the degradation rate due to exposure to high-energy photons in the upper atmosphere (Behringer et al., 2021). These studies also show that lighter, more buoyant molecules tend to have a shorter lifetime as they rise upwards at a greater speed. Other degradation pathways, such as via reaction with hydroxyl or chlorine radicals, occur in the lower atmospheric layers of the troposphere and stratosphere (Bhuvaneswari, 2020). Unlike other greenhouse gases, fluorinated gases, such as CFCs, HCFCs, and HFCs, are not absorbed by the environment, which allows them to have longer lifetimes than CO2, methane, and nitrous oxides, for example.

Currently, most of the emissions associated with refrigeration cycles occur due to residential and commercial AC, followed by refrigeration, accounting for over 50 $MtCO_{2}e$ in the EU alone (EEA, 2022). However, this is a significant reduction from nearly 200 $MtCO_{2,e}$ in 2010, and the phase-out of HFCs continues under the Kigali Amendment to the Montreal Protocol. This amendment came into effect in 2019 and details the scheduled reduction in HFC and HCFC consumption in developed and developing countries. The targets are set at an 85 % reduction in consumption by 2036 (compared to the 2011-13 baseline) in developed nations and an 80 % reduction by 2045 (compared to the 2020-22 baseline) in developing nations (UN, 2016). As such, research into suitable alternatives has gathered pace, in order to satisfy an ever-increasing refrigeration demand during this phase-out.

2.3.5 Blends of Refrigerants

Refrigerants can also be combined to create mixtures that have properties that are more suitable for certain applications. These blends can either behave in an azeotropic or non-azeotropic (zeotropic) nature, depending on the pure components used and their interactions. The naming convention for these mixtures is R-4xx and R-5xx for zeotropic and azeotropic mixtures, respectively. Innovation in mixing refrigerants began to gain traction when high ODP refrigerant replacement was needed, as combinations of HFCs could replicate their properties. The behaviour of these two types of mixtures can be seen in Figure 2.3, where there is a two-phase region that describes a state where the vapour and liquid factions have differing compositions of the two components. The bubble point is defined as the temperature at which the more volatile component first becomes a vapour. Likewise, the dew point is the temperature at which the least volatile component first starts to condense. Since 1990, R410A has become one of the most widespread refrigerants in the developed world and is composed of a 50/50 mixture of R32 and R125. This blend was used as an appropriate replacement for the HCFC R22 thanks to their similar physical properties, which has been reflected in the production rates of R410A, increasing 115 % annually between 2006 and 2017 (Liu et al., 2019).

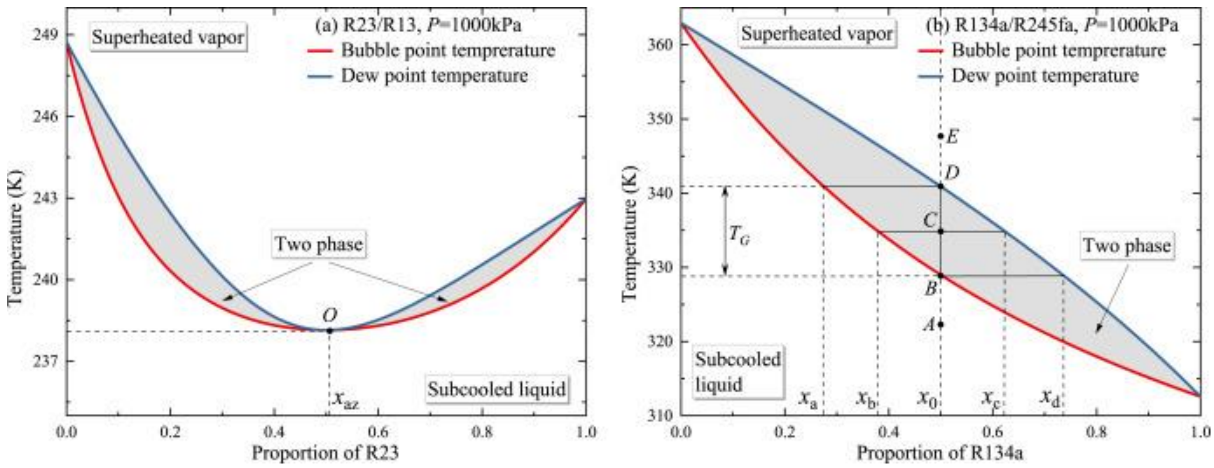

Figure 2.3: Example T-x diagrams for Azeotropic (a) and Zeotropic (b) mixtures (Xu et al., 2021)

This type of refrigerant blend is a zeotropic mixture, as the two liquid components have different boiling points, although R410A is itself a near-azeotropic mixture. The properties resulting in this type of mixture mean that there is often a differential between the saturated vapour and liquid temperatures, as when one of the components has a lower boiling point, it will enter the vapour phase in greater concentrations than the other component. This is defined as the 'temperature glide' and is a property of all zeotropic mixtures. Problems can occur in the evaporator and condenser during the refrigeration cycle if this differential is too large; however, there are ways to mitigate the impact, such as using a counterflow heat exchanger (Wang, 2022). The temperature glide can even be exploited to increase the efficiency of cooling in refrigeration systems, hence reducing power requirements. An increase in Coefficient of Performance (COP) of 40 % in zeotropic hydrocarbon and CO_2 mixtures, compared to pure hydrocarbon, has been reported (Yelishala, 2020).

Azeotropic mixtures, on the other hand, behave as though they were a single compound fluid. This means that they have no temperature differentials and no two-phase region in their mixtures. In Figure 2.3 above, point O in Figure 2.3 diagram (a) shows the azeotropic composition of the mixture R23/R13, which happens to occur at a 50/50 mixture. Heat transfer coefficients in azeotropic mixtures are also typically greater than in zeotropic ones due to the lack of temperature glide and low mass transfer resistance in boiling. Blends of refrigerants with a positive azeotrope (Figure 2.3(a)) can reach lower refrigeration temperatures whilst also requiring less refrigerant charge (volume of refrigerant) (Zhao et al., 2019). These systems are also immune from the fractionation problem that can occur in zeotropic mixtures when there is leakage. This is because zeotropic vapour will have a different composition to the liquid; hence a vapour leak will change the composition and properties of the refrigerant.

Table 2.5: Properties of select Refrigerant Blends

ID	*Composition*	*Azeotropic/Zeotropic*	*Boiling Temp.*	*Critical Temp.*	*GWP*	*Glide Temp.*[4]
#			(°C)	(°C)	(100 years)	(°C)
R404A	R125/R143a/R134a (0.35782/0.60392/0.03826)	Near-Azeotropic	-46.45	72.07	3,922	1.1
R407C	R32/R125/R134a (0.23/0.25/0.52)	Zeotropic	-43.7	86.4	1,624.21	4.9
R410A	R32/R125 (0.5/0.5)	Near-Azeotropic	-48.6	72.9	2,088	0.5
R454B	R32/R1234yf (0.689/0.311)	Zeotropic	-50.5	78.1	466	1.5

2.4 Alternative Refrigerants

As the phase-out of the high GWP refrigerants has come into effect and continues to constrict the use of HFCs, new research has been targeted towards a variety of proposed alternative refrigerants that have not only no ozone depletion properties but also low GWP.

2.4.1 Hydrocarbons

Hydrocarbon (HC) vapour compression cycles were first experimented upon in the 1860s and continued to be utilised until the advent of CFCs in the 1930s. These naturally occurring compounds were applicable to most refrigeration systems of the time, and so were implemented in a variety of industries. However, the most common hydrocarbons, such as propane (R290), butane (R600), and isobutane (R600a), are very flammable, and leakages in early refrigeration systems were frequent. These safety concerns led to the shift away from hydrocarbons to safer CFCs.

More recently, hydrocarbons have been revisited as potential alternatives to ozone-depleting or high GWP refrigerants. The advantage of HC refrigerants in the context of global warming is their significantly reduced GWP when compared to HFCs. Below is a table of select HC refrigerants and their GWP potential. It can be seen that there is a reduction in GWP of several

[4] Data collected from respective manufacturers.

thousand percent, whilst the range of boiling and critical points is diverse, enabling their application in a variety of systems.

Table 2.6: Properties of select Hydrocarbons

ID	*Name*	*Type*	*Boiling Temp.*[1]	*Critical Temp.*[1]	*ODP*[2]	*GWP*[3]
#			(°C)	(°C)		(100 years)
R290	Propane	HC	-42.05	96.8	0	3.3
R600	Butane	HC	-0.2	151.9	0	4
R600a	Isobutane	HC	-11.2	134.6	0	3
R170	Ethane	HC	-88.6	32.2	0	5.5
R1270	Propylene	HC	-47.6	92.1	0	1.8
RC270	Cyclopropane	HC	-33.2	124.9	0	1.8
RE170	Dimethylether	HC	-25.0	127.9	0	1

The flammability of HC compounds is the key concern when investigating the possibility of their use in refrigeration, and the international safety convention identifies the risk posed by these chemicals as the highest flammable classification (A3) (ASHRAE, 2019). However, studies have shown that under the correct operation within manufacturers' guidance, hydrocarbons are safe to use (Harby, 2017). Procedures to limit these concerns of HC operation include low refrigerant charge, elimination of spark sources, and hermetically sealing the fluid within the system. The literature suggests that these HC refrigerants are most suitable for domestic and small commercial applications, which typically have less than 1.5 *kg* of refrigerant per sealed system, in fact, the European domestic fridge market has been dominated by R600a since the turn of the century, whilst 85 *%* of new fridges in China are now also using hydrocarbons (UNEP, 2018). Heat pumps in the UK and Germany are also utilising R290 and R1270 as the favoured refrigerants. The use of HCs as refrigerants is popular in the petrochemical industry, where the control of highly flammable materials is commonplace, and so safety measures are already at a very high standard.

The International Institute of Refrigeration defines the explosion risk as zero with HC charges of less than 0.15 *kg*, and with systems larger than this, there is a negligible risk so long as the size of the room enables the concentration to remain below 0.008 kg/m^3 (Widodo et al, 2021). This is the charge limit for HCs in the EU; however, the US has a much stricter policy at only

0.057 *kg* (Mota-Babiloni, Makhnatch and Khodabandeh, 2017). Adhering to these guidelines could allow HCs to be implemented in smaller refrigeration applications; for example, domestic fridges contain between 0.05 and 0.5 *kg* of refrigerant. In addition to this, hydrocarbons typically have a greater latent heat than CFC and HFC refrigerants, meaning that the compressor size can be reduced whilst also using a smaller refrigerant charge. This has been reported to increase the efficiency of heat pump cycles by up to 11 *%* when compared to R12 (Kim, 1998). Similar results have been published showing that HC refrigeration systems can increase the COP compared to that of HFCs (Figure 2.4). As can be seen in the figure, this investigation was conducted on typical freezer temperature ranges.

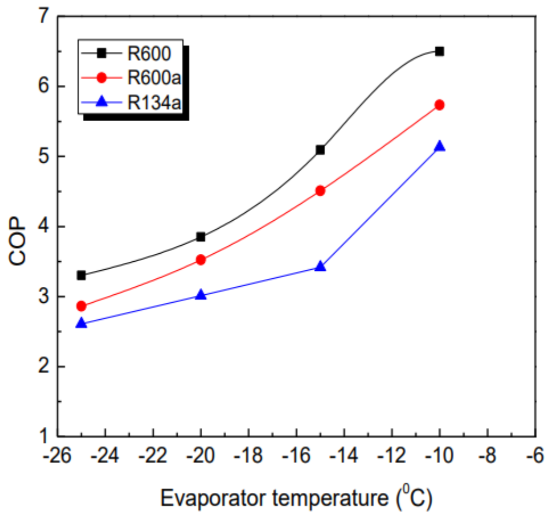

Figure 2.4: Comparison of COP at varying evaporator temperatures for hydrocarbons (R600 and R600a), and HFC (R134a) (Emani, 2018)

2.4.2 Ammonia

Ammonia (R717) is another refrigerant that was popular in early vapour compression systems, but its uses in smaller applications were overshadowed by CFCs. Despite enabling high refrigeration efficiencies and low cost, it causes corrosion of compressors and other crucial components, reducing its attractiveness. It is also an irritant to the human respiratory tract at concentrations above 80 *ppm*, and deadly at approximately 2,000 *ppm*, which led to its application being restricted to industrial and commercial use (NRC, 2008). The penetration in this market is as high as 90 *%* in the US and Europe due to the large enthalpy of evaporation at freezer temperatures (approximately -18 *°C*), meaning that lower charge volumes can be employed (Zhang et al., 2022). As ammonia is also mildly flammable, larger systems are more susceptible to dangerous leakage and explosions. There have been numerous accidents involving ammonia refrigeration systems, and severe cases such as in Jilin, China, where 120 people were killed due to an ammonia explosion, which has hindered the use of ammonia in more applications where it could drastically reduce greenhouse gas emissions (Tan, 2017).

Despite the flammability and toxicity, the physical and environmental properties of ammonia make it one of the most effective and promising refrigerants. Not only does it have a large enthalpy of vaporisation, but it also has a low boiling point (-33 *°C*) and high critical point (132.4 *°C*) whilst also having no global warming or ozone-depletion potential. This means it can be used in very cold storage applications, even at atmospheric pressure. Recent literature reports that efficiencies of ammonia refrigeration are also 3 – 10 *%* improved on competing systems (Shanmugam and Mital, 2019). If safety concerns are addressed for small-scale applications, this could represent a significant reduction in electrical requirements, particularly as cooling demands are increasing at a rapid rate.

Large industrial water chillers have utilised ammonia systems, as well as recent developments in building air conditioning, although it isn't possible to retrofit systems due to the incompatibility with copper alloys and certain types of rubber seals (UK Gov., 2012). However, the production of ammonia is currently dominated by the Haber process, which uses hydrogen generally produced via steam reformation of methane – a carbon-intensive process, with one UK government-backed study suggesting that 2.55 $kgCO_{2e}$ is associated with the production of 1 *kg* of NH_3 (Liu, 2020). Although other processes may reduce these emissions, such as electrolysis for hydrogen production, they are, as of now, uneconomic in comparison, with papers from the Royal Society of Chemistry estimating that the cost per *kg* of 'green' ammonia is approximately four times as much as conventional methods, at $0.92-1.06/*kg* (Lee et al., 2022).

2.4.3 Carbon Dioxide

Carbon Dioxide (R744) is typically thought of as a polluting gas that should be avoided at all costs, as it contributes to 76 *%* of all greenhouse gas emissions (EPA, 2019). However, in comparison to the aforementioned CFCs, HCFCs, and HFCs, it has a much lower GWP whilst also being benign to the ozone layer. The application of CO_2 as a refrigerant is much less widespread; however, as many countries have mandated the removal of refrigerants with GWP greater than 150, it has recently been increasing in popularity (UN, 2016). Carbon dioxide is one of the few natural refrigerants that is non-toxic and non-flammable whilst also being chemically inert, and so avoiding reaction with system components which would increase the likelihood of leakage. Under high pressure, the fluid has a low compression ratio, and studies have proven it to increase the efficiency of current halo-carbon systems (Kim, 2004). However, the difficulties of CO_2 operation are the low critical temperature (31.1 *°C*) and high operational pressures, which means that typically CO_2 refrigeration is transcritical. This leads to more complicated systems and higher specification components being necessary, although there is the advantage of using smaller pipes (for higher pressures). Studies have shown that CO_2 could be used to improve the compactness of systems whilst also consuming less electricity due to having a larger volumetric refrigeration capacity (da Silva, Bandarra Filho and Antunes, 2012). It should be noted that CO_2 systems operate at over 73 *bar* compared to the typical 1 – 20 *bar* for conventional refrigerant systems, although with advancement in material science, this is becoming less of a problem in practice.

The high availability of CO_2 also lends itself to displacing the market share of refrigerants from high GWP gases. Increasing the use of CO_2 in refrigeration applications could also improve the commercial viability of carbon capture and storage systems by generating much greater demand for the gas, and the growth of transcritical CO_2 systems is expected to increase at a rate of 17 *%* each year, from $36 bn in 2020 to $110 bn by 2027 (GVR, 2016). It is forecasts such as this that put CO_2 at the forefront of alternative refrigerant research, and F-gas policies from the EU have accelerated this, whilst the US is also implementing similar regulations in the 2020s.

2.4.4 Hydrofluoro-olefins

Hydrofluoro-olefins (HFOs) are another well-researched alternative refrigerant. They possess very similar thermophysical properties to HFCs, allowing them to be developed as ‘drop-in’ alternatives in some applications, therefore requiring no modification of the system. They are proving popular in American domestic applications, where hydrocarbons are deemed unsafe (Lee, Lee and Jeon, 2018). These gases have no ozone-depleting potential and have a significantly reduced GWP compared to HCFCs and HFCs. This is due to the unsaturated nature of olefins, with a double carbon bond structure, which means that they are broken down in a matter of days by hydroxyl radicals; much more quickly in the atmosphere than previous refrigerants and CO_2 (Nair, 2021).

Recent literature has been focused on four of these compounds: R1234yf, R1234ze(E), R1234ze(Z) and R1233zd(E), and in particular, R1234yf due to its similarity to R134a (HFC), which was the most common HFC refrigerant (Bobbo et al., 2018). Research such as this is positive, as R134a has a GWP of 1,300, whereas, in comparison, R1234yf has a GWP of less than 1.

Table 2.7: Properties of select Hydrofluoro-olefins

ID	*Name*	*Type*	*Boiling Temp.*[5]	*Critical Temp.*[4]	*ODP*[4]	*GWP*[1]
#			(°C)	(°C)		(100 years)
R1234yf	1,3,3,3-Tetrafluoropropene	HFO	-29.5	94.7	0	0.5
R1234ze(E)	2,3,3,3-Tetrafluoropropene	HFO	-19.1	109.4	0	6
R1234ze(Z)	2,3,3,3-Tetrafluoropropene	HFO	9.8	150.1	0	1.4
R1233zd(E)		HFO	18.3	166.5	0	7

HFOs have been coined the fourth generation of refrigerants, and it is thought that they may be the last unnatural refrigeration gases left unexplored. Analysis of the REFPROP chemical database from McLinden (2017), discovered there are unlikely to be any more newly discovered chemicals suitable for vapour compression cycles, and a joint paper with Huber (2020) published these results. Interest in HFOs as a suitable alternative to HFCs, largely began in 2006, with the automotive industry seeking to find gases with a GWP of less than 150 to adhere to the EU regulations coming into force in 2017. Initially, propene was blended with F-gases to experiment with their refrigeration properties; however, these were largely abandoned due to toxicological implications, and some even caused ozone depletion (Spatz, 2007). Investigations into the use of pure HFOs then expanded; for example, R1234yf was deemed a suitable replacement for R134a in mobile air containers in the early 2010s.

However, concerns over the flammability of these gases meant that some manufacturers were reluctant to use them in their cars. Companies such as Mercedes had tested cars utilising R1234yf, leading to explosive events and public anger towards these greener alternatives. Other car manufacturers refuted these results, claiming that the experiments were conducive to ignition, such as spraying the gas on a hot engine with compressor oil, and the manufacturers of R1234yf, Honeywell and DuPont, claim the gas is only ignited at temperatures over 900 *°C* in combination with oils (Spatz, 2008). Despite these concerns, by 2018, over 50 *%* of new car

[5] Nair, V. (2021). HFO refrigerants: A review of present status and future prospects. International Journal of Refrigeration, [online] 122, pp.156–170. doi: https://doi.org/10.1016/j.ijrefrig.2020.10.039.

models used R1234yf as the main AC refrigerant, and in the UK, it has been mandated since 2017 (UK Gov., 2012). Most HFOs are classified as level '*A2L*' under *ASHRAE Standard 34*, meaning they are non-toxic and mildly flammable.

2.5 Thermodynamics and Applications

2.5.1 Refrigeration Cycles

This section will highlight the areas of thermodynamics most crucial to the aims of this project; for further reading, texts such as *Refrigeration Systems and Applications* (Dinçer, 2017) and *Essential Thermodynamics* (Panagiotopoulos, 2011) should be consulted.

The vapour compression cycle is the most widely used refrigeration cycle, particularly in small-scale and domestic applications. This cycle uses a refrigerant as the working fluid, utilising the latent heat of evaporation and condensation to extract heat from cold space and dump it into the warmer, ambient air. In order to avoid breaking the Second Law of Thermodynamics, this cycle is not possible without consuming more electrical power from the compression device than the heat energy that is extracted. The diagram below (Figure 2.6) is a visual representation of the components of the refrigeration cycle, where heat energy is extracted from the indoor environment and expelled into the outdoor environment. This example is an air conditioning unit for indoor cooling, although the process is the same for refrigeration, with the indoor environment being cold storage. The only electrical work consumed by this system is through the compressor as a means of forcing the fluid around the cycle. It can be noted that this is essentially a reversed Rankine cycle, where, conventionally, heat from a fuel source is used to heat a fluid that moves a turbine to *generate* electricity. This cycle is known as a Carnot refrigeration cycle.

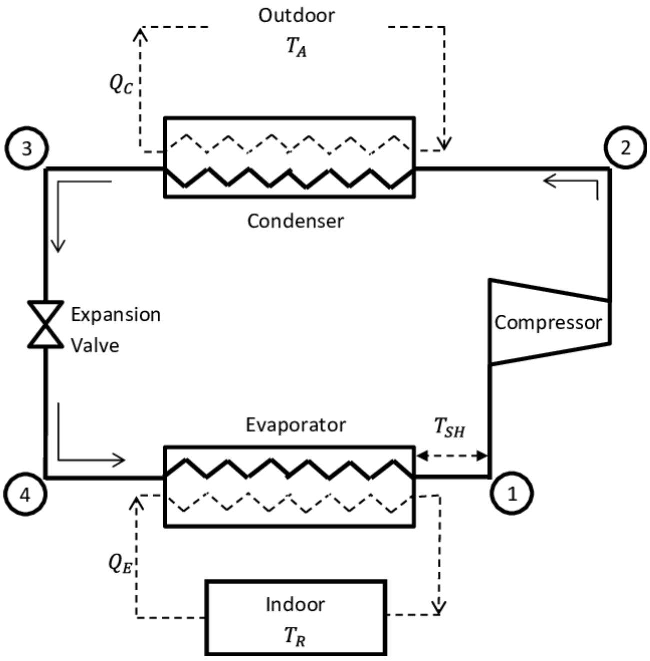

Figure 2.5: Refrigeration Cycle Process Diagram (Sholahudin et al., 2019)

Figure 2.6 shows the relationship between pressure and enthalpy throughout the cycle in relation to the liquid-vapour line (inverted U curve). The numbered points denote each stage of the refrigeration cycle: 1-2 is the compression of the vapour from saturated vapour to superheated, 2-3 is the condensation process, 3-4 is the expansion through the valve (high to low isobars), and 4-1 is the evaporation of the fluid.

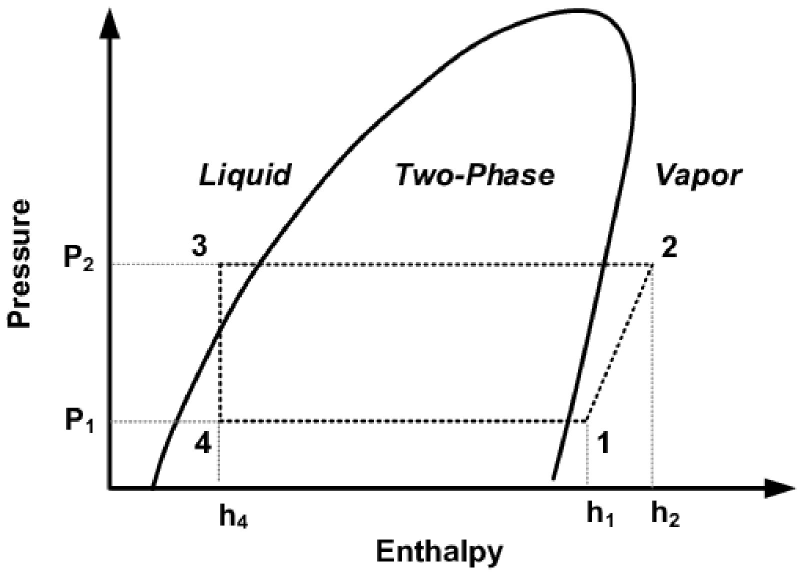

Figure 2.6: Standard Vapour Compression Cycle P-h diagram (Jain and Alleyne, 2011)

The values of the physical properties from each state can be used to calculate the heat work absorbed and expelled as well as the compressor work. Through knowledge of the pressure and temperature at each state, the enthalpies can be known using established databases for the working fluid that is used, such as NIST REFPROP. It should be noted that in Figure 2.6, the expansion process (3-4) is assumed to be isenthalpic, which is not the case in realistic applications but is appropriate for a brief analysis. While for the compression (1-2), this is the realistic compressor power due to the non-isenthalpic nature of vapour compression. In an ideal cycle, the compression would not require any work input.

The following equations show the relationship between each state enthalpy and the respective work.

Compressor Power (Process 1-2):

$$\dot{w}_c = \dot{m}(h_2 - h_1) \tag{2-1}$$

Condenser Heat Rejection (Process 2-3):

$$\dot{Q}_c = \dot{m}(h_2 - h_3) \tag{2-2}$$

Evaporator Heat Extracted (Process 2-3):

$$\dot{Q}_e = \dot{m}(h_1 - h_4) \tag{2-3}$$

Where:

$\dot{Q}$ is Heat (*kW*)
$\dot{w}$ is Electrical Work (*kW*)
h is Enthalpy (*kJ/kg*)
$\dot{m}$ is Refrigerant Mass Flowrate (*kg/s*)

It is important to know these values, as they are used to calculate one of the most important parameters when assessing the performance of refrigeration systems, the Coefficient of Performance (COP). The COP is the most widely used figure to compare the efficiency of systems using a variety of working fluids or in a variety of source and sink temperatures.

Coefficient of Performance (Cooling):

$$COP_c = \frac{\dot{Q}_e}{\dot{w}} = \frac{\dot{m}(h_1 - h_4)}{\dot{m}(h_2 - h_1)} = \frac{(h_1 - h_4)}{(h_2 - h_1)} \tag{2-4}$$

As can be seen from equation (2-4), the COP_C is the ratio between the heat extracted from the cold reservoir (source) and the electrical power consumed by the compressor. This is only correct for a cycle operating at a steady state (Jain and Alleyne, 2011). When the cycle is used for heating applications, the useful heat work is from the condenser (2-3); hence the COP for heating (COP_H) is:

Coefficient of Performance (Heating):

$$COP_H = \frac{\dot{Q}_c}{\dot{w}} = \frac{\dot{m}(h_2 - h_3)}{\dot{m}(h_2 - h_1)} = \frac{(h_4 - h_1)}{(h_2 - h_1)} \tag{2-5}$$

The COP of a refrigeration system is typically larger for those with working fluids that have a higher critical temperature due to the superheating of the vapour in the compressor and gaseous losses (Venkatarathnam and Srinivasa Murthy, 2012).

The ideal COP for the Carnot cycle is determined by the temperature difference between the source and sink used for the heat extraction and ejection. The equation below shows the relationship.

Coefficient of Performance (Ideal Carnot):

$$COP_{ideal} = \frac{T_2 - T_1}{T_2} = \frac{T_{hot} - T_{cold}}{T_{hot}} \tag{2-6}$$

Where:

T_1 is Temperature of the cold reservoir (K)

T_2 is Temperature of the hot reservoir (K)

This means it is possible to estimate the efficiency of applications based on known temperature ranges in their operation. However, real refrigeration systems operate at approximately 50 % of this ideal COP, with a range of between 35 – 60 % (Dinçer, 2017).

2.5.2 Cryogenics

The use of vapour compression cycles for cryogenic temperatures is less common than that of the other applications in this chapter, as there are a wider variety of methods for creating ultra-low temperatures, such as absorption cooling and magnetic cooling. Despite this, vapour compression is used extensively in certain industries such as cryotherapy, cryomilling ceramic powders and food preservation (Rogala and Kwiatkowski, 2022). The temperatures required by these industries vary within the range of 90 to 200 K (– 183 to – 73 $°C$) and are typically unachievable by a single-stage refrigeration cycle. As such, a cascade system is utilised to create these low-temperature evaporator stages, and expel heat to a higher-temperature stage, and each stage uses different refrigerants that have thermophysical properties suited to the operational temperature range.

In the food transport industry, the power generation for the cryogenic cycles is often delivered by diesel engines as opposed to an electrical supply. This creates large amounts of carbon dioxide equivalents and significantly increases the environmental footprint of the industry; with an estimated 12 $MtCO_2$,e emitted in the UK from this industry alone (Rai and Tassou, 2017). At present a third of vapour compression systems are powered in this manner, and the indirect emissions account for approximately 83 *%* of the lifecycle carbon emissions. However, as the method of powering the cycles becomes less carbon-intensive, the refrigerants used will come under greater scrutiny.

The most common low-temperature refrigerant in the post-Montreal era was R23, a hydrofluorocarbon, which was frequently coupled, within a cascade system, with R12 and R22. These refrigerants all have a significant global warming potential, of 14,600, 10,200, and 1,760, respectively; meaning that they are due to be phased out as per the F-gas regulations (Fluorinated Greenhouse Gases Regulations 2018). As of 2020, the maximum carbon dioxide equivalent for HFC systems was restricted to 40 tCO_2,e or the equivalent of 2.74 *kg* of R23. This has led to an increase in research to replace this group of refrigerants with low GWP alternatives that perform comparatively.

There is extensive literature on the thermodynamic analysis of cryogenic cycles, in particular to the liquefaction of natural gas, as this is a major international industry. A thermodynamic review of refrigeration cycles for this application assessed 16 different cycles, with a variety of refrigerant combinations, and concluded that doubling the number of stages resulted in a 25 *%* increase in efficiency, using a combination of propane (R290), ethylene (R1150) and methane (R50) (Chang, 2015). The figure below shows the typical arrangement for a two-stage cascade system for low-temperature applications.

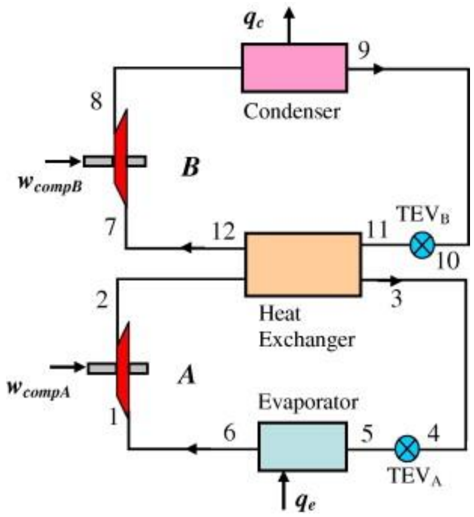

Figure 2.7: Two-stage cascade refrigeration schematic diagram (Kilicarslan and Hosoz, 2010)

It can be seen that the low-temperature stage (A) extracts heat from the environment (q_e) and, through a heat exchanger, expels this to the high-temperature stage (B). This stage then rejects the heat to the ambient environment (q_c). It is noted that the two stages operate with their own separate compressors, as they will utilise different refrigerants, with varying compression properties. In using two different gases, it is possible to achieve very low temperatures, as the colder stage would not be able to reject energy to the ambient environment itself, due to the low boiling point it cannot condense at typical room temperatures.

Aside from the cascade nature of two-stage systems, each separate refrigerant goes through the same changes in state as the single-stage analysis in *Section 2.5.1*.

2.5.3 Refrigeration

Domestic and commercial refrigeration systems are commonplace in almost every corner of the world and are essential for keeping food, medicines, and other products safe for consumers. These devices have revolutionised the modern world by enabling the transportation of products across continents without depreciation in quality or safety. Typically, refrigerators must be kept between 0 – 5 *°C*, whilst freezers are much lower at –23 *°C* to –18 *°C*. In the UK, it is a legal requirement for businesses to keep cold foods stored for sale below 8 *°C*, in order to slow bacterial growth, particularly Escherichia coli (E-coli). The temperature range kept by a freezer for transport or storage prevents bacteria from multiplying, although it doesn't kill them.

The environmental impact of operating refrigeration systems is composed of two aspects: refrigerant leakage and electricity consumption. Domestic appliances often have lifetimes of up to 20 years, and an annual leakage rate of 5 *%*, meaning that without any recharge of refrigerant, there would be a total loss of almost 65 *%*, significantly reducing the performance of the device. In most refrigerators, the amount of charge is between 0.05 and 0.5 *kg*, so the leakage is relatively small; however, there are approximately 1.4 billion fridges in operation worldwide. In older models, more frequently used in developing nations, the leakage rates can be up to four times higher and are more likely to contain high GWP refrigerants.

Given that R600a (Isobutane) is the most common fluid in European refrigerators, with a GWP of 3, the UK government estimates that domestic fridges contribute 0.15 $MtCO_{2e}$ each year from leakages (Foster et al., 2023). The electricity consumption of these domestic appliances is reported to contribute 2.37 $MtCO_{2e}$, due to the carbon intensity of the UK national grid. This illustrates that, at present, the electricity consumed by domestic refrigerators is around 15 times more influential than the leakage of refrigerants.

Commercial refrigerators range from small stand-alone appliances to cold storerooms and can require between 5 to 500 *kg* of refrigerant charge, depending on the cooling demand. Leakage rates for these larger systems are often greater than that of domestic appliances due to their size and complexity, at approximately 10 – 15 *%* per year. In these applications, R404A is still the dominant gas used, which is a blend of three HFCs, has a GWP of 3,922, and thus contributes significantly to the associated carbon emissions. A study published in 2014 found that retail refrigeration produced 4.52 $MtCO_{2e}$ in the UK alone, of which 3 $MtCO_{2e}$ was directly associated with the leakage of refrigerant (SKM Enviros, 2011).

Industrial-scale refrigeration systems can require over 1,000 *kg* of refrigerant for use in warehouses that store large quantities of chilled or frozen foods. Applications of this size typically utilise ammonia as the working fluid, as they are not usually situated in heavily populated areas, and so the risk of operation is reduced. Literature reports there were over 400 warehouses of this type in the UK as of 2018, and as ammonia has no global warming potential, the leakage of any refrigerant has no associated carbon equivalent emissions, although the electricity consumed is reported to be around 3.5 *TWh*, or 0.64 $MtCO_{2e}$ (CCC, 2020).

2.5.4 Heat Pumps

Heat pumps are at the forefront of the UK government's plan to decarbonise heating, both domestic and commercial, in order to reach their net zero ambitions. This has meant that the number of installations each year must increase ten-fold from 60,000 to 600,000, as highlighted in the *'Heat pump investment roadmap'* (UK Gov., 2023). Globally, heat pumps contribute to meeting 10 % of the world's heating demands, predominately due to the increased uptake in the technology across Scandinavia, the US, Northern China, and Oceania (IEA, 2022). In 2022, annual heat pump installations surpassed new gas-fuelled boilers for the first time in several countries, with the increase largely driven by the Ukrainian crisis (EHPA, 2022).

These devices work in a similar way to the refrigeration systems explained previously, except the heat is moved from the outdoor environment to the indoor environment by placing the condenser inside the building. As this cycle uses heat for a purpose, the heat from the compressor work can be effectively utilised, and so the COP_H is larger than that for cooling systems.

It is possible to move heat from a variety of low-temperature sources for utilisation in warm environments; the most common examples are air or ground-source heat pumps for domestic applications, although water is commonly used in larger installations. These systems are proving attractive options for replacing old gas boilers, as with the investment from governments, they are soon to become cost competitive; whilst also being more energy efficient. The COP_H of air and ground-source systems can range from 2 – 5 depending on the source temperature, which means that for each unit of electricity used and paid for by the consumer, the device can produce 2 to 5 units of useful heat. This is much greater than the typical efficiency of the best-performing fossil fuel boilers, ranging from 0.8 to 0.9 (Ala, et al., 2019).

Due to the seasonal variation in air temperature across the whole year, it is typical that the Seasonal Performance Factor (SPF) of ground source heat pumps tend to be slightly greater than the air source. The SPF takes into account the varying COP across the whole year, and reversible heat pumps can include cooling capabilities in summer. As the ground temperature doesn't vary significantly across the year in comparison with the ambient air, the SPF can be up to 1 greater than air source devices, with a range of 2.4 – 3.4 and 3 – 4.6 for air and ground, respectively (Nouvel, 2015). The calculation of SPF and COP for heat pump and air conditioning devices is regulated by the *British Standards BS EN 14825* and allows devices from a variety of manufactures to be compared based on their performance in standardised test conditions (BSI, 2022).

Most mass-produced domestic heat pumps use the refrigerant R410A (HFC) as their working fluid in the UK, which can impact the lifecycle carbon emissions due to its GWP of 1,922. As the number of installations increases, it will become even more important to introduce alternative refrigerants to domestic heat pumps in order to reduce leakage contribution to global warming.

Industrial heat pumps for applications such as district heating or process heating and cooling typically use ammonia, CO_2, or glycol mixtures. This is due to several factors that enable the use of these fluids in larger systems than in smaller domestic devices. The cost-effectiveness of these fluids in comparison to HFCs, due to their ready availability and physical properties, means that they are more suitable. Natural refrigerants are between 3 – 8 times cheaper per kilogram than HFCs (Papasavva, Hill and Andersen, 2010). While issues can arise with the toxicity of ammonia, this is less of a concern in industrial applications due to strict monitoring and operation only with trained personnel. The inefficiency of cooling- or heating-only CO_2 systems restricts the economic viability in these smaller systems; however, in areas where both heating and cooling demands are in close proximity, this can significantly improve the attractiveness over conventional refrigerants (Wang, J, et al., 2022). Applications such as supermarkets and industrial sites that require hot water production and AC cooling are examples that are well suited to a CO_2-based system.

2.6 Summary

To summarise this chapter, the literature review conducted has provided some context for this project and the necessity of research into low GWP refrigerants. The two main driving forces behind these developments were the discovery of the ozone hole and latterly, climate change. Also, refrigerant research is defined by legislation that is developed to restrict the impact that the gases have on these two major events. The expansion of refrigeration systems in the late 20th century, along with the more recent increased demand for cooling systems in developing countries, are also key factors that have led to more extensive research into low GWP refrigerants to curtail direct greenhouse gas emissions. This is particularly due to the vicious circle created by climate change; as temperatures increase, the demand for cooling systems increases, which in turn generates further emissions, and so the greenhouse gas effect is amplified. This chapter also details the major refrigerant groups, namely, chlorofluorocarbon, hydrochlorofluorocarbon, hydrofluorocarbon, natural, and hydrofluoro-olefin refrigerants. The typical physical properties of these groups were explained, along with their respective global warming potential and ozone depletion potential.

Finally, the thermodynamics of the vapour compression cycle was explored, along with a brief description of the applications of this cycle that will be modelled.

3. Modelling Approach

The methodology outlined here was used in order to collect the necessary data for each refrigerant in a number of refrigeration cycles that are modelled based on the parameters of real-life systems. This approach allows for the analysis of technical, environmental, and economic performance, which will provide the basis for fulfilling the objectives described in *Chapter 1*.

This chapter will outline the method used to gather input data, set up simulations, and process the results output. The key software for this analysis were NIST Cycle_D-HX, CoolPack, and MS Excel.

3.1 Software

The software named above were selected as they are well-known and reputable programs developed by the American National Institute of Standards and Technology (NIST), and the Technical University of Denmark (DTU) Department of Mechanical Engineering (CoolPack). They are suitable programs for simulating the vapour compression cycle which is the basis for all of the applications investigated in this project. The results were collected in MS Excel for processing and visualisation. Cycle_D-HX was the main software used thanks to its much larger refrigerant database in comparison to CoolPack, with a variety of refrigerants, from CFCs and HCFCs to HFCs, HFOs, and natural refrigerants, as well as many blended gases. The set up of the model is done with ease thanks to easily accessible user interfaces, and the thermophysical properties are taken from NIST REFPROP.

CoolPack was utilised for cryogenic applications (Case 1) and CO_2 heat pumps (Cases 4 – 8). This program allowed for a larger variety of vapour compression cycles than the NIST software, however, it has a much smaller refrigerant database, with only 14 single and blended fluids to choose from. There are also a number of property calculators, design and analysis tools, as well as auxiliary calculators for the equipment within the cycle. This program coped well with the transcritical nature of CO_2 heat pumps whilst also allowing a two-stage design with different refrigerants in the low and high-temperature loops, so proving useful for the cryogenic model. The output of the simulations takes the form of figures and tables depending on the user's preference.

The NIST Cycle_D-HX program is set up in three steps: Refrigerant selection (Figure 3.1), Cycle Options (Figure 3.2), and Cycle Specifications (Figure 3.3). These can be tailored to the needs of the user for the particular application. The refrigerant database includes 70 single compound refrigerants and over 100 blended fluids, whilst it is also possible to define new custom blends. These can be chosen for modelling in four cycle types: single-stage, two-stage economizer, two-stage compression with intercooling, and three-stage economizer. A heat exchanger can also be added to the system. The final step is to input the constraints on the heat exchangers, compressor, and other auxiliary parameters. This is where the system is customised to each case chosen for modelling by selecting appropriate evaporator and condenser temperatures. The output of the simulations can be presented as a summary table, schematic diagram with state points, or thermodynamic cycle diagrams (temperature – entropy or pressure – enthalpy).

The figures below depict the user interface of the NIST Cycle_D-HX program:

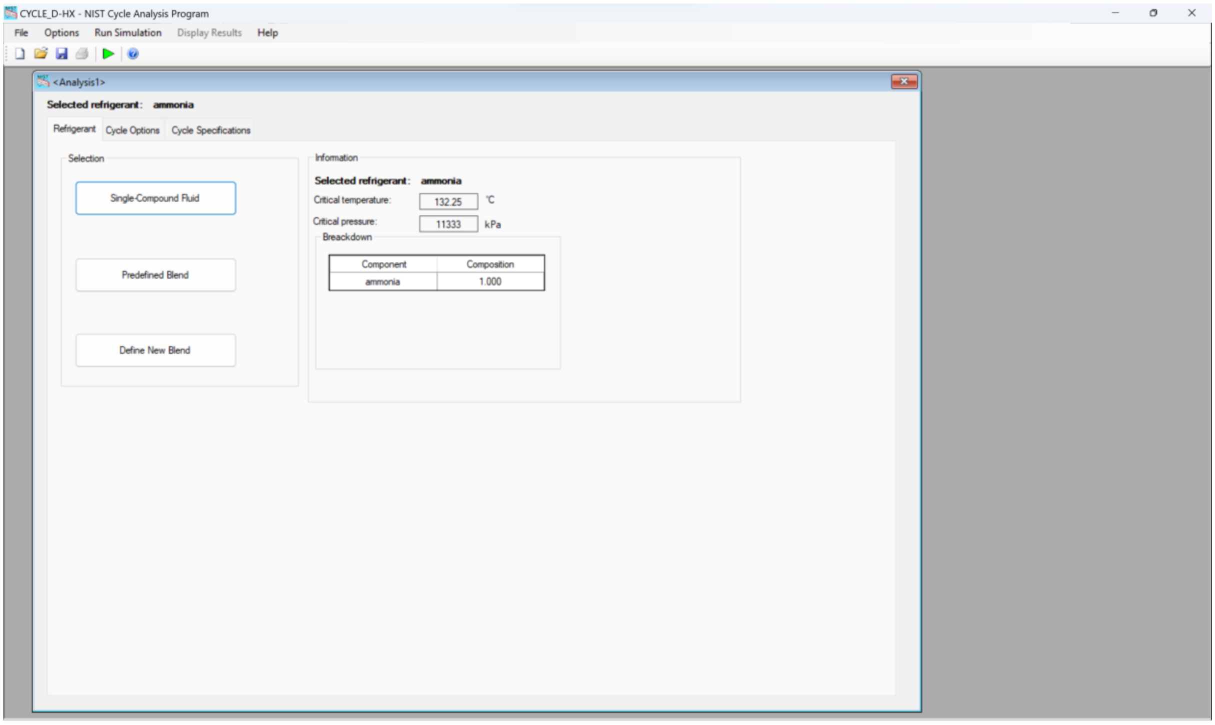

Figure 3.1: Refrigerant selection page

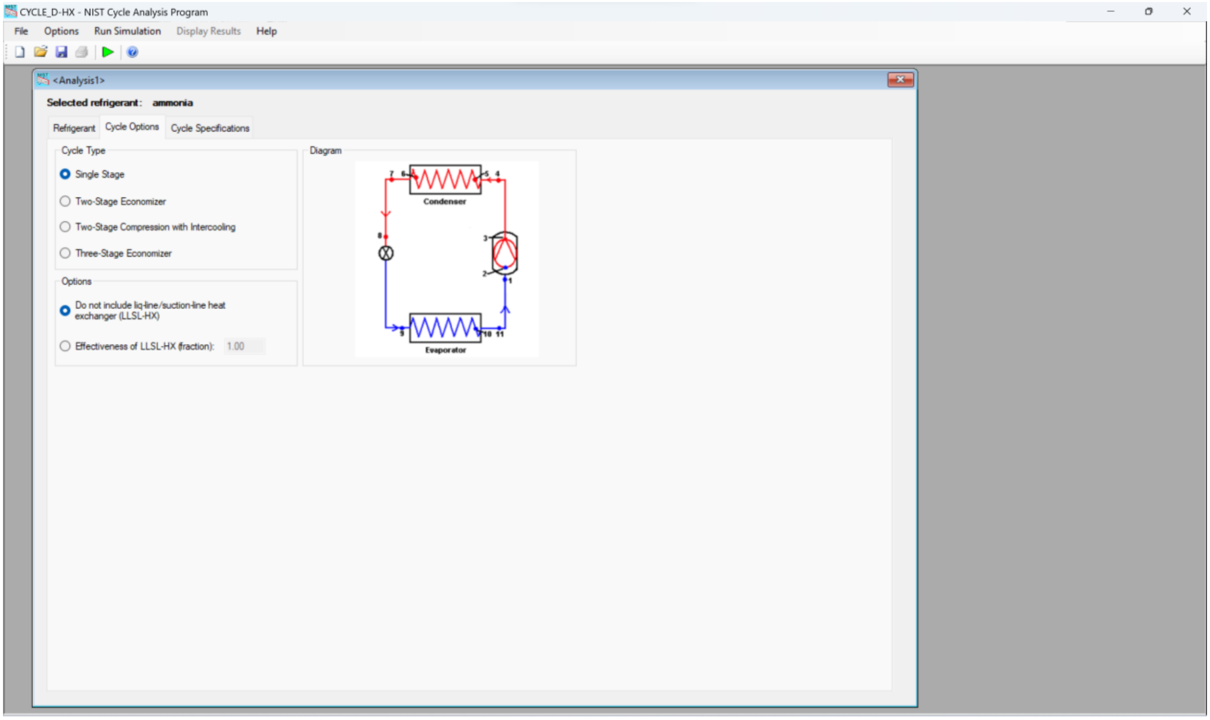

Figure 3.2: Cycle Options page

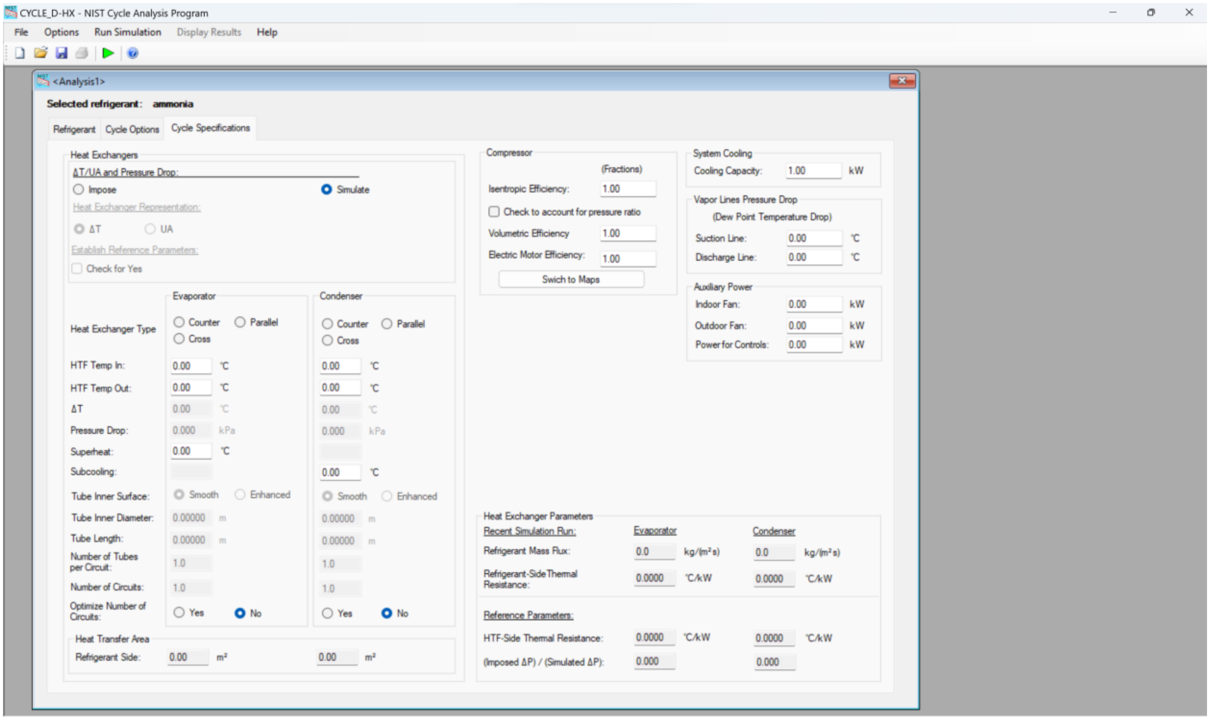

Figure 3.3: Cycle Specifications page

3.2 Refrigeration Selection

In order to achieve the aims of this project, a number of refrigerants were selected for modelling to enable a comparison between the current refrigerants and potential low GWP alternatives. These were specific to the application, as not all refrigerants were suitable for all applications. The following table summarises the selected refrigerants:

Table 3.1: Refrigerants selected for modelling.

Refrigerant	*Group*	*GWP*	*Critical Temp. (°C)*	*Critical Press. (bar)*	*Normal boiling point (°C)*	*Flammability (ASHRAE Class)*
R22	HCFC	1,960	96.15	49	-41	A1
R134a	HFC	1,300	101.06	41	-26	A1
R23	HFC	14,600	26.14	48	-82	A1
R32	HFC	771	78.11	58	-52	A2L
R404A	HFC Blend	3,922	72.20	37	-46	A1
R407C	HFC Blend	1,624.2	86.74	46.2	-43.6	A1
R410A	HFC Blend	2,088	345.28	49	-52	A1
R454B	HFC/HFO	466	77.00	54	-51	A2L
R1234yf	HFO	0.50	94.70	34	-29	A2L
R1234ze(E)	HFO	1.37	109.36	36.4	-18.9	A2L
Ammonia	Natural	0	132.41	113	-33	B2L
CO_2	Natural	1	30.98	74	-78	A1
Ethylene	Natural	4	9.20	50	-104	A3
R290	Natural	3	96.74	36	-42	A3
R600a	Natural	3	134.66	42.5	-11.8	A3

This range of selected refrigerants contains a wide variety of global warming potentials, normal boiling points, and safety classifications (Figure 3.4). This will allow the technical and environmental performance of these fluids to be assessed in several different applications.

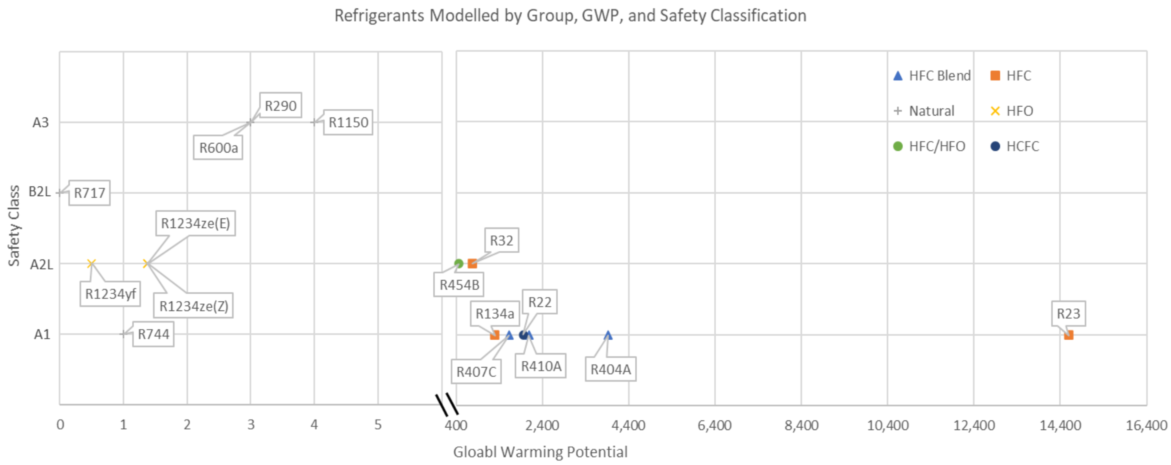

Figure 3.4: Graphical representation of selected refrigerant GWP and safety classification

3.3 Applications Modelled

A range of applications were modelled in order to show if there was any particular case in which current or next-generation refrigerants performed better. These were cryogenics, fridge freezer, air conditioning, air-source and ground-source heat pumps (ASHP and GSHP). These applications are the most common cases of refrigerant use, and each has its own operational temperature ranges. The chosen evaporator and condenser temperatures were determined by researching available literature on each application.

Cryogenic applications can reach temperatures down to 100 K (–170 $°C$), however, this requires fluids such as nitrogen which were not available in the chosen software packages, and instead, the lower limit of –100 $°C$ was used for the evaporator temperature. Domestic and industrial freezers tend to operate in the region of –18 to –25 $°C$, whilst refrigeration must be between 2 and 8 $°C$, in order to prevent bacterial growth and comply with food standards.

Air conditioning temperatures vary based on the device model and user preference but typically will be between 15 and 22 $°C$, with the lower range used for larger spaces or specialist applications such as gyms or swimming pools where considerable heat is being generated by the occupants.

In the case of the heat pump applications, the evaporator temperature for ASHPs was chosen based on the ASHRAE design conditions for selected locations (ASHRAE, 2021), and for the purpose of this project, this was chosen to be Glasgow, UK. This suggested a design condition of –4 *°C* for ASHPs. For GSHPs, the temperature tends to be more consistent throughout the year, and geological surveys of ground temperatures in the UK found that the mean ground temperature at a depth of 100 *cm* in Glasgow is 11.3 *°C* (Busby, 2015).

As these are the 'source' temperatures for the evaporator, there must be a difference in temperature in order to ensure that energy is efficiently transferred from the source to the refrigerant. Typically, this delta T is 5 *°C* (Al-Rashed, 2011).

The condenser temperature is simulated at approximately 10 *°C* greater than the sink temperature, again to ensure there is an appropriate driving force. For cryogenic, freezer and refrigeration applications, this was a minimum of 30 *°C*, as they are typically discharging heat into the ambient room. In the air conditioning application, manufactures suggest that the condenser temperature should be at least 50 *°C*, as this ensures efficient heat rejection to the warm outdoor environment (Sonne and Barkaszi, n.d.). Heat pump condenser temperature is dependent on the situation in which they are used; for example, an air-to-air or liquid-to-air system may only need to produce warm air at 25 *°C*. Typically for space heating, radiators with a large surface area or underfloor heating are used and require water to be heated to 40 – 50 *°C* depending on the building type. Finally, for domestic hot water (DHW) generation, temperatures of over 60 *°C* are necessary in order to prevent the growth of legionnaires disease.

The input data for the modelled applications were as follows:

Table 3.2: Applications modelled.

Case #	*Application*	*Cycle*	*Evaporator Temp. (°C)*	*Condenser Temp. (°C)*	*Refrigerants Modelled*
1	Cryogenic	Two-stage	-100 (-25)	-30 (30)	Stage 1: R404A, R134a, R600a, Ammonia, R1234yf, R1234ze(E), R290 Stage 2: Ethylene, R23
2	Fridge Freezer	Two-stage	-30 (0)	40	R404A, R407C, R134a, R600a, Ammonia, R1234yf, R1234ze(E), R290

Case #	*Application*		*Cycle*	*Evaporator Temp. (°C)*	*Condenser Temp. (°C)*	*Refrigerants Modelled*
3	Air Conditioning		Single stage	10	55	R410A, R32, R22, R454B, R600a, Ammonia, R1234yf, R1234ze(E), R290
4	Air-Source Heat Pump	Air Heat	Single stage	-9	25	R410A, R407C, R32, R600a, Ammonia, R1234yf, R1234ze(E), CO_2, R290
5		Space Heat	Single stage	-9	50	R410A, R407C, R32, R600a, Ammonia, R1234yf, R1234ze(E), CO_2, R290
6		DHW	Single stage	-9	70	R407C, R32, R600a, Ammonia, R1234yf, R1234ze(E), CO_2, R290
7	Ground-Source Heat Pump	Space Heat	Single stage	5	50	R410A, R407C, R32, R600a, Ammonia, R1234yf, R1234ze(E), CO_2, R290
8		DHW	Single stage	5	70	R407C, R32, R600a, Ammonia, R1234yf, R1234ze(E), CO_2, R290

3.3.1 Variables and Assumptions

Several parameters outwith the evaporator and condenser temperatures were varied. The compressor isentropic efficiency was dependent on the refrigerant, and data was collected through literature research. This is presented in Table 3.3 below.

Table 3.3: Compressor Isentropic Efficiency

Refrigerant	*Efficiency (%)*	*Reference*
R22	70%	(Payne and Domanski, n.d.)
R134a	82%	(Zhang et al., 2020)
R23	70%	
R32	70%	
R404A	82%	(Sieres et al., 2021)
R407C	82%	(Aprea and Greco, 2003)

Refrigerant	*Efficiency (%)*	*Reference*
R410A	82%	(Jackson and Brodal, 2018)
R454B	76%	(Sieres et al., 2021)
R1234yf	70%	(Qi, 2015)
R1234ze(E)	70%	(Qi, 2015)
Ammonia	78%	(EPA, 2020)
CO_2	78%	(Jackson and Brodal, 2018)
Ethylene	70%	
R290	84%	(Asdrubali and Desideri, 2019)
R600a	70%	(Asdrubali and Desideri, 2019)

Where appropriate sources were not available, it was assumed that an isentropic efficiency of 70 *%* would be achieved by a compressor, given the range of manufacturers and models available on the market. In fact, the values found in the literature varied by up to 10 *%*, and so the values extracted for this model were the best approximations. The NIST software does allow for a compressor map to be created in order to achieve a more accurate set of results; however, the necessary coefficients were not available for all the refrigerants selected. This approach was taken instead to ensure continuity across all simulations and focus on the relative refrigerant performance rather than the compressor metrics, which are constantly evolving.

The volumetric efficiency of the compressors was kept constant within each model case, as although there is literature that suggests a variation of this parameter between refrigerants, the temperature of the evaporator is a more significant influence. Studies have shown that there is a broad range of volumetric efficiency, from 50 to 90 *%*, with higher temperatures being more efficient (Chen et al., 2020). As such, the value was approximated at 60 *%* for the cryogenic and freezer models and 70 *%* for fridge-freezer, air conditioning, ASHP, and GSHP cases.

Each simulation was for a 1 *kW* cooling capacity system, except for the heat pumps, and the heat exchangers (evaporator and condenser) were set to cross-type. The air- and ground- source heat pumps were simulated using the sized system for the average UK house, at 8 *kW* for heating and 2 *kW* for hot water (Watson, Lomas and Buswell, 2021). The cycle option was kept consistent across all simulations as single-stage without heat exchanger, with the exception of the cryogenic and fridge-freezer models, which were set up as a two-stage system using CoolPack.

The saturated temperature drop was set to 2 *°C* for both the evaporator and condenser, as this was followed in the literature to account for pressure drops with these units (Bell et al., 2019). This journal also suggested superheat and supercool temperatures both set to 5 *°C* in order to prevent liquid from entering the compressor. The temperature glide of refrigerant blends was taken into account by the respective software.

All auxiliary powers were set to zero, as the analysis was focused solely on the impact of the refrigerants on the key performance indicators.

The operational hours were specific to each case, with the following table showing the assumed values.

Table 3.4: Operational Hours by Case

Case	*Operational Hours*	*Notes*
1	7,884	Assuming 90*%* runtime, to account for servicing.
2	3,504	Literature suggests fridge-freezers 'cycle on' for approximately 40 *%* of the day.[6]
3	660	No. of hours of *cooling* assumed for Glasgow, UK, using 2019 weather data. [7]
4 – 9	1,235	No. of hours of *heating* assumed for Glasgow, UK, using 2019 weather data. [6] (For calculation of Seasonal Performance Factor)
Note	For heat pump usage, the units were taken as the annual energy consumption for heating and hot water in UK households. This was 10,400 kWh and 1,460 kWh, respectively[8,9].	

[6] Morales-Fuentes, (2021)
[7] CEDA Archive. UK Daily Temperature Data. Glasgow Bishopton.
[8] Ofgem. (2023). Average gas and electricity use explained.
[9] Energy Saving Trust. (2019). Analysis of the EST's domestic hot water trials and their implications for amendments to BREDEM and SAP

3.4 Technical, Environmental and Economic Assessment Overview

The analysis of the applications detailed above resulted in large amounts of raw data, which was used to assess the performance of each refrigerant in each application. The key performance indicators for each of the three assessments were as follows:

Technical:

- Coefficient of Performance (–)
- Charge per kW capacity (*kg/kW)*
- Compressor Power (*kW*)
- Refrigerant flowrate (*kg/s*)
- Condenser & Evaporator pressures and temperatures (*bar/°C*)

Environmental:

- Direct Emissions
- Indirect Emissions
    i. Electricity requirements
    ii. Manufacture of fluid and device

Economic:

- Capital Expenditure
- Refrigerant Costs
- Electricity Costs

To provide an assessment of the overall feasibility of replacing high GWP refrigerants with low GWP alternatives, the performance in all three of the above analysis will be weighted equally. This follows similar analyses by Zhu et al. (2021) and Yang et al. (2021) on low GWP refrigerants, taking into account both the life cycle climate performance and, technical and economical performances.

3.5 Environmental Analysis

The greenhouse gas emissions associated with the refrigerant simulations were calculated through three main sources: leakage emissions, manufacturing emissions, and electricity carbon intensity. The calculation method was the same across all models, with variables tailored to the case.

3.5.1 Leakage

Calculation of the annual leakage emissions of refrigerant devices followed a method adapted from the literature (Yang et al., 2021), which is represented by the following equation:

$$E_{leak} = GWP * C * ALR * EOL \qquad \left(\frac{kg_{CO2e}}{yr}\right) \tag{3-1}$$

Where:

C = Refrigerant Charge (kg)

ALR = Annual Leakage Rate ($\%$)

EOL = End of life leakage ($\%$)

The ALR was found from well-cited literature for each application, and the approximate refrigerant charge per kW of cooling capacity was also sourced for each refrigerant. The EOL is dependent on the methods of disposal for the device, and the annualised figure depends on the device's lifespan. As the aim of this project is to directly compare the refrigerants, this value was kept constant across all models and refrigerants, using an end-of-life discharge of 15 $\%$ and a lifetime of 15 years, based on life cycle analysis literature (Yang et al., 2021).

Table 3.5 details the values for ALR used in this project.

Table 3.5: Annual Leakage Rates by application

Case	Annual Leakage Rate (%)	Reference
1	1 %	(IPCC, 2005)
2	10 %	(UNDP, 2022)
3	5 %	(UNDP, 2022)
4 – 9	3.48 %	(UK Gov., 2014)

The amount of refrigerant charge required for a 1 kW simulation is shown in Table 3.6.

Table 3.6: Charge requirements by refrigerant

Refrigerant	*Charge per kW (kg)*	*Reference*
R22	0.409	(Rajendran, 2011)
R134a	0.667	(Andrew Pon Abraham and Mohanraj, 2018)
R23	0.409	
R32	0.183	(Jin et al., 2023)
R404A	0.500	(Heredia-Aricapa et al., 2020)
R407C	0.389	(Sieres et al., 2020)
R410A	0.474	(Inshi etal., 2002)
R454B	0.296	(Shen, Li and Gluesenkamp, 2022)
R1234yf	0.377	(Rajendran, 2011)
R1234ze(E)	0.545	(Honeywell, 2016)
R717	0.260	(Gilmour, 2014)
R744	0.157	(Li et al., 2023)
R1150	0.033	(Jones, Wolf, and Kwark, 2022)
R290	0.060	(Fraunhofer, 2022)
R600a	0.033	(Jones, Wolf, and Kwark, 2022)

3.5.2 Manufacture Emissions

The manufacturing of both the refrigerants and the device is not without carbon dioxide emissions. In order to assess the full lifecycle emissions of each case, these emissions were quantified through the following method.

Data on the emissions associated with the production of each unit of refrigerant was collected and presented in Table 3.7 below.

Table 3.7: Refrigerant Manufacture emissions

Refrigerant	*Production Emissions ($kg_{CO2}/kg_{refrigerant}$)*	*Reference*
R22	390	(Spatz and Yana, 2004)
R134a	8	(Pspasavva, Hill, and Andersen, 2010)
R23	390	(Spatz and Yana, 2004)
R32	7.2	(IRR, 2015)
R404A	16.7	(IRR, 2015)

Refrigerant	*Production Emissions ($kg_{CO2}/kg_{refrigerant}$)*	*Reference*
R407C	18	(Spatz and Yana, 2004)
R410A	10.7	(IRR, 2015)
R454B	18	(Spatz and Yana, 2004)
R1234yf	13.7	(Baral, Minjares, and Urban, 2013)
R1234ze(E)	13.7	(Baral, Minjares, and Urban, 2013)
R717	2.4	(IEA, 2021)
R744	3.7	(Pspasavva, Hill, and Andersen, 2010)
R1150	1.56	(Keller, Lee, and Meyer, 2020)
R290	2	(Spatz and Yana, 2004)
R600a	5.6	(Spatz and Yana, 2004)

It should be noted that several of the references are more than 10 years old, so manufacturing practices are likely to be less carbon-intensive at the time of this project. This was due to a lack of available well-cited reports and manufacturers being unwilling to publish detailed information on the production of their refrigerants.

The manufacture of the refrigeration device is also to be considered in the environmental analysis, as this can contribute over 100 *kg* of CO_2 to the lifecycle analysis. Below is a breakdown of the materials and associated emissions of a refrigeration device (Yang et al,. 2021).

Table 3.8: Carbon emissions from the unit

Material	*Composition of Refrigeration Device (%)*	*Virgin Emissions ($kg_{CO2}/kg_{material}$)*	*Recycling Emissions ($kg_{CO2}/kg_{material}$)*
Steel	46	1.8	0.07
Aluminium	12	12.6	
Copper	19	3	
Plastics	23	2.8	0.015

Using the weighted composition, the emissions associated with manufacturing the unit (UME) is approximately 3.590 kg_{CO2}/kg_{unit}.

The total mass of the device is dependent on the refrigeration or heating capacity, but for the purpose of this analysis, the total device mass was kept to 70 *kg* for all cases, based on typical manufacturer specifications for fridge-freezers (LG), integrated air-conditioning units (Samsung), and heat pumps (Grant).

The manufacturing emissions were then calculated as follows:

$$E_{man} = (GWP * RME * C) + (m * UME) \qquad \left(\frac{kg_{CO2e}}{yr}\right) \tag{3-2}$$

Where:

RME = Refrigerant Manufacturing Emissions ($kg_{CO2}/kg_{refrigerant}$)

m = mass of unit (*kg*)

UME = unit manufacturing emissions (kg_{CO2}/kg_{unit})

This figure was annualised, using a 15-year lifetime, for comparison with the other costs that were calculated as part of the analysis.

3.5.3 Electricity Carbon Intensity

The carbon dioxide emissions that are indirectly produced as a result of the energy consumption of the refrigeration device is another key source for the environmental analysis. The calculation of this parameter is straightforward, using data from the National Grid on the carbon intensity of the electricity generation in the UK, the power of the compressor and the running hours per year of the device.

In 2022, the carbon emissions associated with each kilowatt-hour of energy produced in the UK was 182 gCO_2/kWh. Across the year, this value is variable depending on the amount of renewable energy that is generated at any given time, and the 'greenest' day in 2022 saw an average of 39 gCO_2/kWh, whilst the most polluting was 280 gCO_2/kWh. As this value is expected to decrease due to the progressive decarbonisation of the UK's electricity generation, a sensitivity analysis was conducted using a variety of figures for this parameter. The UK Gov. Department for Business, Energy and Industrial Strategy (BEIS) released a report in 2020 detailing the predicted fall in grid carbon intensity between 2020 and 2040, with the forecast that in 2030 and 2040, the carbon intensity will be 90 and 67 gCO_2/kWh, respectively (UK Gov. 2020a). Further modelling also found that based on several possible scenarios for the future electricity generation mix, the minimum system cost would be between 5 and 25 *gCO_2/kWh* in the year 2050 (UK Gov. 2020b). This was concluded through a detailed analysis of hundreds of cases which included varying compositions of nuclear, hydrogen, and carbon capture utilisation and storage (CCUS), along with the current wind and solar projections. These four figures were considered for the sensitivity analysis along with the 2022 carbon intensity (Table 3.9).

Table 3.9: Electricity Carbon Intensity Sensitivity

#	*Emissions (gCO_2/kWh)*	*Note*
1	182	Current Intensity
2	90	2030 Forecast
3	67	2040 Forecast
4	25	Upper Economic Bound 2050
5	5	Lower Economic Bound 2050

The electricity indirect emissions were then calculated as follows:

$$E_{elec} = I_{grid} * E_{consumed} \qquad \left(\frac{kg_{CO2e}}{yr}\right) \tag{3-3}$$

Where:

I_{grid} = Carbon Intensity of the UK grid (*$kgCO_2/kWh$*)

$E_{consumed}$ = Energy consumed per year by the compressor (kWh)

3.6 Economic Analysis

The final analysis undertaken was the economic analysis. This was used to complete the overall objective of assessing the feasibility of replacing current fluids with low GWP alternative refrigerants through a three-pronged analysis. Several factors contribute to the economic performance of a refrigeration system, and for this project, the following factors were considered: the capital expenditure of the systems, refrigerant costs, and electricity costs.

3.6.1 Capital Expenditure

The capital expenditure of a refrigeration system (or simply CAPEX) is the amount of money needed to purchase the equipment that will fulfil the heating or cooling requirements. This value varies depending on several factors such as manufacturer brand, country of purchase, and size of the system. The value will also increase or decrease with rising or falling demands from the market and over time, may change with advancements in technology. Due to a lack of publicly available data, in order to keep the analysis consistent across the cases, only the size of the system was taken into account, and the values per *kilowatt* of capacity for each application were sourced from literature and online vendors (Table 3.10).

Table 3.10: CAPEX for each application

Case #	*CAPEX (£/kW)*	*Reference*
1	1,731	(Luyben, 2017)
2	1,000	Typical UK Classic Fridge-Freezer (Samsung, 2023)
3	700	(UK DECC, 2020)
4-6	1,100	(Myers et al., 2018)
7-9	1,650	(Myers et al., 2018)

3.6.2 Refrigerant Costs

The costs of each refrigerant were collected on a price *per-kilogram* basis from online retailers or research papers if publicly available (Table 3.11). This information was combined with the refrigerant charge required for each case to determine the overall cost of the refrigerant fluid.

Table 3.11: Refrigerant Costs

Refrigerant	*Price* (*£/kg$_{refrigerant}$*)	*Reference*
R22	51.11	(Angi, 2023)
R134a	25.52	(Alpha Wholesale, 2023)
R23	4.70	(Note: Not available in the UK, price taken from Indian market)
R32	22.13	(Alpha Wholesale, 2023)
R404A	23.40	(Alpha Wholesale, 2023)
R407C	26.72	(Alpha Wholesale, 2023)
R410A	23.43	(Alpha Wholesale, 2023)
R454B	46.39	(Alpha Wholesale, 2023)
R1234yf	103.00	(Lamb, 2016)
R1234ze(E)	74.57	(BHL, 2023)
R717	8.23	(BOC online, 2023)

Refrigerant	*Price ($£/kg_{refrigerant}$)*	*Reference*
R744	2.77	(Wygonik and Goodchild, 2011)
R1150	29.06	(BOC online, 2023)
R290	14.00	(Gas UK, 2023)
R600a	16.00	(Gas UK, 2023)

It should be noted that the purchase of most refrigerants requires a valid trading licence, and so the data was difficult to obtain from a range of sources, hence the values found must be used only as a best approximation. Similarly, data from literature that is more than three years old may be outdated due to market changes and advancements in the respective production processes.

3.6.3 Electricity Prices

The consumption of electricity by the compressor is another contributor to the economic performance of each model. This parameter is closely related to the technical performance of the refrigerant, as a device with a greater COP will require less electrical energy, and so the costs associated with powering the device are lower. Due to several macroeconomic factors, the price of electricity in the UK has experienced a sharp increase in the past 18 months, with average consumer prices in the region of 30 *p/kWh*, at the time of writing (Ofgem, 2023). This is much greater than the historical average, ranging between 10 – 20 *p/kWh*. Similar to the costs associated with the manufacturing and refrigerants for the devices, the electricity prices are likely to continue to fluctuate, and as such, a sensitivity analysis was conducted on this variable (Table 3.12).

Table 3.12: Electricity Price Sensitivity

#	*Price (p/kWh)*	*Note*
Current	30.0	Current Price
1	15.9	2010 – 2020 Average (BEIS, 2023)
2	13.8	2050 Forecast (NIC, 2018)

The total cost associated with each case was then calculated using the following formula:

$$C_{annual} = \frac{(C_{CAPEX} + C_{refrigerant})}{n} + E_{consumed\ p.a} * \frac{E_{price}}{100} \qquad \left(\frac{£}{yr}\right) \tag{3-4}$$

Where:

C_{annual} = Annualised cost of the device (*£/year*)

C_{CAPEX} = Capital expenditure of model device (*£*)

$C_{Refrigerant}$ = Cost of refrigerant (*£*)

$E_{consumed\ p.a}$ = Energy consumed each year (*kWh/year*)

E_{price} = Electricity unit price (*p/kWh*)

n = assumed device lifetime (*year*)

4. Results and Discussion

4.1 Sample results from NIST Cycle_D-HX

This section will detail the key outputs delivered by NIST Cylce_D-HX for the air conditioning application model. All result tables for other applications can be found in the *Appendix*.

Below are the schematic diagrams for the ammonia-based air conditioning model, annotated with both temperature (°*C*) (Figure 4.1) and pressure (*bar*) (Figure 4.2). These figures show the set-up of the model in reflection of a real-life device and mimic the same basic cycle described in the *Literature Review* chapter.

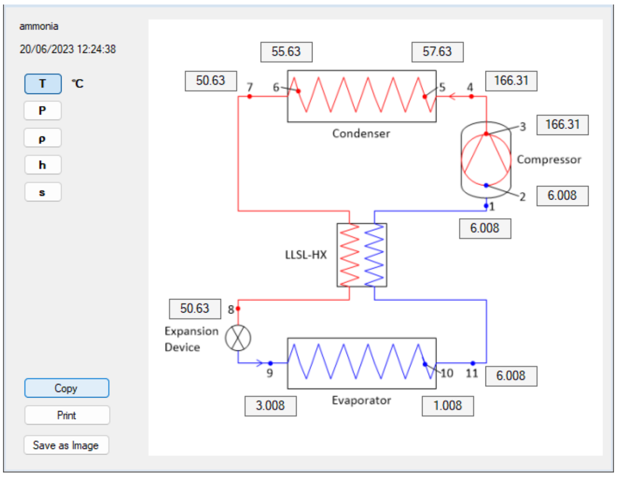

Figure 4.1: Ammonia AC Temperature schematic diagram

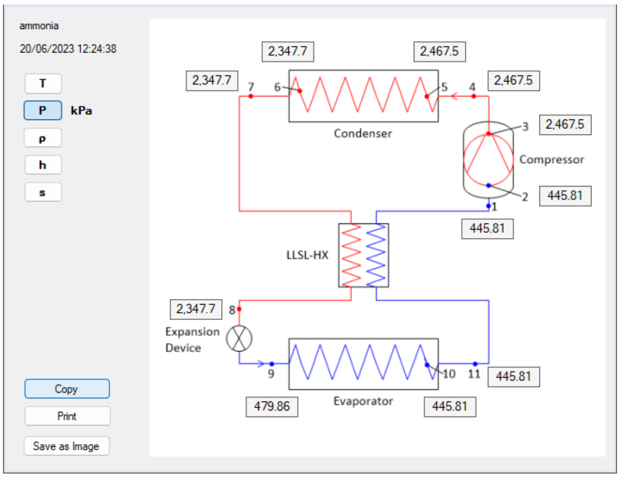

Figure 4.2 Ammonia AC Pressure schematic diagram

In this example result output, the ammonia refrigerant behaves as expected throughout the cycle; beginning at state point 1, the fluid entering the compressor is at 6 °*C* and 4.458 *bar*, before experiencing a great increase in temperature to 166.31 °*C* after being compressed to 24.675 *bar*. The superheated fluid then rejects heat into the outdoor environment through a phase change in the condenser at 55 – 57 °*C* (a temperature drop is modelled to incorporate assumed pressure losses, despite the use of an azeotropic fluid), and supercooled by 5 °*C*. The expansion device reduces the fluid pressure from 23.477 *bar* to 4.7986 *bar*, in order to allow evaporation at 3 °*C*. The evaporation of the refrigerant is enabled through the extraction of heat from the indoor environment, and so a cooling effect is provided by the air conditioning device.

The refrigeration cycle is also represented by the following thermodynamic diagrams.

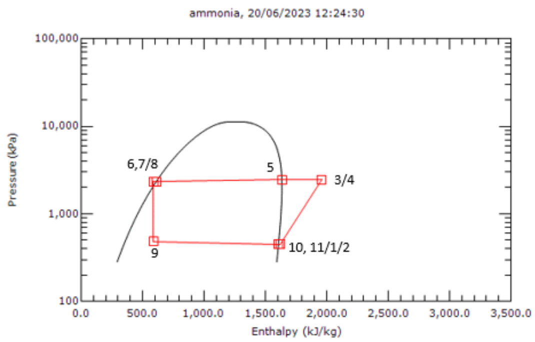

Figure 4.3: Ammonia AC P-h diagram

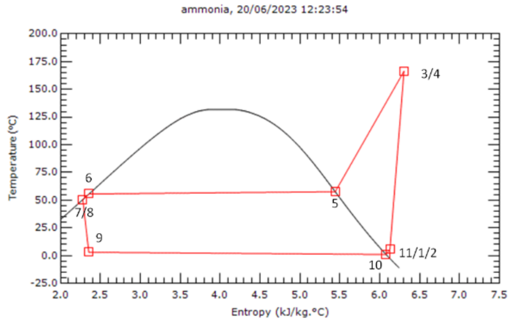

Figure 4.4: Ammonia AC T-s diagram

These figures show the change of state that occurs across the cycle, as the black line represents the saturated liquid-vapour state, with the left region being liquid only and the right region being vapour only. The T-s diagram (Figure 4.4) shows that the compressor causes the fluid to reach critical temperatures at the high pressure generated, as the state points 3 and 4 are above the peak of the saturation line.

The results from NIST Cylce_D-HX are also given in tabular form (Figure 4.5), which was then used to extract the technical data to MS Excel. This table clearly states the data required for comparison between the refrigerants, such as coefficient of performance, compressor power, refrigerant mass flowrate, and the physical parameters at each state point.

```
----------------------------------Input Data--------------------------------

Refrigerant: ammonia
System cooling capacity (kW)     =  1.00

Compressor:
     Isentropic efficiency            =  0.780
     Volumetric efficiency            =  0.500
     Electric motor efficiency        =  1.000

Heat Exchangers:                                 Evaporator       Condenser
     Configuration                        =           Cross           Cross
     HTF inlet temperature            (C) =           10.00           50.00
     HTF outlet temperature           (C) =            5.00           55.00
     ΔT                               (C) =            5.00            5.00
     Saturation temperature drop      (C) =            2.00            2.00
     Superheat/Subcooling             (C) =            5.00            5.00

Effectiveness of the llsl heat exchanger = 0.00

Saturation temperature drop in the suction line   (C) =   0.0
Saturation temperature drop in the discharge line (C) =   0.0

Parasitic powers (kW): indoor fan  = 0.000      outdoor fan  = 0.000
                       controls    = 0.000


----------------------THERMODYNAMIC CYCLE RESULTS---------------------------

    STATE                  T         P        H         V         S        XQ
                          (C)      (kPa)   (kJ/kg)  (m^3/kg)  kJ/(kg C)

 1  Compr. shell inlet    6.0     445.8   1457.4   2.86E-1   5.36922    1.000
 2  Cylinder inlet        6.0     445.8   1457.4   2.86E-1   5.36922    1.000
 3  Cylinder outlet     166.3    2467.5   1797.2   8.16E-2   5.54498    1.000
 4  Condenser inlet     166.3    2467.5   1797.2   8.16E-2   5.54498    1.000
 5  Cond. sat. vapor     57.6    2467.5   1470.8   5.19E-2   4.68374    1.000
 6  Cond. sat. liquid    55.6    2347.7    450.2   1.81E-3   1.59862    0.000
 7  Condenser outlet     50.6    2347.7    424.6   1.78E-3   1.52033    0.000
 8  Exp. device inlet    50.6    2347.7    424.6   1.78E-3   1.52033    0.000
 9  Evaporator inlet      3.0     479.9    424.6   4.91E-2   1.59600    0.184
10  Evap. sat. vapor      1.0     445.8   1444.1   2.79E-1   5.32117    1.000
11  Evaporator outlet     6.0     445.8   1457.4   2.86E-1   5.36922    1.000

    Work = 339.78 kJ/kg    Qevap =1032.83 kJ/kg    Qcond =1372.61 kJ/kg
                           COPc  =   3.040         COPh  =   4.040
    Two-phase glide:  evaporator =   2.0 C     condenser =   2.0 C
    Condenser superheat          = 108.7 C     P(3)/P(2) =   5.53
    Liquid line subcooling due to llsl heat transfer     =   0.0 C
    Suction vapor superheat due to llsl heat transfer    =   0.0 C
    Volumetric capacity:     cooling                 heating
       @ vol. eff. = 0.50    1805.7 kJ/m^3           2399.8 kJ/m^3


---------------------COMPRESSOR AND SYSTEM RESULTS---------------------------

Compressor power            =   0.329 kW
Compressor COP: COPc        =   3.040                COPh =   4.040
Compr. suc. vol. flow rate  =   0.997 m^3/h

Refrigerant mass flow rate  = 9.6822E-04 kg/s  Total power =   0.329 kW
```

Figure 4.5: Ammonia AC Summary Table

In this ammonia air conditioning example, it can be seen that the COP for cooling is 3.040, requiring a compressor power of 0.329 *kW*, and utilising a mass flowrate of 9.6822 x 10^{-4} *kg/s*. The maximum temperature and pressure of the fluid are 166.3 *°C* and 24.675 *bar*, respectively.

4.2 Sample results from CoolPack

This section will describe a sample result from the fridge-freezer case, where a single fluid and circuit are required to provide cooling at two separate temperatures. The CoolPack program provides a simple tool to simulate this as a two-stage refrigeration cycle, with the low-temperature stage at –30 *°C* and the high-temperature stage at 0 *°C*, with a rejection temperature of 40 *°C* into the ambient air. The following figure shows the input page of the program, where it is possible to configure the cycle specification.

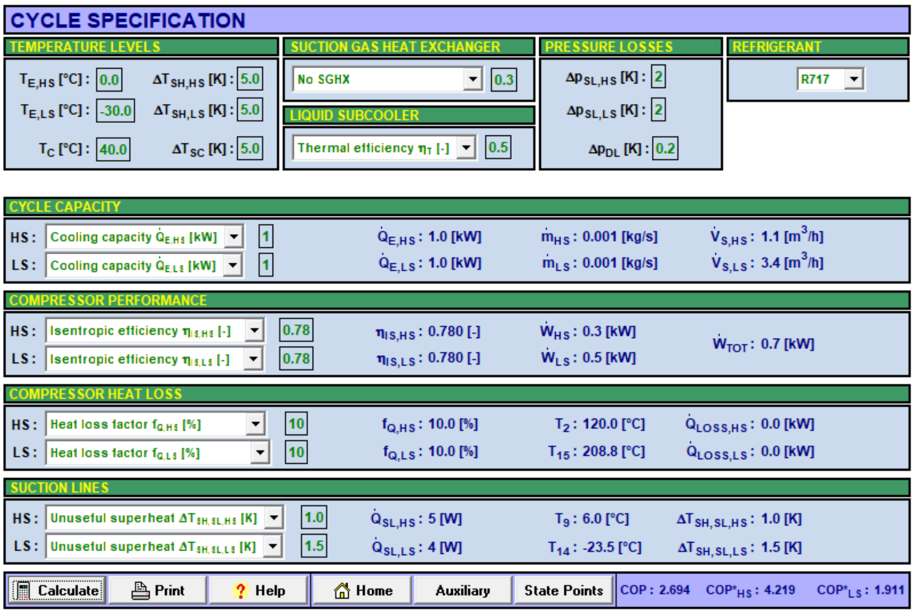

Figure 4.6: CoolPack Cycle Specification Interface

The assumptions outlined in *Section 3.3.1* are implemented here in the temperature levels, pressure losses and compressor performance boxes. All parameters are kept constant between the different refrigerant simulations with the exception of compressor isentropic efficiency, which is tailored to the fluid. Compressor heat losses and suction line inputs were left untouched from the default given by the program. The green text in black boxes represents user-defined variables, and the bold blue text is the output results of the model simulation. Another results page shows the logP– h diagram, as can be seen in Figure 4.7.

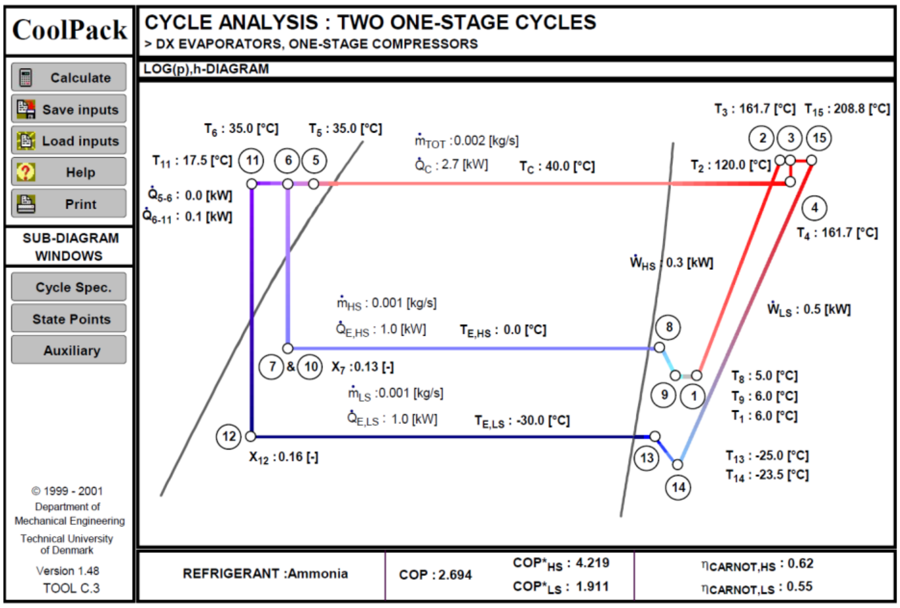

Figure 4.7: Ammonia Fridge-Freezer CoolPack diagram

The red central horizontal line represents the condenser heat rejection to the environment at a rate of 2.7 *kW*, whilst the middle horizontal line shows the high-temperature evaporator cooling capacity of 1 *kW* in the fridge compartment. The lower horizontal dark blue line represents the evaporator in the freezer, also with a cooling capacity of 1 *kW*.

The key performance indicators from this output are the COP_C at 2.694, total compressor work of 0.742 *kW*, and a maximum temperature of 208.8 *°C*.

4.3 Processed Results

4.3.1 Case 1: Cryogenic

Technical:

The cryogenic model was performed using the input parameters detailed in *Section 3.3*, with the first stage of the cycle utilising a variety of refrigerants capable of cooling at temperatures down to – 30 *°C* from an ambient environment. The technical performance of these refrigerants is well described by Figure 4.8, which shows the cooling COP and mass flowrate required of each simulated fluid. Here it is clear why R134a has thus far been one of the most popular refrigerants in this application, as it achieves the highest COP_C (2.596), although it is very closely followed by R600a (2.593). It is also shown that all the natural refrigerants outperform the HFC blend R404A, both in terms of a greater COP_C and also utilising a smaller refrigerant flowrate. All of the natural refrigerants were found to have a COP_C at least 7 *%* greater than R404A, whilst also using less than 50 *%* of the refrigerant mass. This means the device and compressor sizing can be made smaller and may lead to cost savings in the manufacturing process. However, the hydrofluoro-olefins perform comparatively poorly, with a COP_C approximately 16 *%* less than R134a, and although they require a smaller mass flowrate, this advantage is not significant enough to overcome the lack of cooling efficiency.

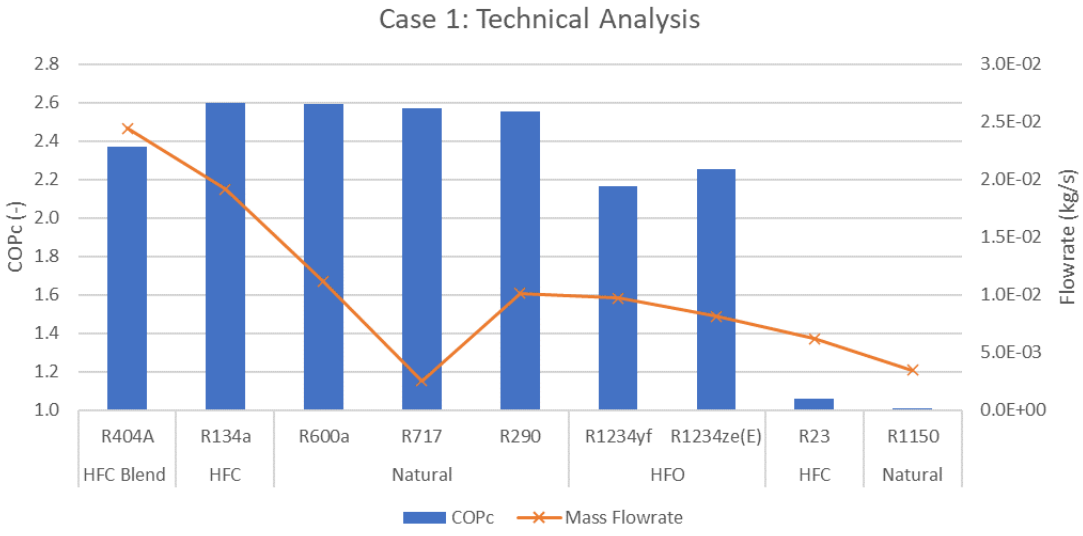

Figure 4.8: Case 1 Technical Performance

The second analysis of operational performance is the physical conditions experienced within the refrigerant cycle. In particular, the condenser pressure and maximum temperature can have an impact on the suitability of the device to be successful on a wide scale. Higher temperatures and pressures require more advanced materials and construction methods, which can significantly increase the capital costs of the device, and it is, therefore, beneficial to perform the desired application with a lower maximum temperature and pressure system. Figure 4.9, shows that R600a has the lowest maximum temperature at 39.1 *℃* whilst also having the lowest maximum pressure at 4.064 *bar*. The other simulations yielded operating pressures in the range of 7 – 14 *bar*, which is well within the typical operating limits of mass-produced devices. Similarly, the maximum temperature of most other models was between the range of 45 – 65 *℃*. However, the maximum temperature of the R717 model was far in excess of the other refrigerants, at 159 *℃*, which would likely restrict the application of this refrigerant to highly specialist devices that encompass a strict safe operating procedure.

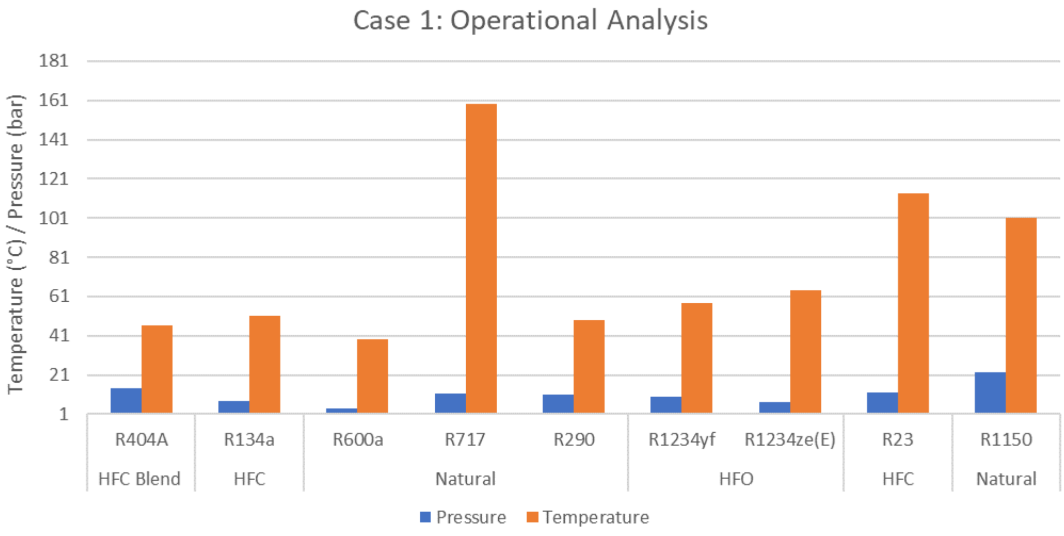

Figure 4.9: Case 1 Operational Performance

The second stage of the cryogenic model utilised two other refrigerants, which have the capacity to cool the cryogenic chamber to temperatures of –100 *°C*. The fluids capable of this extremely low temperature were R23 and R1150 (ethylene). The following figures (Figure 4.10, Figure 4.11) show that the refrigerants are both similar in their performance, although R23 can perform the application with a 5 *%* greater COP_C. However, in absolute terms, this is a difference of 0.051. Both of the simulations show a maximum pressure and temperature that is within the capabilities of widespread materials.

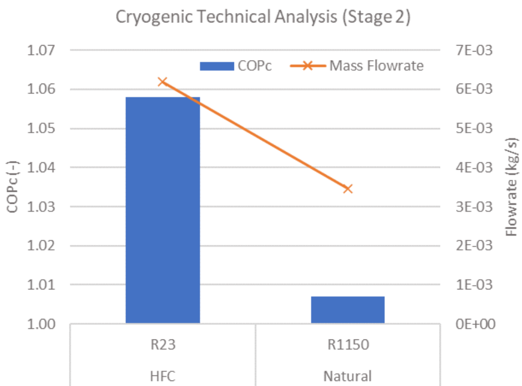

Figure 4.10: Case 1 (Stage 2) Technical

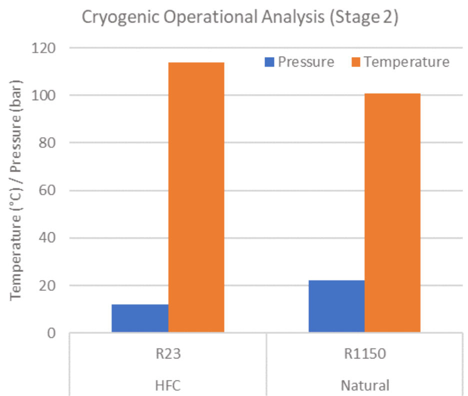

Figure 4.11: Case 1 (Stage 2) Operating

Environmental:

The figure below (Figure 4.12) shows the environmental performance of each refrigerant in the cryogenic model. It can be seen that the HFC and HFC blend had significant direct emissions due to refrigerant leakage, along with their high GWP. In comparison, the emissions of the natural and HFO gases were dominated by the indirect emissions from electricity consumed by the compressor. This was to the advantage of these groups, as the slight differences in COP_C meant there was little difference in the indirect emissions of R134a in comparison to the natural gases, and the lack of direct emissions improved their environmental impact in comparison.

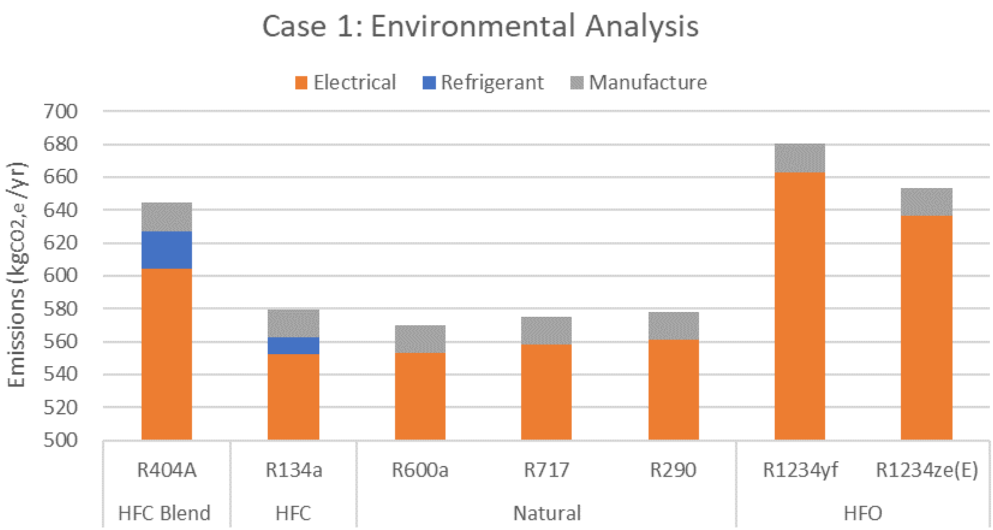

Figure 4.12 Case 1 Environmental Analysis

The HFO R1234yf has the largest environmental impact, despite its low GWP (0.50), as the compressor required larger amounts of energy across the year, due to the low COP_C, as described in the technical analysis above. In this simulation, for a 1 kW cooling stage of the cryogenic model, R600a performed the best, with emissions of approximately 9.6 kg of CO_2,e per year less than R134a (1.7 $\%$ reduction).

The analysis for stage 2 of the cryogenic model yielded similar results, with the natural refrigerant R1150 outperforming the HFC R23 (Figure 4.13). This was a consequence of the extremely large GWP of R23 (14,600), which contributed 68 kg of CO_2 per year, in comparison to 0.0015 kg for R1150. The indirect emissions from electricity consumption was lower in the R23 simulation, due to the greater COP_c, but the difference was small, and not enough to overcome the direct emissions. The manufacture of R23 is also more carbon intensive than R1150, and contributed 27.39 $kg_{CO2},e/year$, in comparison to 16.76 $kg_{CO2},e/year$. Even though the gas is an extremely potent greenhouse gas, the direct emissions contributed only 4.6 $\%$ of the annual emissions.

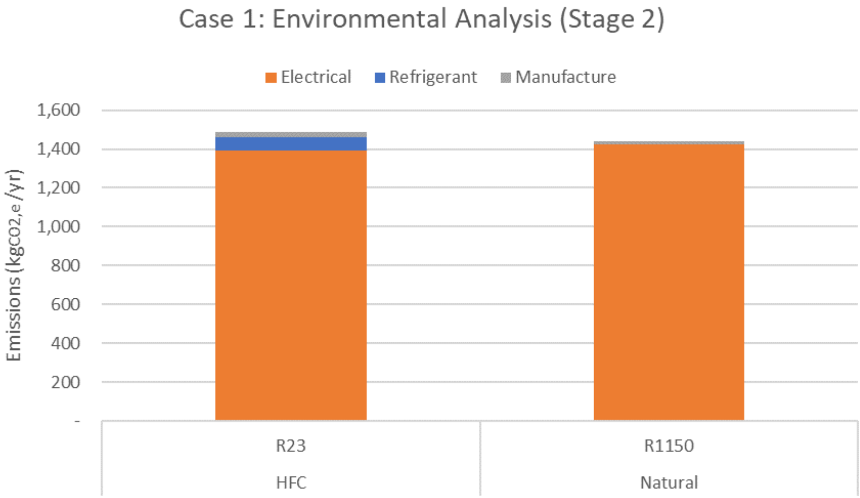

Figure 4.13: Case 1 Environmental Analysis (Stage 2)

Economic:

The economic analysis of the cryogenic model shows that the annual costs are dominated by the purchase of electricity in all the refrigerants simulated. The refrigerant expenditure is negligible in comparison for all gases, with the exception of the HFOs R1234yf and R1234ze(E), due to their exceptionally high production costs, and in the case of R1234yf, the cost of refrigerant is 7.7 % of the annual expense. It is also clear that the second stage is much more expensive than the first stage because of the lower COP_C achieved by the cryogenic stage leading to increased electricity consumption at the compressor. The R23 refrigerant is the more economical choice in comparison to R1150, as it is approximately 3.2 % cheaper to operate.

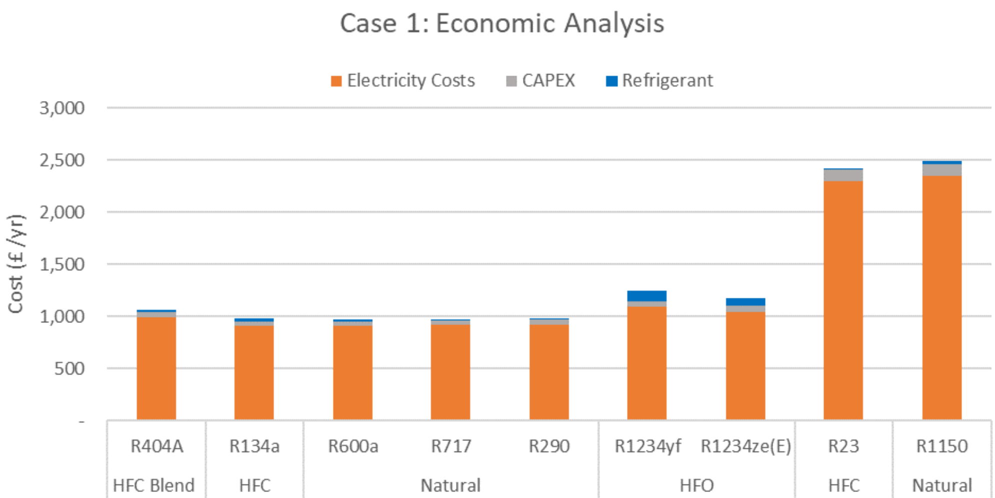

Figure 4.14: Case 1 Economic Analysis

Overall:

The feasibility of replacing the high GWP refrigerants is assessed by combining the performance of the refrigerants in all three analyses.

In the cryogenic application of the modelled refrigerants, three gases stood out in their overall performance: R134a, R600a, and R717 (Table 4.1). There was little to separate their technical or economic performance, although R600a was the most environmentally friendly refrigerant. This should lead to the conclusion that the optimal choice for stage 1 of a cryogenic refrigeration system is R600a, as it performed the best in the economic and environmental analyses whilst also second in the technical analysis, with a COP_C only 0.116% poorer than R134a.

Table 4.1: Case 1 Overall Analysis

Ranking	HFC		Natural			HFO	
	R404A	R134a	R600a	R717	R290	R1234yf	R1234ze(E)
Technical	5	1	2	3	4	7	6
Environmental	5	4	1	2	3	7	6
Economic	5	3	1	2	4	7	6
Overall Score	15	8	4	7	11	21	18

For the analysis of stage 2, the refrigerant R23 performed marginally better in the technical and economic analyses by 5.0 and 3.2 %, respectively. However, the natural refrigerant, R1150, performed 3.6 % better in the environmental analysis, and although this may not outweigh the difference in the other analysis, it is likely dependent on the views of the consumer. Given the shift in EU regulation to phase out gases such as R23, the low GWP alternative can be determined as a feasible replacement due to the close comparison in the other two analyses.

4.3.2 Case 2: Fridge – Freezer

Technical:

The technical results of the fridge-freezer model are presented in Figure 4.15, R407C is the only addition to the Case 1 refrigerants, as it is available at this temperature range. It can be seen that similar to Case 1, R600a and R134a produce the more desirable results, although R600a is able to perform using a smaller flowrate of refrigerant, and with a 4.2 % increase in COP. The COP_C of R404A and R717 are lower in comparison to the other natural and HFC gases, and their relative performance is much reduced compared to Case 1. Again, it is found that the HFOs are the most inefficient group of gases at this temperature range, as R1234yf has a COP_C 27 % poorer than the best-performing refrigerant, whilst also requiring the largest refrigerant mass flowrate.

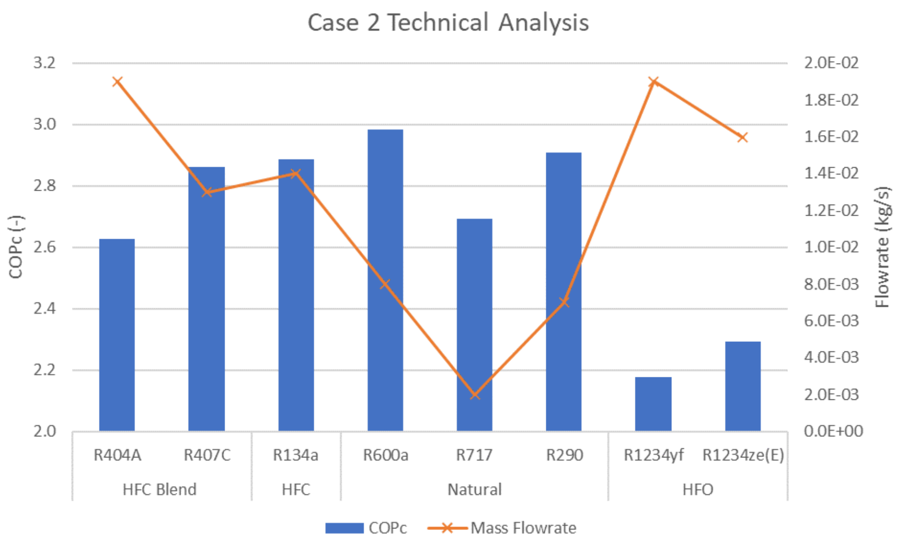

Figure 4.15: Case 2 Technical Analysis

The operational performance of the refrigerants can be seen in Figure 4.16, where R600a has the most attractive results. The maximum cycle temperature reaches 47.8 *°C* and the maximum pressure is 5.31 *bar*, so there is less risk of accidental leakage, whilst also requiring less expensive materials to contain the gas. This is an advantage to the gas, as it is highly flammable, so these conditions improve its perceived safety with respect to other gases; for example, R717, which is operating under 15.67 *bar* and 161.7 *°C*, whilst also being mildly toxic and flammable. The other refrigerants simulated operate under similar conditions, within the range of 9 – 18 *bar* and 57.0 to 69.7 *°C*.

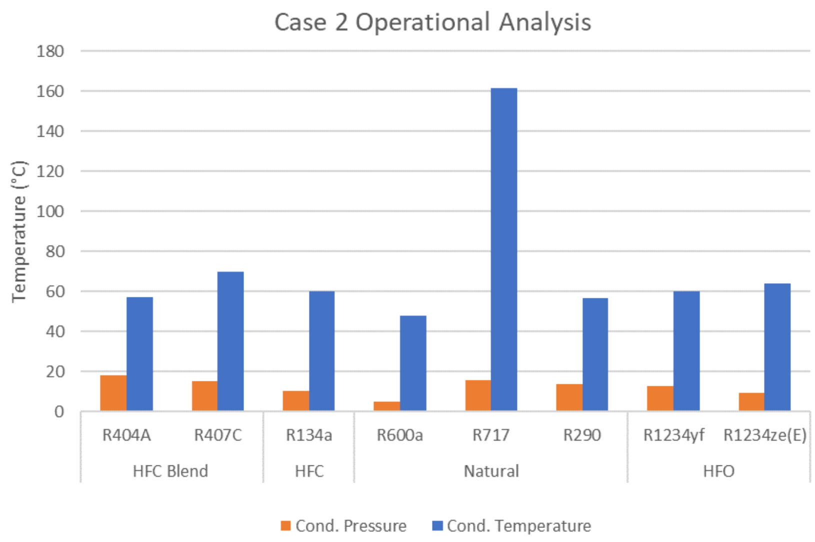

Figure 4.16: Case 2 Operational Analysis

Environmental:

The environmental analysis of this case clearly shows that R600a is again the best-performing refrigerant, with an annual emission of 427.86 *$kgCO_2/year$* (Figure 4.17). In fact, the best three refrigerants in this analysis are the natural gases, due to their low GWP, reducing annual emissions by up to 12 *%* on the HFC R407C. Similar to the previous Case, the HFOs performed poorly in their environmental impact, due to the low COP_C achieved in the simulation. The indirect emissions from electrical energy consumption alone were more than the total emissions of the high GWP refrigerants R407C and R134a, and so these gases are an unattractive environmental alternative for this application.

The manufacturing emissions for all refrigerants are responsible for a very small proportion of the overall annual emissions ranging from 0.23 *%* for R717 to 1.48 *%* for R404A.

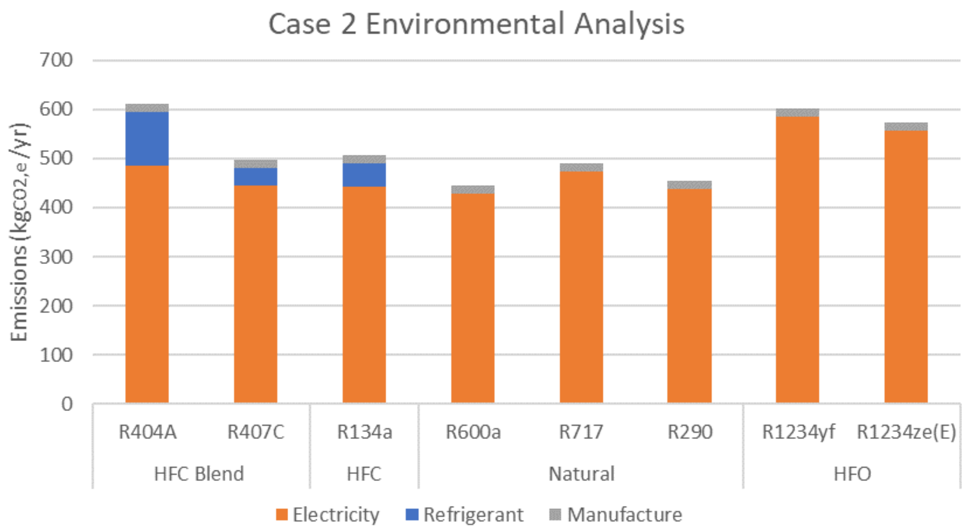

Figure 4.17: Case 2 Environmental Analysis

Economic:

The economic analysis of Case 2 shows that R600a again performs the best of the simulated refrigerants, with and annual expense of £750.06 (Figure 4.18). This is approximately 2.5 % less than the next best (R290) and more than 25 % better than R1234yf. There was also a small improvement of 4.3 % when compared to R407C; however, R717 was more expensive than two of the three HFCs. The annual expense of all simulations was dominated by the cost of electricity for the compressor, although the proportion of the total expense was reduced compared to Case 1 due to the reduced operating hours per year.

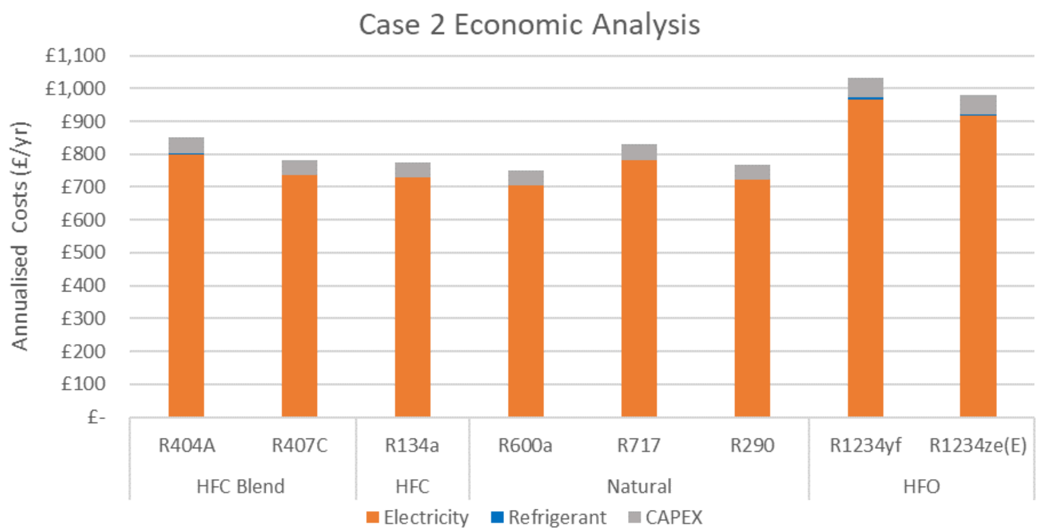

Figure 4.18: Case 2 Economic Analysis

Overall:

The best-performing refrigerant in all three analyses was R600a, closely followed by R290, and so these would prove suitable alternatives to the popular HFC blend R407C and the HFC R134a (Table 4.2). This is consistent with current trends, as R600a and R290 have become popular fridge-freezer refrigerants in Europe over the past decade, although this is not, as of yet, followed in other regions. Ammonia (R717) performed well in the environmental analysis due to its GWP of 0, and if high-specification materials, to contain the high condenser temperature, were available it would also be a suitable alternative to the HFCs. This is the case in industrial fried-freezers or large chiller rooms for supermarkets, as the refrigerant charge for these systems is often much larger than can be deemed safe for the hydrocarbon gases (R600a and R290). Regular maintenance by trained personnel enables the safe operation of R717, as there is a much-reduced risk of exposure to the gas than in domestic applications, where there is likely no maintenance schedule.

Table 4.2: Case 2 Overall Analysis

Ranking	HFC			Natural			HFO	
	R404A	R407C	R134a	R600a	R717	R290	R1234yf	R1234ze(E)
Technical	6	4	3	1	5	2	8	7
Environmental	8	4	5	1	3	2	7	6
Economic	6	4	3	1	5	2	8	7
Overall Score	20	12	11	3	13	6	23	20

4.3.3 Case 3: Air Conditioning

Technical:

The technical performance of the refrigerants in Case 3 is displayed in Figure 4.17, where it can be seen that R600a is able to perform with the greatest COP_C, closely followed by R717 and R22. Again, it is shown that the natural refrigerants, on the whole, perform better than the current generation of refrigerants (HFC/HCFC) whilst also requiring a smaller mass flowrate for the same cooling capacity. The HFO performance follows the trend from the previous two Cases, as they have the lowest COP_C and R1234ze(E) has the largest flowrate. When compared to R32, the most widely used air-conditioning refrigerant, the HFO R1234yf was 18.8 % less efficient, although it did require less than a quarter of the refrigerant flowrate.

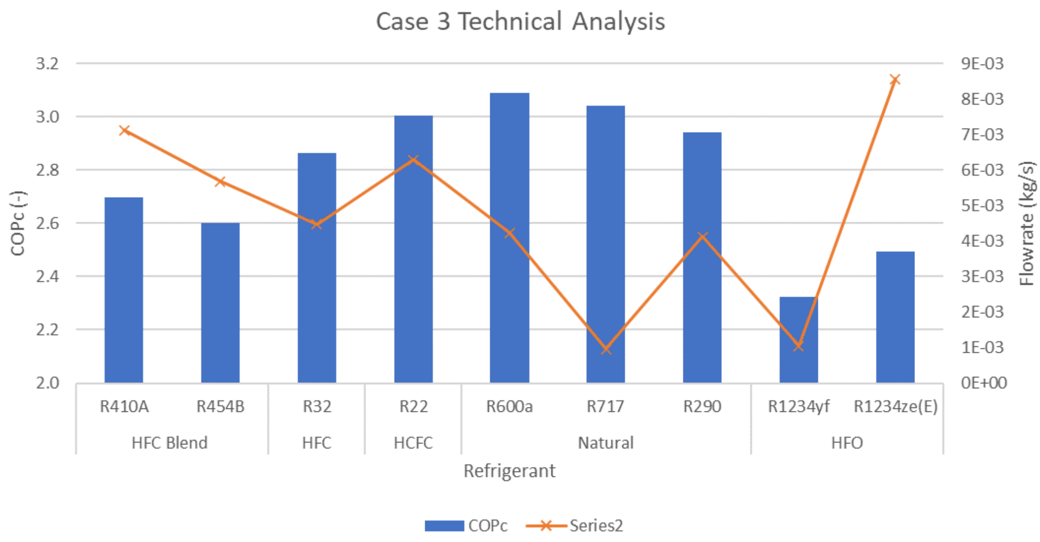

Figure 4.19: Case 3 Technical Analysis

The operational results of each model show that the maximum temperature achieved in the condenser is again greatest in R717, and the pressure is largest in the HFC R32 (Figure 4.20). All alternative refrigerants perform under more favourable conditions than the current gases, with the exception of the high temperatures experienced in the R717 simulation.

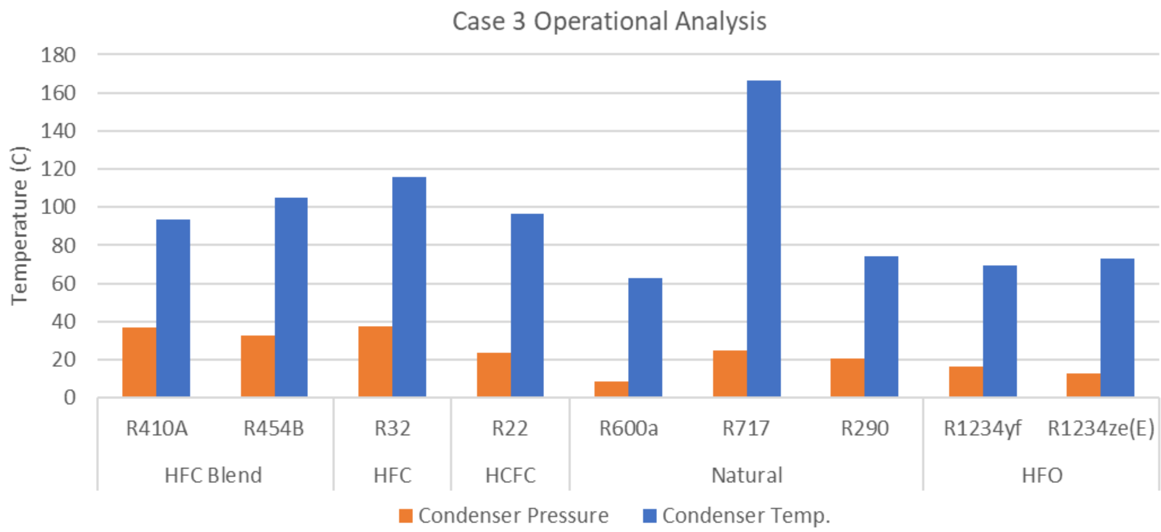

Figure 4.20: Case 3 Operational Analysis

Environmental:

The environmental analysis conducted on Case 3 shows a much-changed composition of emissions in comparison to the previous Cases, with a larger portion of annual CO_2,e emissions coming from refrigerant leakage in the current generation of refrigerants (Figure 4.21). In the case of R410A and R22, the direct emissions from leaks account for 66.9 % and 60.0 % of the total emissions, respectively. The reasoning for this result is the reduced annual operating hours of the air conditioning model compared to the other Cases, the location simulated (Glasgow, UK) is of a temperate climate that rarely reaches temperatures necessary for air conditioning. Although leakage emissions are reduced with less operation, there is still substantial leakage, particularly compared to the high specification of cryogenic and freezer applications. The equipment is also likely to be left for long periods without any use, as cooling is only necessary in the months of June, July, and August, which can lead to degradation of the system components and cause further leaks (Fenaughty et al., 2018).

The results would differ is the simulation was assumed in a hot climate that required more extensive use of the AC system, and the annual hours of operation where the indirect electricity emission is equal to the leakage emission for the R410A simulation is 1,585 hours per year, which would be expected in a southern Mediterranean climate. The operational hours for an AC system in Glasgow, UK will likely increase in the coming decades due to global warming. Forecasting from The James Hutton Institute suggest that the mean maximum summer temperature could rise by 4 *°C* by 2050 compared to the 1960 – 1990 average, in Scotland, leading to a doubling of cooling demand (The James Hutton Institute, 2022).

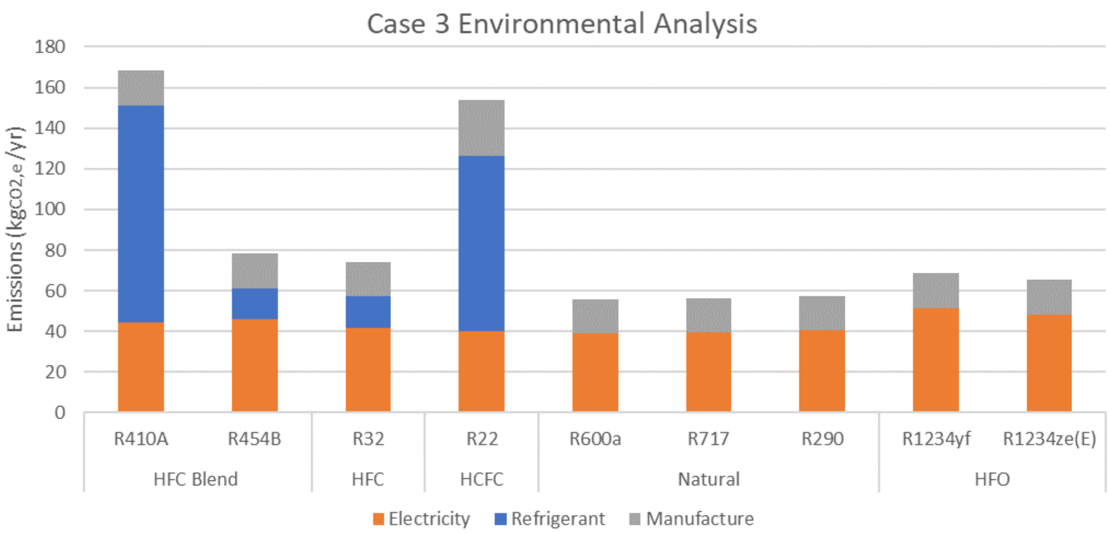

Figure 4.21: Case 3 Environmental Analysis

Despite the poorer efficiency of the HFO simulations, due to their low GWP, they have a much-reduced environmental impact compared to R410A and R22 (reduction of 59 and 55 *%*, respectively), whilst also outperforming R454B and R32, by 12 *%* and 7 *%*.

Economic:

Analysis of the cost associated with the Case 3 simulations shows that the natural group of refrigerants are the most economical choice (Figure 4.22). All of these gases have an annualised cost of between £80 – £84, which is an improvement in the region of 3 – 8 % compared to R32 devices.

Similar to the previous Cases, the results of the HFO simulations are the least attractive, as they have the greatest costs associated with both electricity consumption and purchasing the refrigerants. Although this might improve in the future as the efficiency of the HFO devices increases, or the cost of production reduces, at present many AC applications, such as domestic appliances may not be suited to convert to this group. Their use in automobile AC systems is partly due to legislation and enhanced safety consideration when compared with natural refrigerants as alluded to in the *Literature Review*.

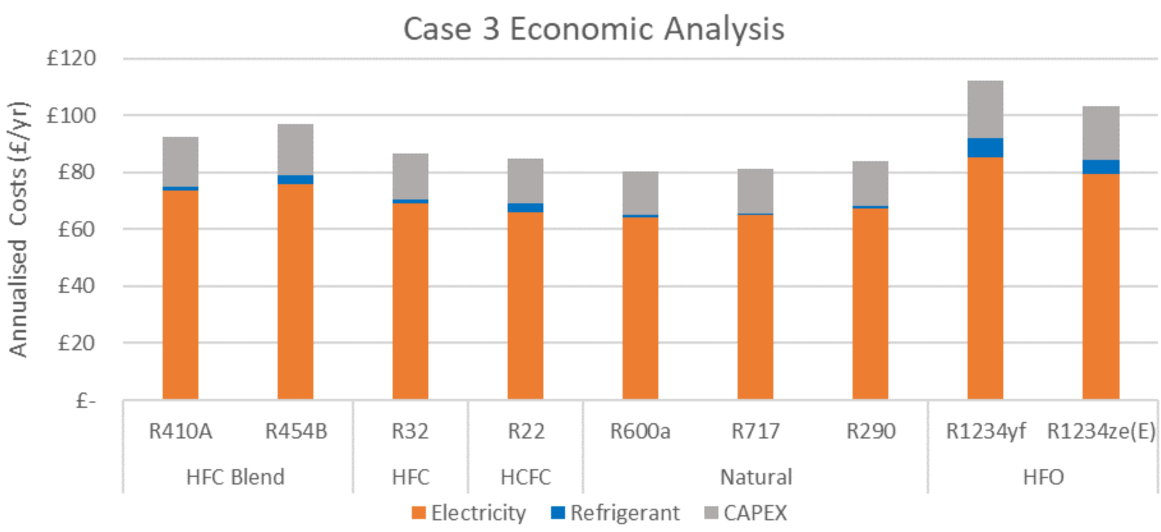

Figure 4.22: Case 3 Economic Analysis

Overall:

The table below presents the output of the three analyses, ranking the refrigerants from best to worst. It can be deduced that again the best performer is R600a, followed by R290 and R717. This would lead to the conclusion that they are all suitable replacements for the current generation of refrigerants, although the safety concerns over the flammability of R600a and R290, as well as the toxicity of R717, must be overcome. The legislation surrounding charge limits on R600a and R290, would suggest that they would be most effective in smaller AC applications, such as domestic or window-mounted devices; whereas R717 would be more suitable as an alternative in larger commercial systems for supermarkets or office complexes.

In these settings, the gas can be controlled in a safe manner by trained and regulated professionals. Some industries such as oil refineries are already accustomed to handling flammable substances, and so the use of R600a and R290 may be successful there.

Table 4.3: Case 3 Overall Analysis

Ranking	HFC Blend		HFC	HCFC	Natural			HFO	
	R410A	R454B	R32	R22	R600a	R717	R290	R1234yf	R1234ze(E)
Technical	6	7	5	3	1	2	4	9	8
Environmental	9	7	6	8	2	3	1	5	4
Economic	6	7	5	4	1	2	3	9	8
Overall Score	21	21	16	15	4	7	8	23	20

4.3.4 Case 4 – 6: ASHP

All three of these Cases pertain to the winter standard for ASHPs in Glasgow, United Kingdom. This represents a minimum design temperature of – 4 *°C* for this location, and the model was conducted on three types of heating systems. The first was Air – to – Air (Case 4), which would provide warm air to the indoor environment, much like the reverse of an air conditioning device. The second was an Air – to – Space heating (Case 5), where heat is extracted from the outdoor air and provided via a large water system, such as underfloor heating. Case 6 was the final ASHP model, which would provide domestic hot water at a temperature of between 65 and 70 *°C*.

Technical:

The technical performance of the refrigerants varied between each Case, due to the varying heat delivery temperature, the figures below show the COP_H of each model for the respective Cases. It can be seen that R600a is again the standout performer in Case 4, along with R290. These were found to achieve a COP_H of 4.99 and 4.90, respectively; and both were more efficient than the most popular current refrigerant R407C (4.63). The refrigerant flowrates required by these gases were also reduced by over 30 *%*.

The results of R744 (CO_2) show that as the delivery temperature increased from warm air to hot water, its efficiency relative to the other refrigerants increased. This is consistent with other studies, that report the use of R744 for high-temperature heat pumps as being the most effective application of that refrigerant (Mateu-Royo et al., 2020).

Similarly, the performance of R717 was also more desirable in Cases 5 and 6, outperforming most of the other refrigerants, expect R744 and R600a in Case 5.

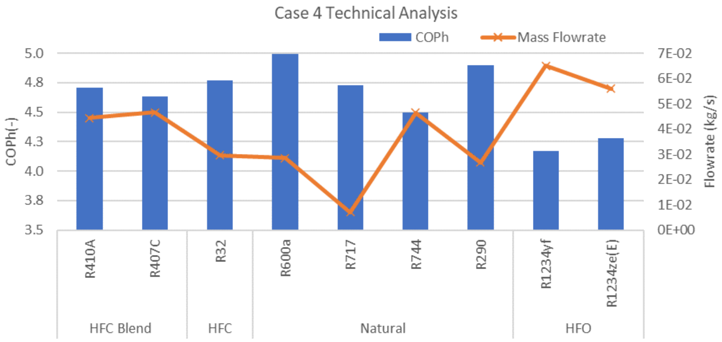

Figure 4.23: Case 4 Technical Analysis

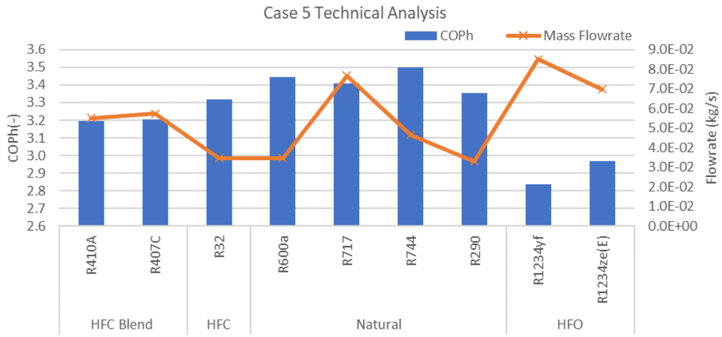

Figure 4.24: Case 5 Technical Analysis

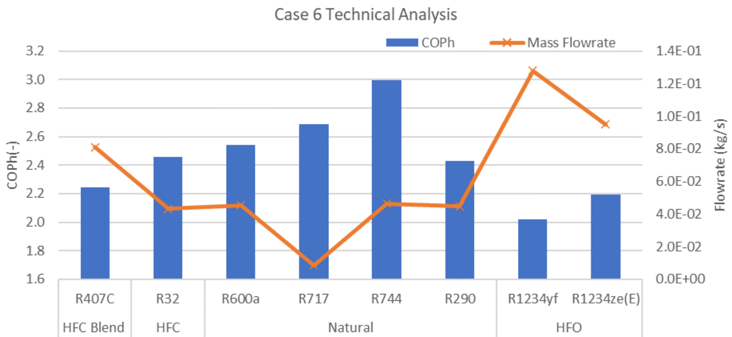

Figure 4.25: Case 6 Technical Analysis

Note that in Case 6, R410A was not simulated as its thermophysical properties are not suitable for the delivery of heat at the hot water temperature.

Environmental:

The environmental impact of an ASHP is a critical parameter as they are touted as the future of heating both domestically and commercially in the UK government route to Net Zero. As such the analysis of the carbon emissions associated with the refrigerants in all three ASHP cases is presented in the figures below. It is also reiterated that this analysis was not conducted on the number of hours of operation, as in the other Cases, but rather using an annual energy consumption for space and DHW heating as defined in *3.3.1*. This was used to reflect the average usage of UK households. To reflect this, the simulation was also conducted on an 8 kW capacity for Cases 4 and 5, whilst Case 6 is 2 kW.

The analysis shows that due to the reduced electrical consumption compared to Cases 1 and 2, the refrigerant leakage has a much greater impact on the total emissions. In the model for DHW generated by an R407C ASHP, 53 % of the emissions would be as a result of refrigerant leakage. Of course, it is unlikely that a heat pump would be installed only for hot water production, and so, the analysis for the Seasonal Performance Factor (Page 69) is conducted on a dual system of space heating and DHW, across the whole year.

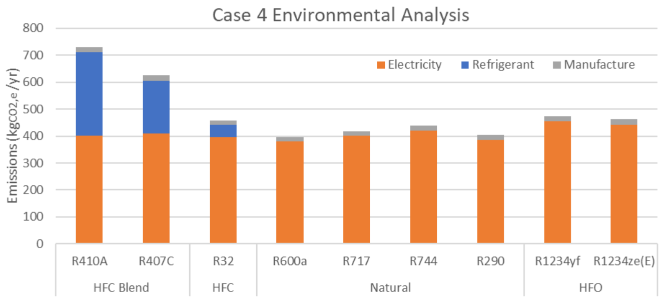

Figure 4.26: Case 4 Environmental Analysis

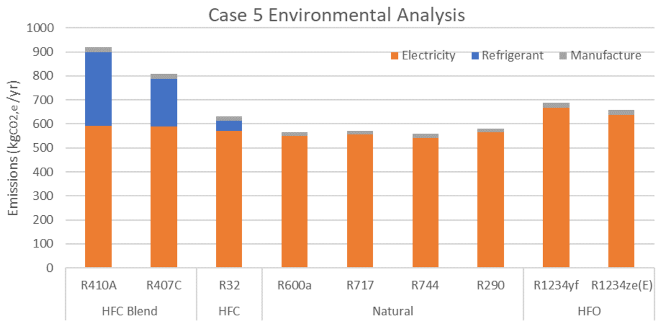

Figure 4.27: Case 5 Environmental Analysis

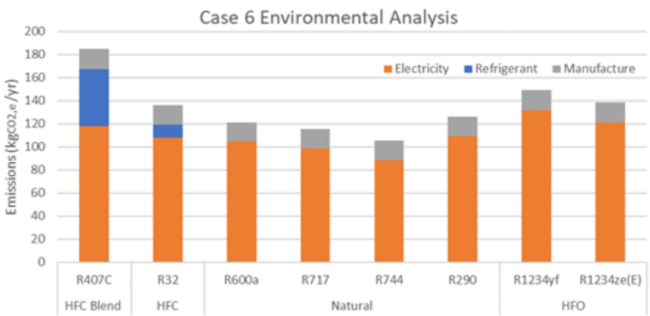

Figure 4.28: Case 6 Environmental Analysis

As a result of this increased contribution of emissions from refrigerant leakage, the environmental performance of all the low GWP refrigerants is significantly better than that of R410A or R407C. However, the poor COP_H of the HFO refrigerants means that overall, they have a larger carbon footprint than the HFC R32.

A relevant comparison for these Cases is to a typical gas boiler for domestic heating. Using the same aforementioned consumption figures, it can be calculated that the carbon dioxide emissions from this form of heating is approximately 2,400 $kg_{CO2,e}/year$ [10]. This puts into context the figures above for the ASHP models, as although there appears to be a large variation in emissions, they all result in a significantly smaller environmental impact than traditional heat sources.

[10] Natural gas emissions factor: 0.18 $kg_{CO2,e}/kWh$. Thermal efficiency of a condensing gas boiler: 90 % (UK Gov., 2022)

Economic:

The economic analysis of the ASHP models reflects the technical results, showing that the operational costs from electricity consumption have the greatest impact on the annual expense (Figure 4.29 to Figure 4.31).

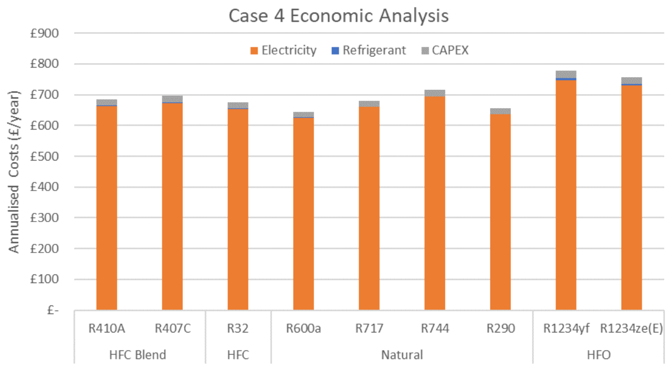

Figure 4.29: Case 4 Economic Analysis

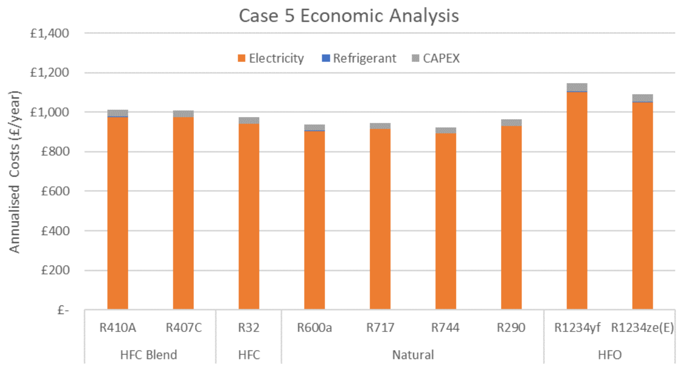

Figure 4.30: Case 5 Economic Analysis

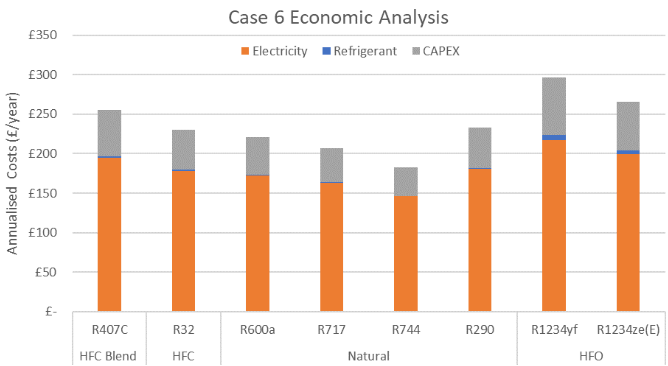

Figure 4.31: Case 6 Economic Analysis

The variation in annual costs between the most (R290) and least (R1234yf) economical across the scenarios was approximately 24 %. Within the natural refrigerant group, there was little difference over the three models, as only 2.1 % separated the annual running costs of R600a, R290, R717, and R744.

Seasonal Performance Factor:

In order to represent the efficiency of the ASHP models in a way that would be achieved in a real-world application, the Seasonal Performance Factor (SPF) is calculated. This provides a metric that allows the refrigerants to be compared across a range of evaporator temperatures, and so their COP_H is modelled using a range of average ambient air temperatures.

Temperature data for Glasgow, UK is available online, which was used to generate a heating profile based on the average temperature on each day across the year. Processing this data to find the number of days within temperature bands of 5 *°C* allowed the calculation of the number of heating hours at each evaporator temperature (Figure 4.32).

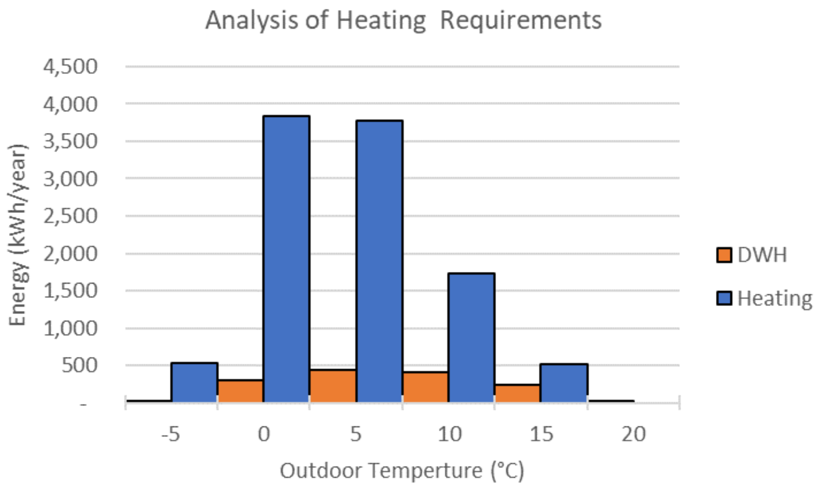

Figure 4.32: Analysis of heating in Glasgow, UK

This data was input into the model for each refrigerant using the Case 5 heating and Case 6 DHW supply temperature. The results produced a weighted SPF for an ASHP system that combined heating and DHW supply, known as a hybrid heat pump. Figure 4.33 shows that such a device would be most efficient using an R744 refrigerant, with all natural gases outperforming the HFCs. It is also seen that the performance of the HFOs is 22 – 24 *%* worse than that of R744, and not competitive with R407C.

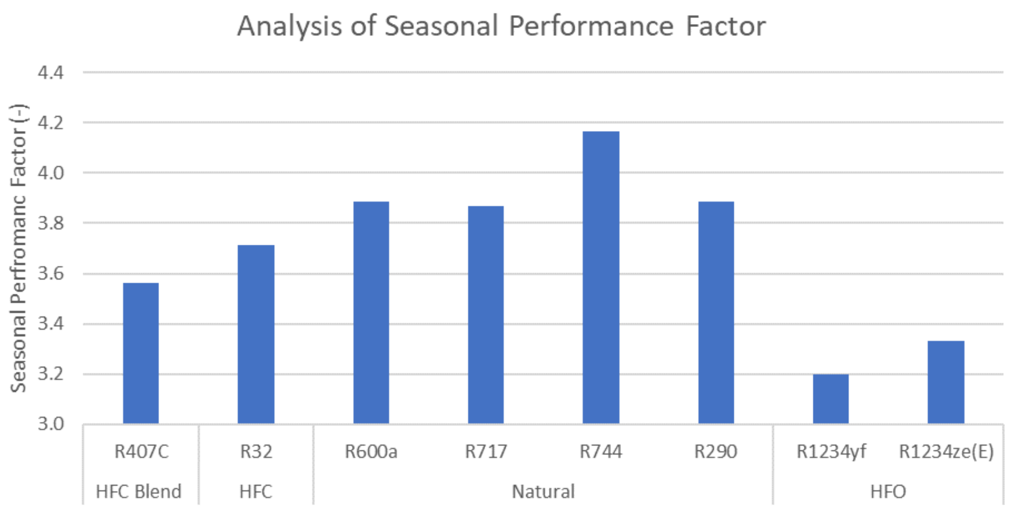

Figure 4.33: Seasonal Performance Factor for ASHP

As mentioned in the *Variables and Assumptions* section, these numbers don't include the effect of any auxiliary equipment, or parasitic load, from fans and other devices within the ASHP. There are also heat losses within the system, especially through piping, and cycling of the system to defrost the evaporator coils. This is particularly problematic in humid climates such as Glasgow, as the water vapour condenses on the external coils, reducing heat transfer to the refrigerant within. This can reduce the SPF by up to 15 % depending on the location and other install-specific factors and so a more realistic analysis is carried out (Chesser et al., 2021). The figure below shows the corrected analysis, where the horizontal orange line depicts the predicted SPF of an ASHP in the UK, found through a European-wide mapping model by Nouvel, R. (Nouvel et al., 2015). According to EU legislation in 2016, the minimum SPF required to receive funding for installation is 2.5 (black line); however, this is due to change to 2.1, in order to improve the uptake in ASHP devices (EU Directive 2018/2001).

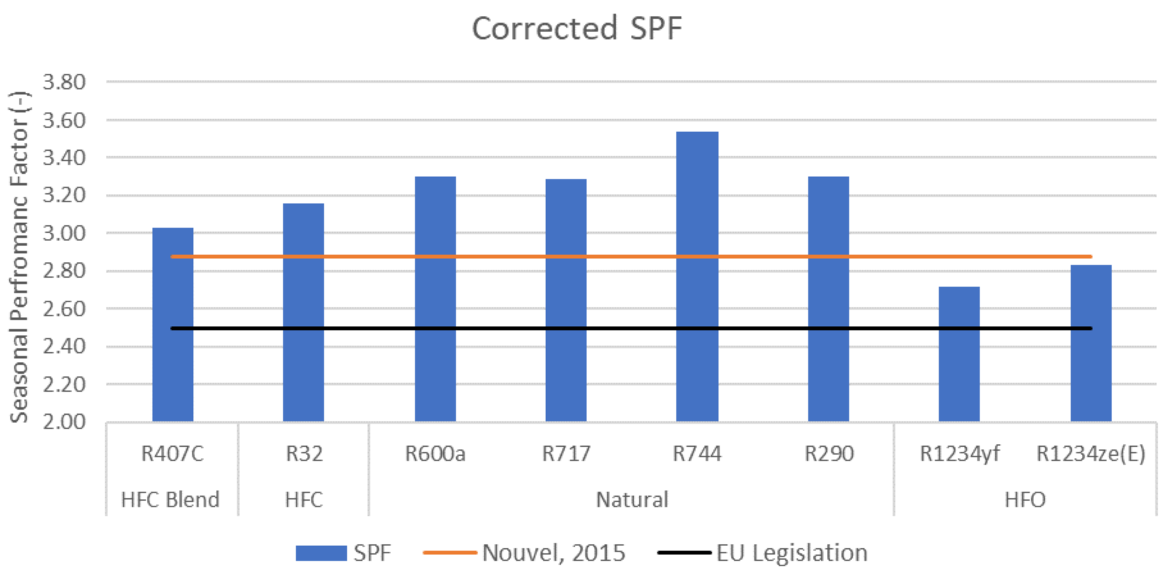

Figure 4.34: Seasonal Performance Factor (Corrected)

Overall:

The table below shows the overall analysis of the air-source heat pump model, using the results from the three analyses above. This analysis was conducted based on the weighted performance of space and water heating, as described in the previous section. It can be seen that R744 is the best performer in this model, with the best technical and economic performances. This can be explained by its high thermal conductivity and latent heat of vapourisation, extracting more heat in comparison to the HFC and HFO gases. R290 was the seconded best refrigerant, with the best environmental performance. The natural group were the top four refrigerants, outperforming all the HFC and HFO gases. The current popular refrigerant, R407C, did not perform well relative to the alternatives, only beating one of the six modelled low-GWP refrigerants.

Table 4.4: ASHP Case Overall Analysis

Ranking	HFC Blend	HFC	Natural				HFO	
	R407C	R32	R600a	R717	R744	R290	R1234yf	R1234ze(E)
Technical	6	5	3	4	1	2	8	7
Environmental	8	5	3	4	2	1	7	6
Economic	6	5	3	2	1	4	9	7
Overall Score	20	15	9	10	4	7	23	20

4.3.5 Cases 7 – 8: GSHP

This analysis is conducted on the ground-source heat pump (GSHP) model, with the input data simulated for an average household in the climate of Glasgow, UK.

Technical:

The figures below show a similar trend in the technical performance of each refrigerant as that seen in the ASHP Cases above. The relative performance of R717 and R744 improves with the increasing delivery temperature, while all the natural refrigerants prove more efficient than the HFCs in Cases 7 and 8. As the ground temperature at depths of over 10 *m* doesn't fluctuate across the seasons, it can be reasonably assumed that these COP_H will be available throughout the year. This analysis compared to the SPF in the previous section is consistent with literature that suggests that the overall performance of GSHPs is greater than that of ASHPs (Nouvel et al., 2015).

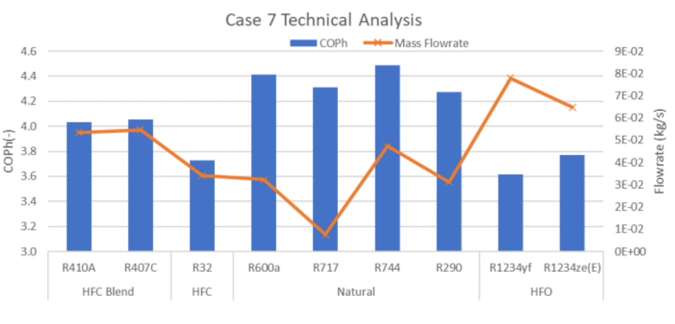

Figure 4.35: Case 7 Technical Analysis

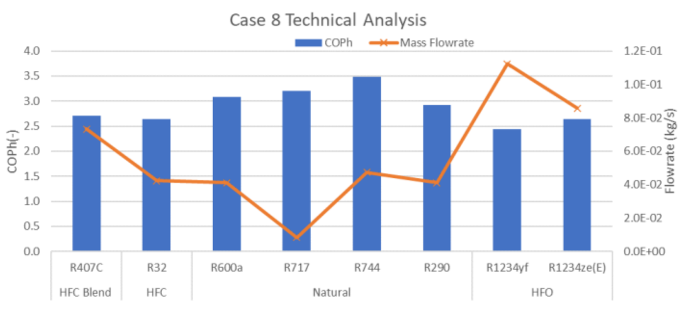

Figure 4.36: Case 8 Technical Analysis

Applying weighting to the typical consumption of heating and DHW in an average UK household, the overall COP_H is calculated for this GSHP system (Figure 4.37).

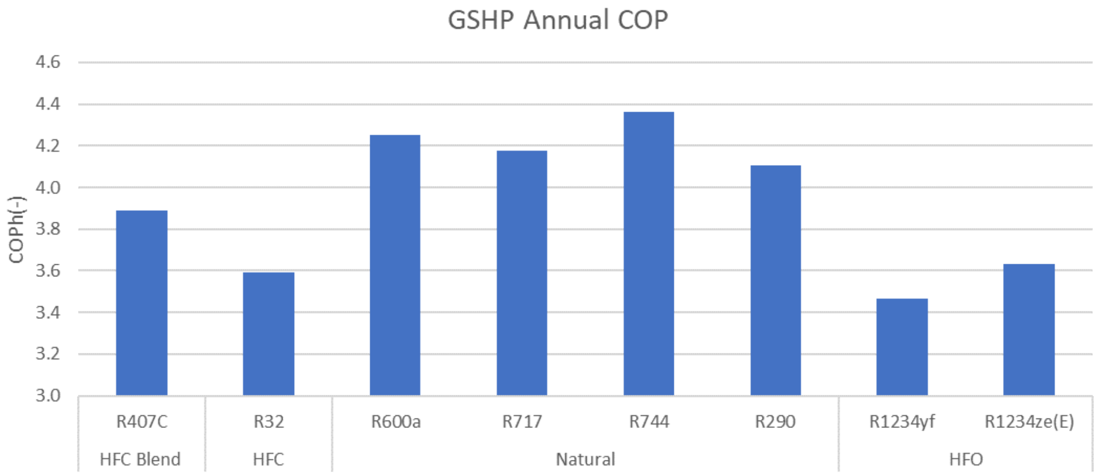

Figure 4.37: Overall GSHP COP Analysis

This figure shows that a GSHP utilising R744 would be most efficient for combined heating and DHW application, closely followed by the other natural refrigerants R600a, R717, and R290.

Environmental:

The environmental impact of the GSHP model shows that refrigerant leakage accounts for 36.5 % and 27.3 % in the R410A and R407C simulations for space heating (Figures below). This is significantly greater than the portion of direct emissions in the low GWP models, which accounted for between 0 % (R717) and 0.04 % (R1234ze(E)). Due to the large amount of refrigerant emissions, all the alternatives modelled generated fewer emissions when compared to the most popular current generation gas, R407C.

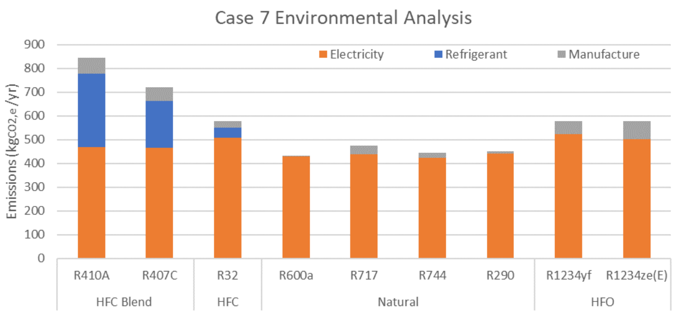

Figure 4.38: Case 7 Environmental Analysis

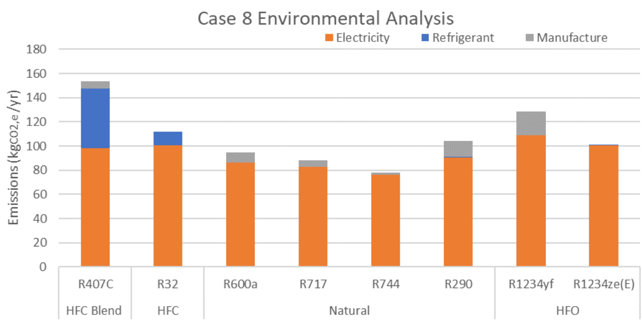

Figure 4.39: Case 8 Environmental Analysis

Annual emissions for a space heating and DHW system ranged between 428 to 738 $kg_{CO2,e}/year$ for the worst and best-performing refrigerants, R744 and R407C, respectively. This represents an improvement of 42.0 %.

Economic:

The economic performance of the refrigerants in the GSHP model is closely related to the technical performance. Following the trends from the previous cases, the electrical costs comprise the largest component of annual expenditure (figures below), and so the refrigerant with the greatest COP_H is also the cheapest to operate (R744). In Case 8 (DHW production), the R744 model was £189.97 per year cheaper to run in comparison to R407C, a reduction of 13.7 %.

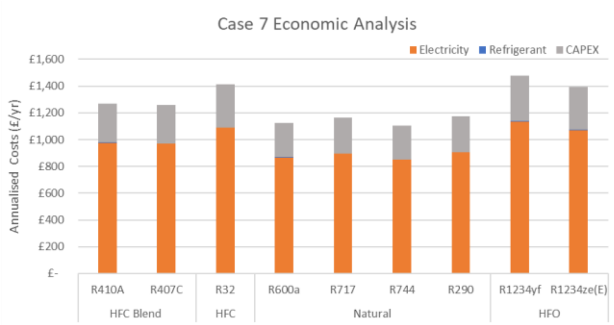

Figure 4.40: Case 7 Economic Analysis

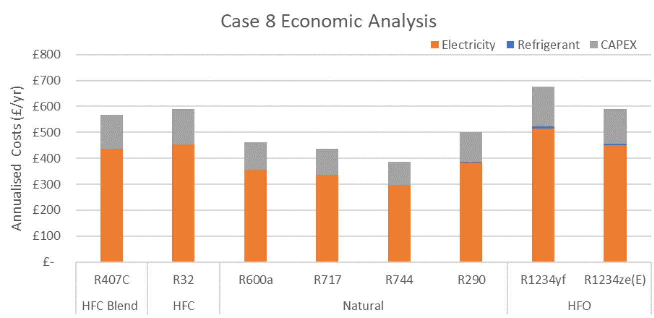

Figure 4.41: Case 8 Economic Analysis

It can also be seen that the refrigerant costs are negligible when compared to the cost of purchasing the GSHP device and the electrical costs associated with heating the average house and generating sufficient hot water. The GSHP also required the greatest capital expenditure for the initial device and installation of all the domestically available device (all models with the exception of Case 1: Cryogenic). This is in particular due to the large amount of excavation work required to install the device at depths of between 1 – 30 *m*, depending on the individual system.

Overall:

The overall analysis for the ground-source heat pump model is presented below. For a concise analysis, the performance in space and water heating has been weighted to the typical annual requirements in Glasgow, as defined in *3.3.1*. This analysis found that the best-performing refrigerant was R744, and, similar to the ASHP analysis in the previous section, the natural refrigerants outperformed all other groups. The popular HFC blend R407C also performed worse than the HFO R1234ze(E), so there could be multiple groups of low-GWP refrigerants researched further for implementation in heat pumps in the future.

Table 4.5: GSHP Case Overall Analysis

Ranking	HFC Blend	HFC	Natural				HFO	
	R407C	R32	R600a	R717	R744	R290	R1234yf	R1234ze(E)
Technical	5	7	2	3	1	4	8	6
Environmental	8	7	2	3	1	4	6	5
Economic	5	7	2	3	1	4	8	6
Overall Score	18	21	6	9	3	12	22	17

4.4 Sensitivity Analysis

A sensitivity analysis on three key parameters of each of the environmental, economic, and technical analyses above was undertaken. This was achieved by varying the carbon intensity, electricity unit price, and compressor isentropic efficiency. In order to keep the presentation concise, for the ASHP and GSHP results, the weighted performances of the space heating and DHW Cases were considered only. This represented the most realistic data for these applications, as devices performing both tasks are the most common.

4.4.1 Carbon Emissions

The effect of the carbon intensity of the National Grid on the indirect emissions was modelled, in order to reflect the movement towards are net-zero economy by 2050 in the UK. As explained in *Section 3.5.3*, this analysis was chosen to reflect the current carbon intensity, as well as four future values, as forecast by the UK government. The manufacture emissions were omitted from this analysis, as they did not represent a significant component of emissions in comparison to leakage and electricity.

The results of this analysis can be seen in Figure 4.42.

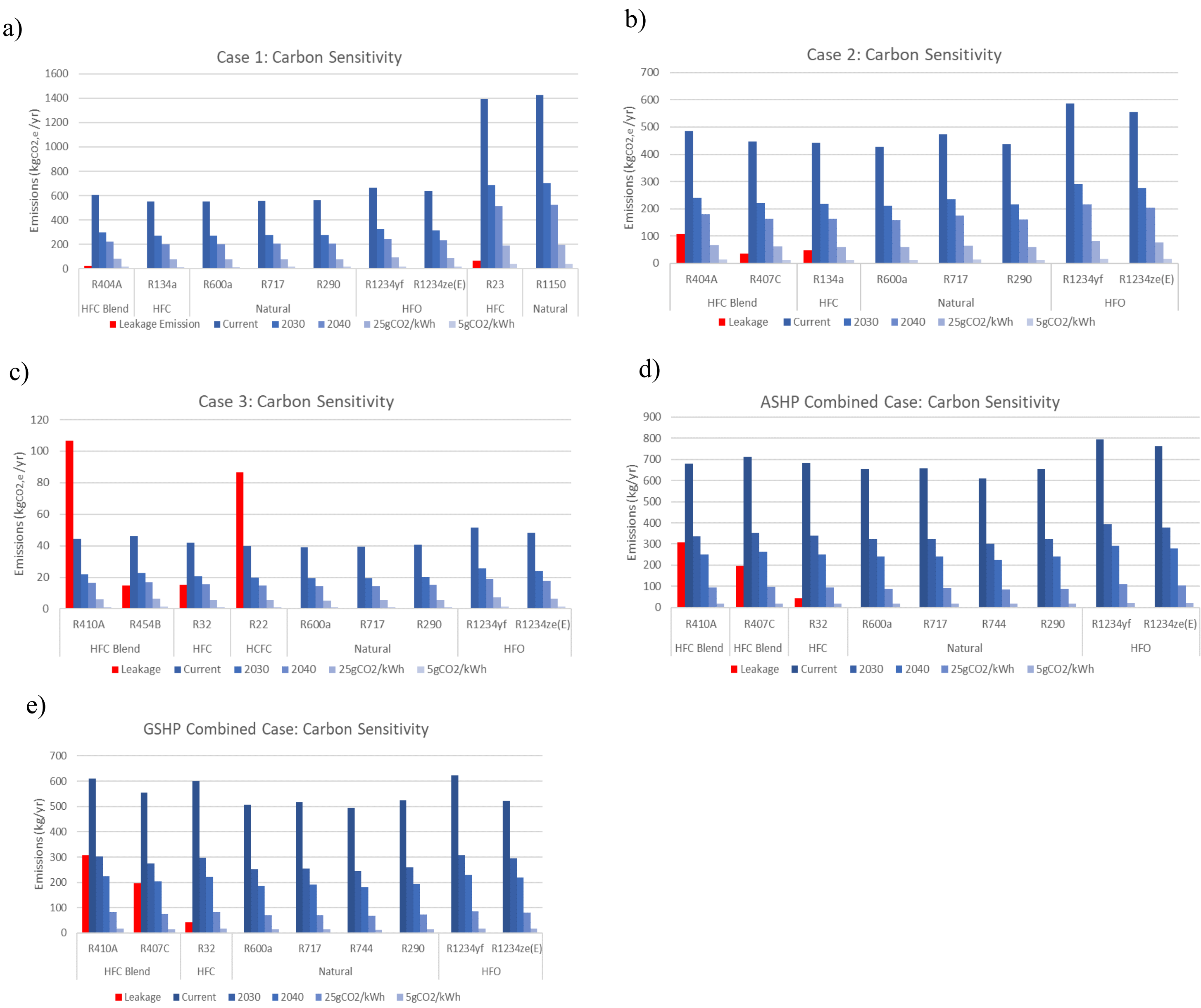

Figure 4.42: Carbon Emissions Sensitivity Analysis (a: Case 1, b: Case 2, c: Case 3, d: ASHP Combined Case, e: GSHP Combined Case)

These figures show the large proportion of emissions that are caused by refrigerant leakage (red bars) in the HFC, HFC blends, and HCFC simulation. When comparing the HFO and natural refrigerant leakage emissions, these are negligible in comparison to the conventional refrigerants, and also compared to the current indirect emissions from the UK grid carbon intensity. As discussed in the *Results Section*, for the air conditioning (Case 3) model, the direct leakage emissions are already more significant than indirect emissions for R410A and R22, due to the fact that AC is not necessary for a large proportion of the year in the climate of Glasgow.

As the UK electricity supply decarbonises, the indirect emissions will reduce in their contribution to the overall emissions of all the simulated refrigeration cycles. It was found that the grid carbon intensity that leads to parity in direct and indirect emissions for the current refrigerants in Cases 2, ASHP, and GSHP were as follows.

Table 4.6: Carbon Intensity where direct and indirect emissions are equal (kg$_{CO2}$,e/kWh).

Case	*Refrigerant*				
#	R404A	R410A	R407C	R134a	R32
1	11.9	-	-	8.9	
2	40.7	-	14.3	19.8	-
ASHP	-	94.7	60.6	-	14.0
GSHP	-	119.5	76.6	-	15.7

The table above shows that for these selected Cases, there is a strong likelihood that in the future the direct emissions will become a more significant source of CO_2,e than that from the electrical energy consumption. In fact, in ASHP and GSHP the most common refrigerant (R407C), will be responsible for more emissions than that of its consumed electricity in the years between 2030 and 2040.

As the direct emissions of the current generation of refrigerants are so much larger than the low GWP alternative, the figures below exclude them in order to analyse the impact of grid decarbonisation on these simulations.

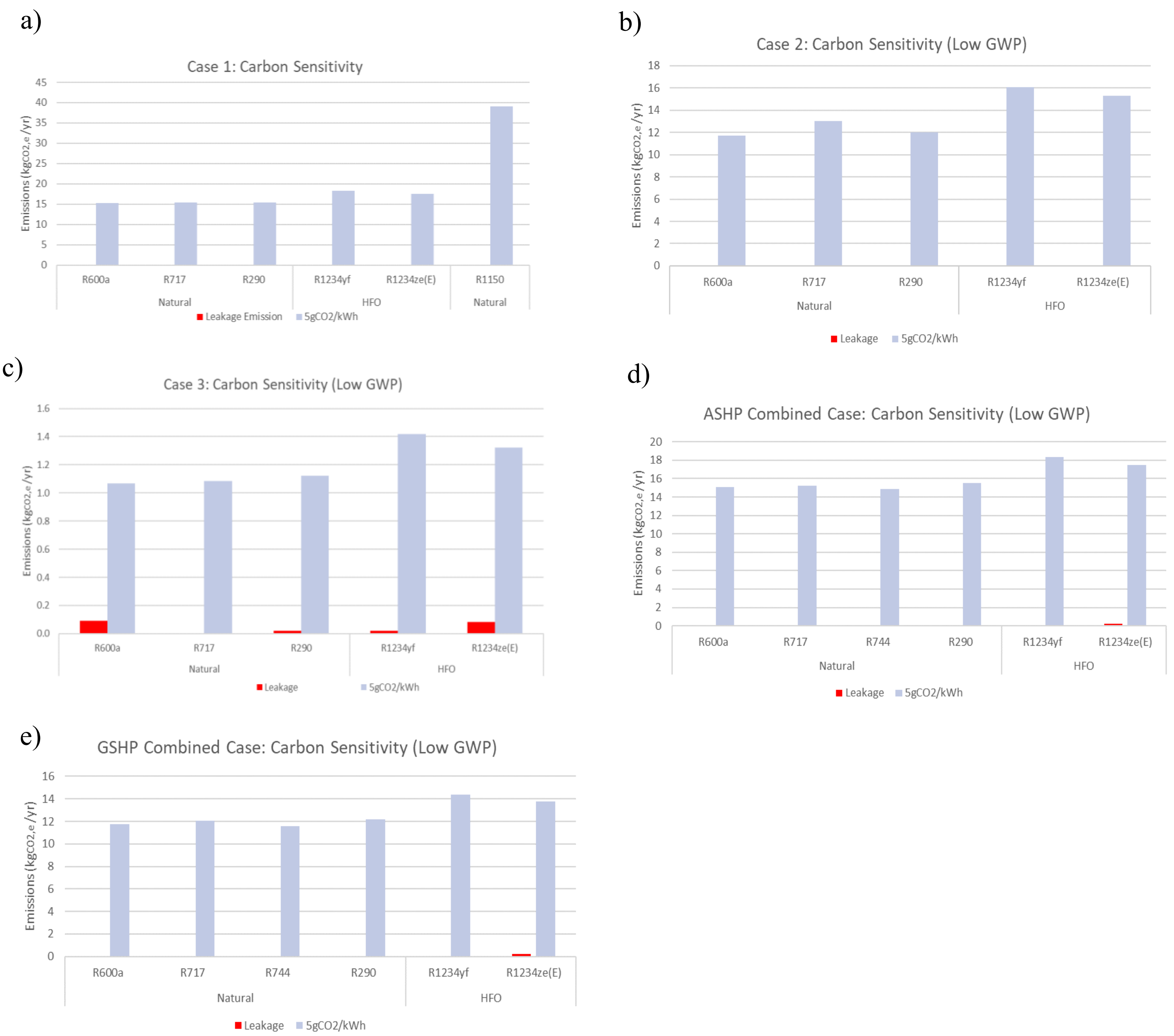

Figure 4.43: Low GWP Analysis (a: Case 1, b: Case 2, c: Case 3, d: ASHP Combined Case, e: GSHP Combined Case)

These figures clearly show that for all the low GWP alternative refrigerants, and in all simulations, the direct carbon equivalent emissions due to leakage of refrigerant is negligible in comparison to the indirect carbon emissions. Even at the best-case scenario for carbon intensity as forecast by the UK government, the emissions would account for less than 8 % of emissions in the air conditioning case, which had the largest annual leakage rate. In the 5 $g_{CO2,e}/kWh$ models for fridge-freezer, ASHP, and GSHP, the direct emissions accounted for, at most, 0.05 %, 0.36 %, and 0.46 %, respectively, across all the low GWP refrigerants.

This is a stark contrast to the current situation with the popular HFC refrigerants in these simulations, as the table below outlines the percentage of emissions currently associated with direct leakage of refrigerant.

Table 4.7: Portion of emissions associated with refrigerant leakage in current simulation.

Case	*Emissions from leakage (%)*						
#	R134a	R22	R32	R404A	R407C	R410A	R454B
2	6.2			12.7	4.5		
3		56.2	20.6			63.4	19.1
5			6.9		24.3	33.5	
7			7.7		28.8	38.8	

It is noted that the direct emissions comprise a smaller portion in Case 2 due to the far greater number of hours that fridge-freezers are utilised in comparison to the heating or cooling systems in Cases 3, 5, and 7.

4.4.2 Electricity Pricing

It was apparent in the above *Results Section* that in all Cases the most significant factor in the economic analysis was the cost associated with purchasing electricity for the compressor in each refrigeration cycle. In order to assess the impact that a varying unit price for electricity may have on the economic results, a sensitivity analysis was conducted in accordance with the values described in *Section 3.6.3*, using the current price, past decade average (#1), and NIC forecast (#2). The results of this sensitivity are presented in Figure 4.42 below.

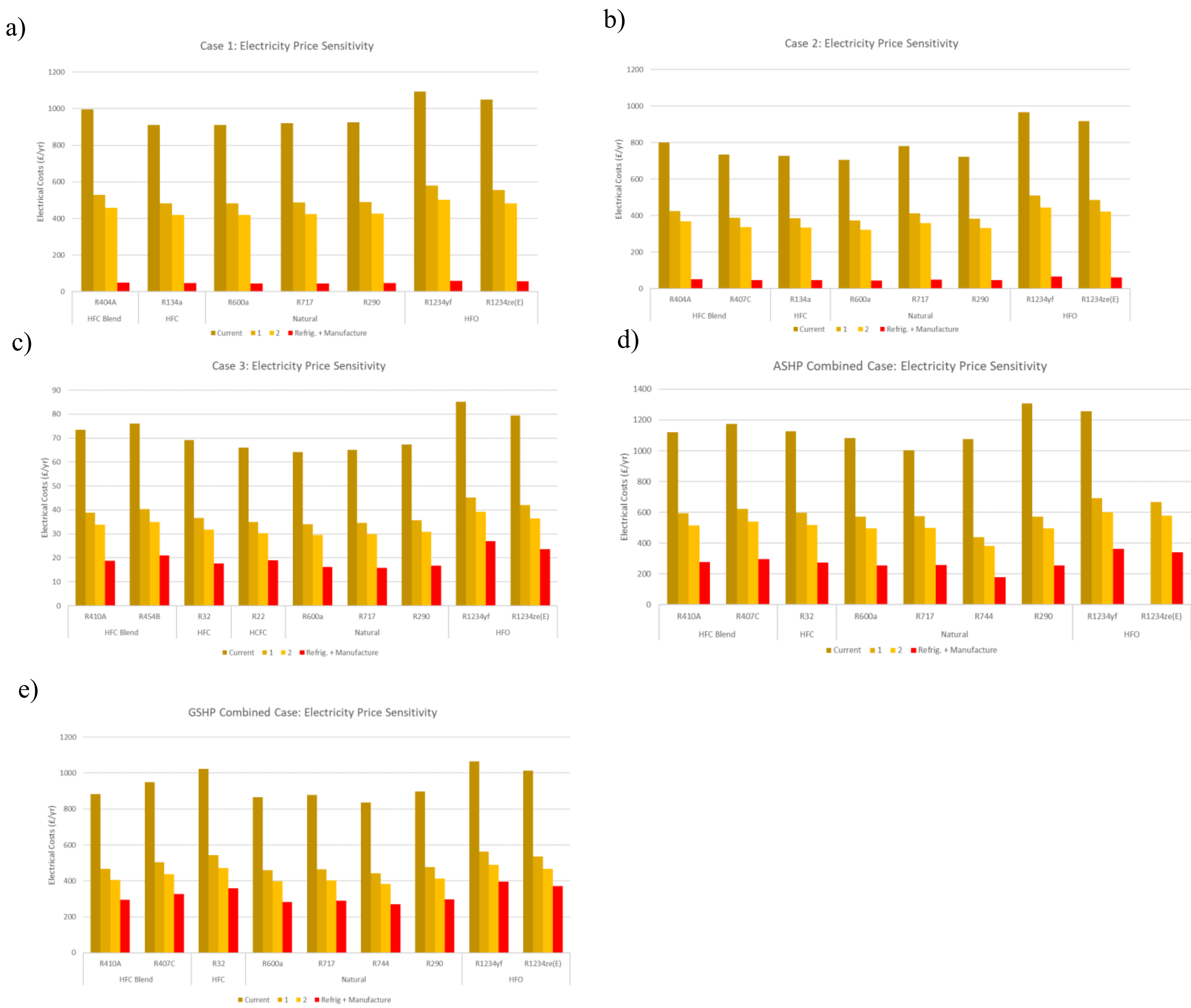

Figure 4.44: Low GWP Analysis (a: Case 1, b: Case 2, c: Case 3, d: ASHP Combined Case, e: GSHP Combined Case)

In Figure 4.44 a) and b), it can be seen that the electricity costs will likely always be much more significant than the cost of refrigerant and capital costs of the device, even at the lowest assumed unit price per *kWh*. For example, at 13.8 *p/kWh* in Case 1, the portion of annual cost associated with electricity is between 89.3 *%* and 90.3 *%*, for the least (R1234yf) and most (R600a) efficient refrigerants, respectively. Similarly, in Case 2 the range was found to be between 86.7 *%* and 87.8 *%*. This can be explained by the operational hours assumed for these Cases, being 7,884 and 3,504 *hours/year*, and so they will consume a large amount of energy to power the compressor for this length of time, hence the electricity costs are much more significant than the cost of the device and refrigerant.

However, in Cases 3, 5, and 7 (Figure 4.44 c), d), and e)), the electricity costs are smaller in comparison to Cases 1 and 2. At current electricity prices (July 2023), the electricity costs account for 76.0 % to 80.4 %, of the total cost per year for Case 3; however, if the pricing forecast by the NIC is correct, this could potentially reduce to between 59.3 % and 65.3 %. A similar trend is seen in Case 5, where the cost of electricity may reduce to between 56.9 % and 63.6 % of total annual cost, from 73.3 % to 78.9 %. In Case 7, it is possible that the cost of electricity to power the GSHP could reach as low as 55.5 % if utilising an R717 or R290 refrigerant, as opposed to the current scenario of between 75.9 % and 77.1 %.

This analysis shows that, at present, high electricity prices result in the great majority of annual expenditure for each simulation being purchasing the electrical energy to power the compressor. Although, based on the average unit price for the past decade (#1) and price forecasting (#2), it is possible that the cost of refrigerant and device manufacture may begin to play a greater role in the economic analysis of refrigeration devices. This is an important finding, as it may be the case that in the future, due to legislation or product scarcity, the cost of the refrigerant may be a more influential factor in economic decision-making than the efficiency or COP of the refrigeration cycle. This could favour the natural refrigerants, and even the HFOs in the future, as the price of HFC and HFC blends could increase due to phase-out legislation such as those put in place by the EU, whilst production costs of alternatives decrease, or subsidies are provided.

4.4.3 Compressor Efficiency

The input parameter that had the greatest effect on the technical performance output of the simulations was the compressor efficiency. The impact that varying this parameter had on the COP of the models was tested in Cases 1, 2, 3, 5, and 7. As detailed in the *Assumptions Section*, the compressor efficiency was tailored to each refrigerant using the available literature on the subject; however, this area is constantly developing, with new technology and devices being made available each year. It is also noted that some of the literature sourced were several years old, which may not reflect the most up-to-date compressors available. As such, a range of compressor efficiencies between 65 – 90 % was used to conduct a sensitivity analysis.

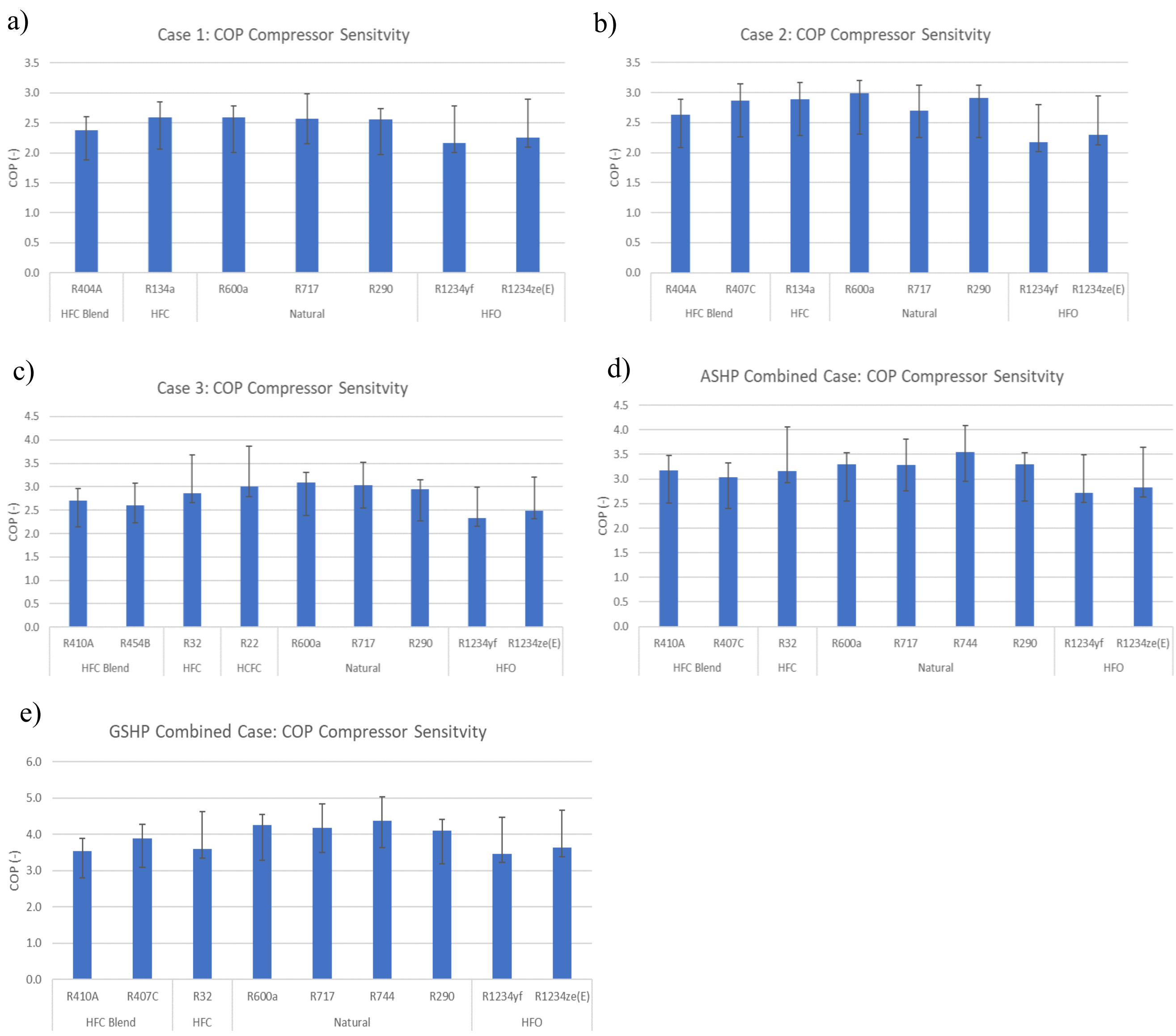

Figure 4.45: Effect of Compressor Efficiency on COP Sensitivity Analysis (a: Case 1, b: Case 2, c: Case 3, d: ASHP Combined Case, e: GSHP Combined Case)

The key takeaway from this analysis is that there is a significant range of overlap between the lower and upper ranges of COP across the refrigerants. The values for compressor efficiency for R600a and R290 were the greatest at 84 %, which likely led to their excellent performance across many of the models shown in the *Results Section*. Similarly, the poor performance of the HFOs in almost all of the Cases is a result of the compressor efficiency assumed for their simulations being the smallest (70 %), and it is possible that they may prove a suitable alternative to the current refrigerants, performing significantly better with a more efficient compressor. Further to this, if all the compressor efficiencies across the refrigerants are made equal, the relative performance of the HFO group improves significantly, with at least one of R1234yf or R1234ze(E) ranking in the top three for COP in Cases 1, 3, 5, and 7.

4.4.4 Levelised Compressor Efficiency

In order to compare the refrigerants independently of the compressor efficiency, the assumed value was set to 85 % for all refrigerants in all Cases. The findings of this levelised analysis are presented below.

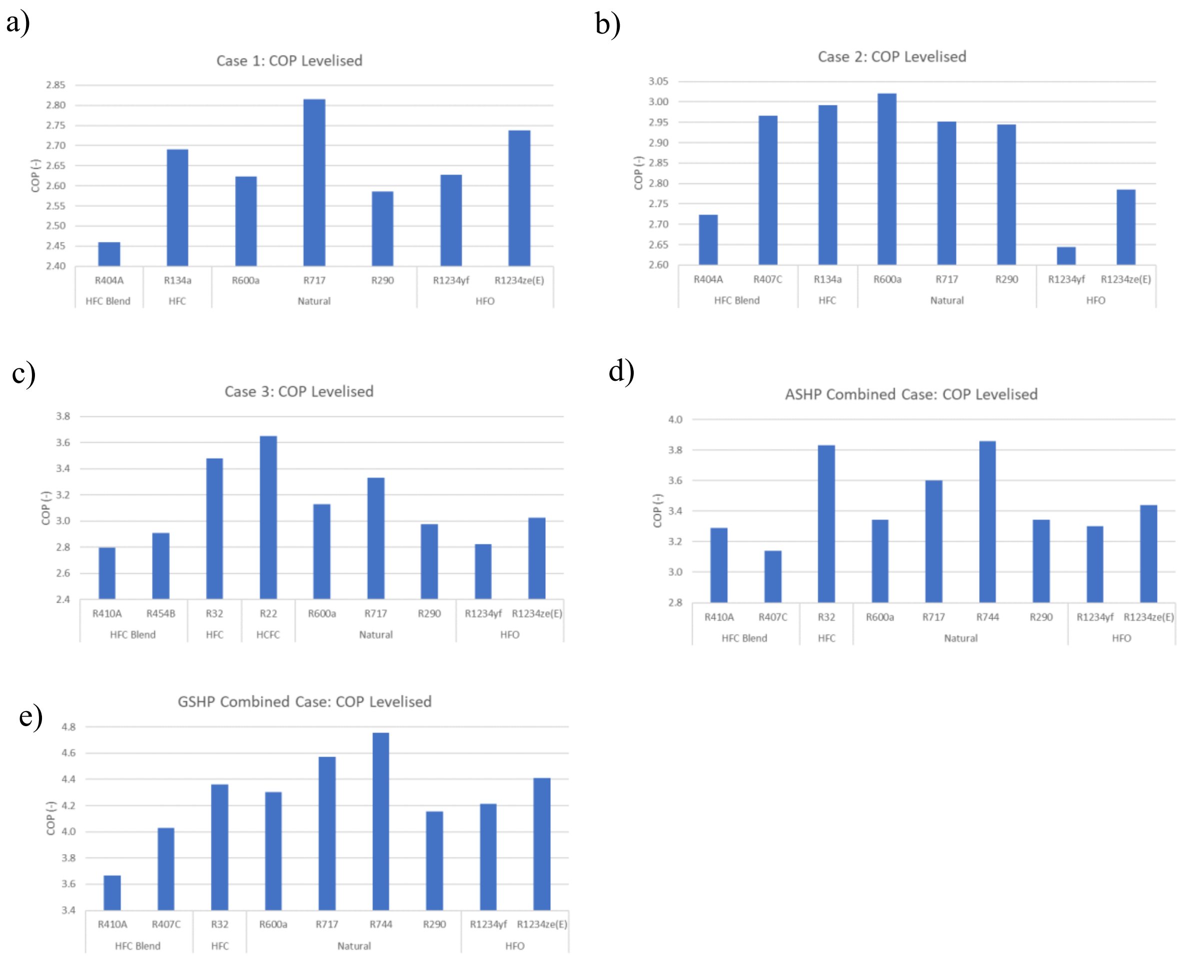

Figure 4.46: Levelised Compressor Efficiency for Comparison of COP (a: Case 1, b: Case 2, c: Case 3, d: ASHP Combined Case, e: GSHP Combined Case)

These results show that the high compressor efficiency assumed for R600a and R290 were critical in their successful performance in the *Results Section*, and that in fact, they are not stand-out performers if compressor efficiency is levelised. In the cryogenic case (Figure 4.46a), R717 was the most efficient refrigerant, with a COP 5 % greater than the second best, R134a. This could be a result of the lower boiling point of R717, along with a significantly greater latent heat of vapourisation, meaning that more heat is extracted by the fluid per *kilogram*. For the fridge-freezer model (Figure 4.46b), R600a has the greatest COP, although there is only a 3 % difference between the top five performing refrigerants. In the air conditioning analysis (Figure 4.46c), the HFC R32 and HCFC R22 were the top two performers, which is reflected in their popularity in current and previous commercial systems (as R22 is now banned). However, the natural refrigerant group all outperform the HFC blends, along with the HFOs also being comparable in their achieved COP. This is promising for this application as it is expected that demand for AC systems could increase rapidly in the coming years (*Chapter 2*). In the ASHP model (Figure 4.46d), R744 marginally outperforms R32 (3.86 vs 3.83, respectively), with R717 being the third most efficient refrigerant in this application. This reflects the current popularity of R32 systems (although R407C and R410A are becoming more popular in the UK) and these top three refrigerants in this case all have a lower boiling point than the other gases, which could explain their improved performance. Finally, in the GSHP model (Figure 4.46e), R744 has the largest COP (4.76) followed by R717 (4.57) and R1234ze(E) (4.41). In this model, the HFO group performed strongly compared to the other cases, as a result of their higher boiling points and critical temperatures. This analysis suggests that this could be the most promising application of HFOs, in systems operating at an evaporator temperature above 5 *°C*.

Across all of the above models, with a levelised compressor efficiency, it can be concluded that R717 is the most versatile refrigerant, performing well relative to the other gases in all Cases, whilst, in the heat pump models, R744 was the most efficient. It is also seen that the natural refrigerants are typically more efficient than the HFC blends which have been used as an intermediate replacement for high GWP refrigerants, and so could be well suited to replace this group. The HFO gases also performed much better than in the previous analysis from the *Results Section*, which suggests that the assumed value for compressor efficiency severely impacted their relative performance, and if compressors were tailored to their properties they would be viable replacements for HFCs in several cases.

4.5 Model Validation

In order to validate the findings of this project, the results must be compared to that found in well-cited literature. This section will detail the similarities and discrepancies between the model used for the above analyses and the values collected from the literature. As the performance of a refrigeration system is defined largely by the Coefficient of Performance of the model, this parameter was the most obvious choice for comparison to the literature. However, as has been demonstrated in this project, the COP of the system is affected greatly by the source and sink temperatures, and so literature with similar input is needed to accurately compare the results. In addition, papers reporting experimental data will likely incorporate losses and auxiliary power consumption that this model could not. This significantly reduced the number of suitable papers that could be used to validate the model; however, to remedy these difficulties, the performance of each refrigerant was compared relative to a chosen reference which could then be validated against similar relative analyses in literature. As CoolPack did not have as large a database as Cycle_D-HX it could only be used for comparison for some refrigerants; however, it proved useful to compare the two tools.

The figures below (Figure 4.47 to Figure 4.50) present a graphical comparison of the modelled results to well-cited papers. Note that the NIST model series includes the error range defined by the compressor efficiencies, as described in *4.4.3*. Case 1 is omitted due to a lack of similar literature to compare the findings of this project.

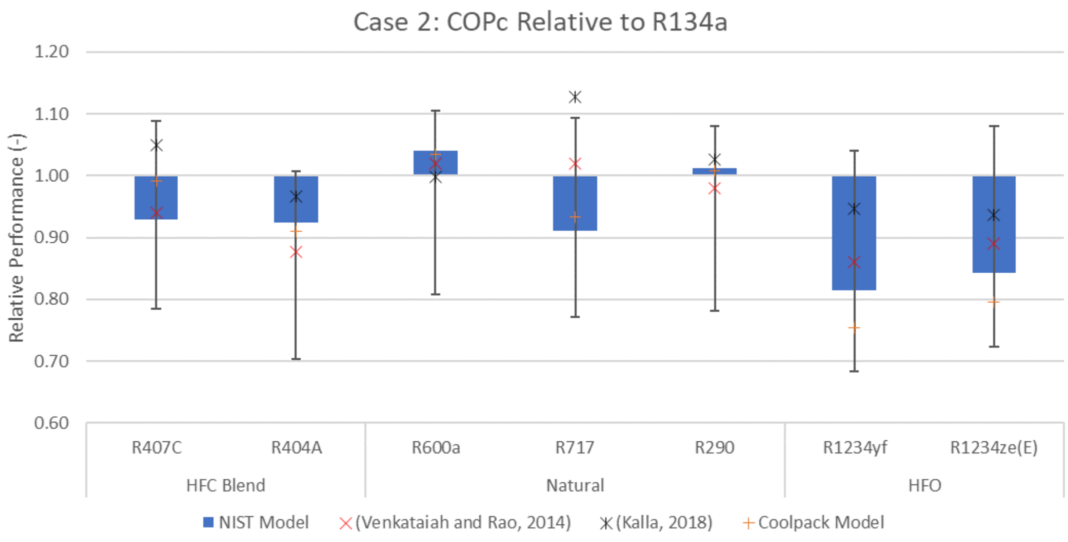

Figure 4.47: Case 2 Validation

The literature reviewed for the fridge-freezer (Case 2) temperature ranges specified showed a general agreement with the trends found in this project, with natural refrigerants performing better than the two other groups. In fact, the data collected is within the error range of all but one refrigerant (R717). This could be a consequence of *Kalla (2018)* referencing experimental data, which they suggest improves the relative performance of R717 due to its lower required mass flowrate. The data points for R600a and R290 are much closer to the NIST model results, suggesting that the compressor efficiency for these gases was in line with experimental data collected by these papers; whilst the assumptions for the other refrigerants may have been further from their systems. There was also little variation in the results of the two software packages, with the largest discrepancy being 7 % in the R1234yf result. This general agreement improves the validity of the results and provides a stronger basis for the conclusions of this project.

It was also found that literature sourced for air-conditioning systems also broadly agreed with this project's NIST model. Figure 4.48 shows that two recently published papers concluded findings that were within the error range of the NIST model, with the exception of one data point for R22. This suggests that the losses associated with an R22 system are large, given that the compressor efficiency assumed by the model (70 %) was the same as the literature. Similar to Case 2 above, the performance of R717 was found to be between 8 and 15 % greater in literature, perhaps showing that theoretical analysis of this model would benefit from tuning with empirical data for this refrigerant.

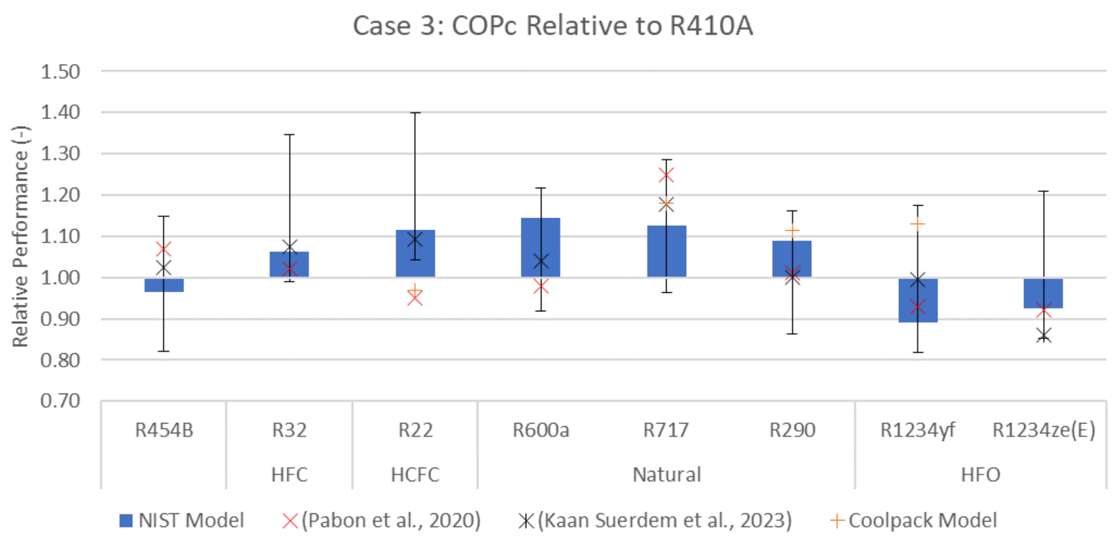

Figure 4.48: Case 3 Validation

The results of the ASHP Case were also compared to the literature; however, due to the recency of research on low GWP refrigerants in this sector, there were few papers with similar input parameters to the NIST model. Despite this, the data that was available showed that the natural refrigerants perform even better than the results of the model, and all refrigerants were found to have a larger COP_H in comparison to R410A than the findings of this model. This suggests that the model may provide inflated results for R410A compared to experimental data, perhaps as the model weighting for space and water heating did not correlate with that of the literature, which were not conducted in the UK.

The results of the CoolPack model were in general agreement with the NIST software, with the exception of R600a, as the CoolPack software suggested a 12 % comparative increase in COP. In fact, it is seen that all of the results from the CoolPack model are slightly greater than the NIST model. This could be a consequence of the equations of state used in the respective models deviating at greater temperatures compared to the previous Cases.

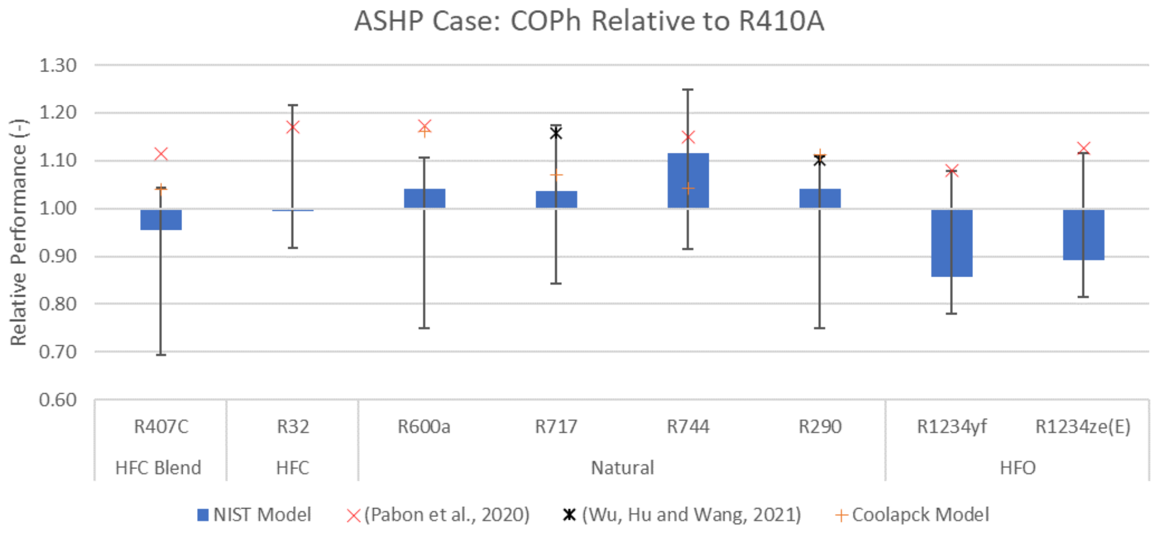

Figure 4.49: ASHP Case Validation

Similar to that of the ASHP, the literature for low GWP refrigerants in GSHPs was scarce due to the relatively new growth of these systems, in comparison to refrigeration and air conditioning. The trend of relative performance was found to be in agreement for the natural and HFC refrigerants, although, the HFO group performed up to 10 % better in literature than the NIST model suggests (Figure 4.50). All values collected were within the error margins for the model, and the discrepancy between the model and literature was within 5 % for all but the two HFO simulations.

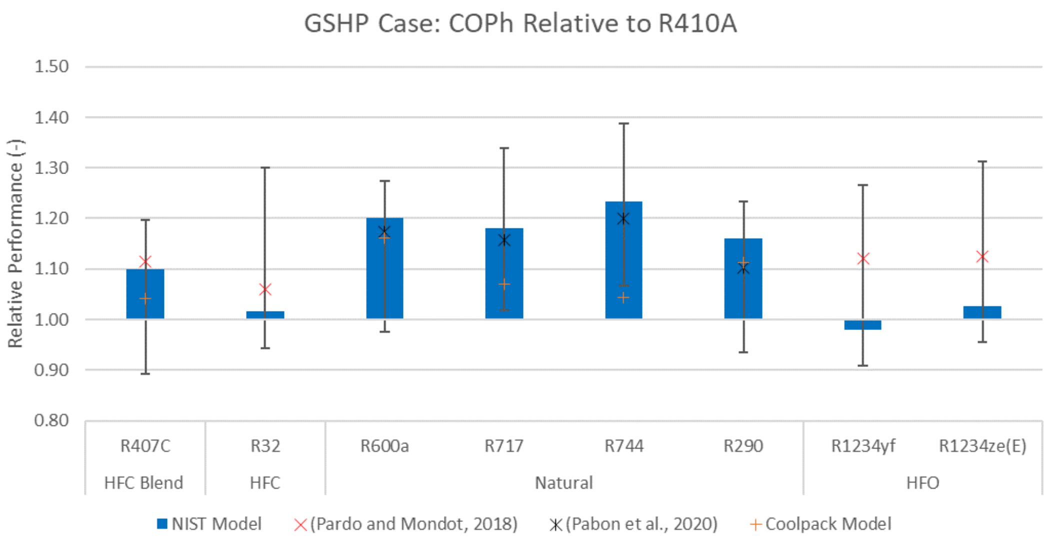

Figure 4.50: GSHP Case Validation

To summarise this validation section, it has been shown that the models used closely follows trends observed from experimental data in the literature, and only 8 % of the data points collected were out with the error margins of the models. However, this analysis would benefit from further investigation, and as more papers are published in the heat pump field, it is hoped that this would strengthen the model credentials.

4.6 Limitations to the Model

Although the software used in this project are sophisticated and reputable, there are several factors that were not taken into account that may have implications for the results and analysis of the refrigerant performance. The models analysed in this chapter provide a suitable comparison between the refrigerants, they don't reflect the behaviour and operation of real applications.

In the applications utilising evaporator temperatures below 0 *°C*, namely Cases 1, 2, and winter ASHP Cases 4 – 6, the model was unable to account for frosting effects. Ice crystals can accumulate on the evaporator coils as when energy is removed from the air and into the refrigerant, the moisture in the air cools to below the freezing point of water. These crystals form a layer on the coils, reducing the heat transfer coefficient, whilst also reducing the air flowrate across the coil surface. It is also commonly found that the frosting is non-uniform across the evaporator due to varying mass transfer coefficients and humidity gradients which, in the cryogenic and fridge-freezer applications, could lead to an uneven cooling of the interior environment. To prevent the effects of frosting from affecting the operation of the refrigeration cycle, methods have been developed that limit frost formation, such as electrical heating and reverse defrost cycling. However, these both require energy that would otherwise contribute to the desired cooling or heating function. This is called the energy penalty, and in the case of the electrical heater, a small wire is wrapped around the coils which is heated using a current. Not only does this consume additional electricity, but the temperature of the coils is increased and so the device is unable to remove as much heat from the cooled environment.

Reverse cycling also reduces the overall efficiency of the system as, during this defrosting process, the cycle is powered by the compressor to provide the opposite effect to its design (warming a fridge for example). Whilst a heat pump is defrosting, it is removing heat from the warm environment and in very cold outdoor conditions constant defrosting may lead to insufficient heating being supplied inside. Other physical methods of frost prevention include hydrophobic coatings of the evaporator coils and dehumidification of the intake air. Both zeolite and activated carbon have been researched as methods of desiccating the air surrounding the coils and have been shown to improve the COP in winter by 15 % (Song et al., 2018). Similarly, silica-based hydrophobic coatings have been researched for implementation on household appliances, as no auxiliary devices are needed. These have been shown to reduce frost thickness by between 8.5 % and 16 %, whilst improving heat transfer by 9 – 20 % (Liang and Wu, 2022).

These effects were not incorporated into the model used in this project, which although it is unlikely to impact the relative performance of the refrigerants, the absolute values will be affected in real-world applications. Figure 4.51 shows the correlation between the COP_C of an R600a system as simulated, using the model above, and the evaporator temperate. The condenser temperature was 50 *°C*, and all other variables were also kept constant.

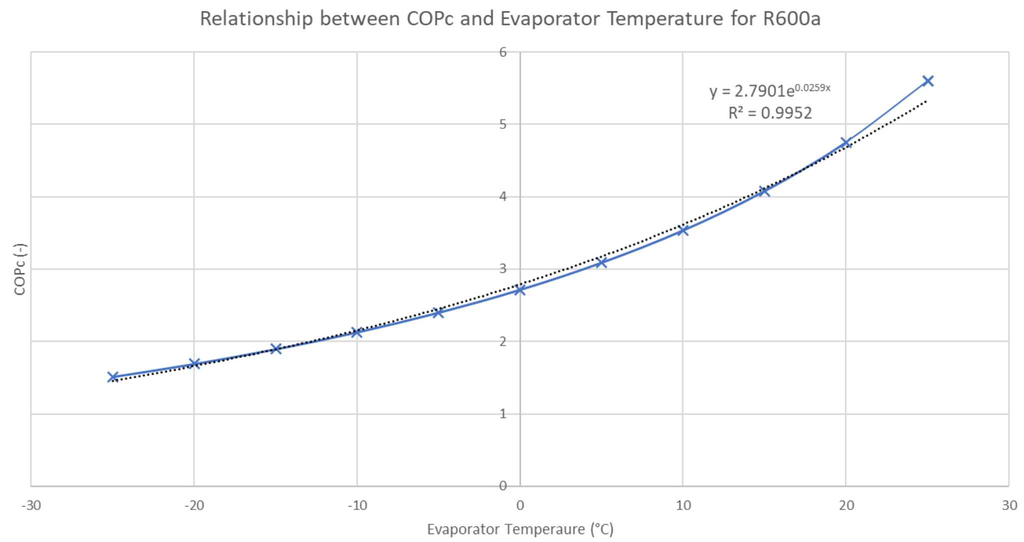

Figure 4.51: Relationship between COPc and Evaporator Temperature for R600a

This proves the software is unable to take into account the frosting effect, as the relationship follows a smooth exponential increase with greater evaporator temperatures. It is expected that there would be a decreasing shift in COP between 0 and 5 *°C*, due to the build-up of ice crystals at this temperature. The figure below is an extract from literature conducted on real heat pumps in Italy.

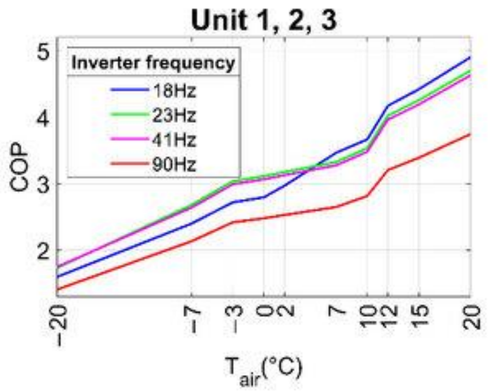

Figure 4.52: Literature on COP with frosting effect (Rossi di Schio et al., 2021)

The model would have also benefitted from the utilisation of experimental data, rather than solely theoretical modelling. Although this would have come at greater expense and time constraints restricted the potential for experimental data, the model could in future be modified to include effects of specific compressor maps, heat exchanger efficiency, and other ambient conditions such as air pressure or velocity. These additions would aid the model's accuracy in reflecting performance indicators such as those achieved by installed devices.

4.1 Summary

To summarise the results section, the data collected from the model and presented here has proved that several low GWP refrigerants could prove suitable alternatives to current HFCs in a variety of vapour compressions cycle applications. Specifically, R600a was found to be extremely consistent in outperforming the other simulated gases and was closely followed in most Cases by R290 and R717. This is likely due to the large latent heat of vaporisation and condensation of these fluids, in comparison to the HFC group, which allows more energy to be extracted and transferred per unit mass, and in turn, reduces the energy consumption of the compressor. These physical properties are responsible for the improved COP, as suggested by the literature in *Chapter 2*. The environmental and economic analyses also showed that the low GWP refrigerants are more attractive in both respects, which may lead to further funding and research into their development for more widespread use. As discussed, at present the only low GWP refrigerants currently utilised at large scale are R600a and R290, in EU fridge-freezers, with a much smaller market penetration also seen for R717, in commercial applications. However, the hydrocarbons (R290 and R600a) are both very flammable gases, which could be a hindrance to their increased uptake. As discussed in *Chapter 2*, charge limit regulation on these refrigerants is slowly being increased, and they could be an attractive replacement in systems that operate in highly restricted conditions such as the chemical industry.

5. Conclusions and Future Work

The objective of this project was to review the low global warming potential refrigerants and model a select number in several vapour compression cycle systems. The necessity of a study such as this was detailed in the literature review, with key impacts of refrigerants on both the ozone layer and climate change. In particular, the leakage of conventional refrigerants contributes to global carbon equivalent emissions due to the significant global warming potential and atmospheric lifetime of these gases. The history of refrigerants from the mid to late 19th century to the present day was briefly covered, along with the driving forces that initiated changes to regulations, such as the Montreal Protocol.

The modelled refrigeration systems ranged from very low-temperature cryogenic freezing to fridge-freezers and air conditioning, whilst also investigating heat pump systems. Three analyses were conducted on the low GWP refrigerants, as well as their conventional counterparts, namely technical, environmental, and economic, to compare the respective refrigerant groups.

Assessment of the suitable low GWP refrigerant groups was conducted using the NIST Cycle_D-HX and CoolPack software packages, and the key performance indicators were presented. A comparison of coefficient of performance, associated carbon emissions, and annualised operating costs, were used to compare each refrigerant in each separate model.

Sensitivity analyses were also conducted on three input parameters to assess the implications for certain assumptions used in the initial model. The key findings of these sensitivity analyses were that although direct emissions from leakage account for a relatively small proportion of total emissions, this will increase as the grid decarbonises. It is thought that by 2040, in the heat pump models, the direct emissions from HFC devices will be the major contributor to the annual emissions. Similarly, as the price of electricity fluctuates, the costs associated with the purchase of the device and refrigerant may play a greater role in the system's economic viability. The NIC unit price forecast would suggest that in the future the direct and indirect costs associated with air conditioning and heat pump systems will be similar. The cryogenic and fridge-freezer models did not show as much of an impact due to their longer hours of operation.

The results of this project conclusively show that low GWP refrigerants can perform the same function in the replacement of HFC-containing gases, whilst in all Cases modelled, at least one alternative achieved the most promising performance across the analyses. Overall, R600a performed the best in the majority of modelled cases, largely due to the high compressor efficiency (84 %) that is available at present. In the cryogenic model, R600a performed at an almost identical COP to the HFC R134a and at a similar annualised cost of operation, whilst also reducing the annual emissions by 1.7 %. The fridge-freezer model also showed the hydrocarbon gases improved COP by 4.2 %, with a 4.3 % reduction in costs and also a 12 % reduction in emissions, when compared to the popular HFC R407C. Similar trends were also found in the air conditioning model, although due to their fewer annual hours of operation, the leakage of refrigerant in HFC models had a much larger component of annual emissions. This meant that the natural and HFO refrigerant groups reduced annual emissions by 60.0 – 66.9 %, compared to HFC R410A. In the heat pump cases, R744 was the top performer, as it was suited to the specified temperature ranges. The economic analysis suggests that the annual costs of an R744 heat pump are 13.7 % lower than that of the common R407C device.

The levelised compressor efficiency analysis showed a direct comparison between the COP of each refrigerant system, without the influencing factor of assumed efficiency values from the literature. It was shown that the natural refrigerants outperformed the HFC blends, and with the exception of the air conditioning case, they also had the greatest efficiency in all models. In contrast to the main results section, R600a was not the stand-out performer, which suggests that if compressors were tailored to specific refrigerants, it may not be the most obvious replacement for high GWP gases. In similar disagreement, the efficiency of HFO refrigerants was much improved over the original analysis, performing particularly well in the heat pump models, relative to the other gases. As the environmental and economic analyses are predominantly influenced by the COP of each model, these findings would likely be reflected in these analyses.

In conclusion, this project has shown that low GWP refrigerants are proven to be suitable alternatives in a wide variety of refrigeration cycle applications. These gases will duly replace the HFC group, in line with international agreements, and will significantly reduce the direct emissions associated with refrigeration devices, whilst also reducing the indirect emissions thanks to improved cycle efficiency.

Future works could build and improve on these findings by addressing the limitations highlighted in the previous section. In particular, the addition of experimental data from systems both in the lab and in situ would aim the results of the model by allowing for the inclusion of losses within particular systems, along with parasitic power drain from smaller devices such as induction fans. This could provide the foundation for a more accurate model that could take into account the intricate features of refrigeration cycle operation, such as the reverse cycling or defrost mechanisms used in real applications. The use of hydrophobic coatings or desiccation systems are also areas in which future projects could investigate their implications for cycle efficiency and operational costs, along with the environmental impact of manufacturing such additional systems.

Further research could also refine the compressor efficiency of each fluid using the compressor map function if appropriate coefficients were available. This would improve the robustness of any comparisons between the refrigerants. Improvements in the modelling of the transcritical cycle with carbon dioxide could also be researched, as the behaviour of the gas is difficult to simulate, and experimental data could be used to increase the accuracy of a model.

6. References

Ala, G., Orioli, A. and Di Gangi, A. (2019). Energy and economic analysis of air-to-air heat pumps as an alternative to domestic gas boiler heating systems in the South of Italy. Energy, 173, pp.59–74. doi: https://doi.org/10.1016/j.energy.2019.02.011.

Al-Rashed, A.A.A.A. (2011). Effect of evaporator temperature on vapor compression refrigeration system. Alexandria Engineering Journal, 50(4), pp.283–290. doi: https://doi.org/10.1016/j.aej.2010.08.003.

Andrew Pon Abraham, J.D. and Mohanraj, M. (2018). Thermodynamic performance of automobile air conditioners working with R430A as a drop-in substitute to R134a. Journal of Thermal Analysis and Calorimetry, 136(5), pp.2071–2086. doi: https://doi.org/10.1007/s10973-018-7843-1

Aprea, C. and Greco, A. (2003). Performance evaluation of R22 and R407C in a vapour compression plant with reciprocating compressor. Applied Thermal Engineering, [online] 23(2), pp.215–227. doi: https://doi.org/10.1016/S1359-4311(02)00160-6.

Asdrubali, F. and Desideri, U. eds., (2019). Chapter 7 - High Efficiency Plants and Building Integrated Renewable Energy Systems. [online] ScienceDirect. Available at: https://www.sciencedirect.com/science/article/pii/B9780128128176000401#s0425 [Accessed 21 Jun. 2023].

ASHRAE (American Society of Heating, Refrigerating and Air-Conditioning Engineers). (2019). Standard 34: Designation and Safety Classification of Refrigerants. New York.

ASHRAE (American Society of Heating, Refrigerating and Air-Conditioning Engineers). (2021). Standard 169, Climatic Data for Building Design Standards. New York.

Balmer, R. (2011). Modern Engineering Thermodynamics

Baral, A., Minjares, R., Urban, R.A. (2013). Upstream climate impacts from production of R-134a and R-1234yf refrigerants used in mobile air conditioning systems. International Council On Clean Transportation.

Barry, E. (2022). Air-Conditioning Is Rare in the U.K. Could Heat Waves Change That? Time Magazine.

Behringer, D., Heydel, F., Gschrey, B., Osterheld, S., et al (2021). Persistent degradation products of halogenated refrigerants and blowing agents in the environment: type, environmental concentrations, and fate with particular regard to new halogenated substitutes with low global warming potential. Umweltbundesamt, Germany

BEIS. (2023). Department of Business, Energy & Industrial Strategy. Domestic Energy Price Indices. May 2023.

Bell, I.H., Domanski, P.A., McLinden, M.O. and Linteris, G.T. (2019). The hunt for nonflammable refrigerant blends to replace R-134a. International Journal of Refrigeration, 104, pp.484–495. doi: https://doi.org/10.1016/j.ijrefrig.2019.05.035.

Bhamare, K.D., Rathod, M.K., et al. Energy and Buildings. Volume 198.

Bhuvaneswari, R., Senthilkumar, K., First principle studies on the atmospheric oxidation of HFC-C1436 initiated by the OH radical. New Journal of Chemistry. Royal Society of Chemistry.

BMJ. (2022). Why do NHS hospitals struggle to handle heatwaves? Volume 378

Bobbo, S., Nicola, G.D., Zilio, C., Brown, J.S. and Fedele, L. (2018). Low GWP halocarbon refrigerants: A review of thermophysical properties. International Journal of Refrigeration, 90, pp.181–201. doi: https://doi.org/10.1016/j.ijrefrig.2018.03.027.

Britannica, T. Editors of Encyclopaedia (2020, July 14). Refrigeration. Encyclopaedia Britannica.

BSI (British Standards Institution). (2022). BS EN 14825:2022: Air conditioners, liquid chilling packages and heat pumps, with electrically driven compressors, for space heating and cooling, commercial and process cooling. Testing and rating at part load conditions and calculation of seasonal performance. London: British Standards Institution. Available at: https://bsol.bsigroup.com/Bibliographic/BibliographicInfoData/000000000030419055. (Accessed: 31 May 2023).

Busby, J. (2015). UK shallow ground temperatures for ground coupled heat exchangers. Quarterly Journal of Engineering Geology and Hydrogeology, 48(3-4), pp.248–260. doi: https://doi.org/10.1144/qjegh2015-077.

CCC (Cold Chain Federation). (2020). The Sixth Carbon Budget F-Gases. https://www.theccc.org.uk/wp/content/uploads/2020/12/Sector-summary-F-gases.pdf

Chang, H.-M. (2015). A thermodynamic review of cryogenic refrigeration cycles for liquefaction of natural gas. Cryogenics, 72, pp.127–147. doi: https://doi.org/10.1016/j.cryogenics.2015.10.003.

Chen, X., Liang, K., Li, Z., Zhao, Y., Xu, J. and Jiang, H. (2020). Experimental assessment of alternative low global warming potential refrigerants for automotive air conditioners application. Case Studies in Thermal Engineering, 22, p.100800. doi: https://doi.org/10.1016/j.csite.2020.100800.

Chesser, M., Lyons, P., O'Reilly, P. and Carroll, P. (2021). Air source heat pump in-situ performance. Energy and Buildings, 251, p.111365. doi: https://doi.org/10.1016/j.enbuild.2021.111365.

Cox, S. (2012). Losing Our Cool. The New Press

da Silva, A., Bandarra Filho, E.P. and Antunes, A.H.P. (2012). Comparison of a R744 cascade refrigeration system with R404A and R22 conventional systems for supermarkets. Applied Thermal Engineering, 41, pp.30–35. doi: https://doi.org/10.1016/j.applthermaleng.2011.12.019.

Danlami Musa, S., Zhonghua, T., O. Ibrahim, A., Habib, M., China's energy status: A critical look at fossils and renewable options. Renewable and Sustainable Energy Reviews. Volume 81

Dinçer, I. (2017). Refrigeration systems and applications. Chichester, West Sussex, UK: John Wiley & Sons, Inc.

EEA. (2022). European Environment Agency. Indicators. Hydrofluorocarbon phase-down in Europe. 9 Nov 2022

Elkins, J. (1999). The Chapman & Hall Encyclopedia of Environmental Science, edited by David E. Alexander and Rhodes W. Fairbridge, pp pp.78-80, Kluwer Academic, Boston, USA

Emani, M.S., Mandal, B.K., (2018). IOP Conf. Ser.: Mater. Sci. Eng. 377 012064

Energy Saving Trust. (2019). Analysis of the EST's domestic hot water trials and their implications for amendments to BREDEM and SAP

EHPA. (2022). European Heat Pump Association. Market Data 2022. [online] Available at: https://www.ehpa.org/market-data/

EPA (2019). Inventory of U.S. Greenhouse Gas Emissions and Sinks | US EPA. [online] US EPA. Available at: https://www.epa.gov/ghgemissions/inventory-us-greenhouse-gas-emissions-and-sinks.

EPA. (2020). Energy Efficiency Opportunities in Industrial Refrigeration. Available at: https://www.epa.gov/sites/default/files/2020-10/documents/p2webinar_energy_ind_refrig_061720.pdf.

EPA. (2020). Updating the Atmospheric and Health Effects Framework Model: Stratospheric Ozone Protection and Human Health Benefits. EPA Publication Number 430R20005

European Commission. (2019). European Green Deal. Climate Pact

EU. Directive 2018/2001. Methodology for calculating the amount of renewable energy used for cooling and district cooling. Available at: https://eur-lex.europa.eu/legal-content/EN/TXT/PDF/?uri=CELEX:32022R0759

Fenaughty, K., Parker, D. and Center, F.S.E., 2018. Evaluation of Air Conditioning Performance Degradation: Opportunities from Diagnostic Methods. Florida Solar Energy Center, editor.

Flerlage, H., Velders, G., de Boer, J. (2021). A review of bottom-up and top-down emission estimatesof hydrofluorocarbons (HFCs) in different parts of the world. Chemosphere. Volume 283.

Foster, A., Brown, T., Evans, J. (2023). Carbon emission from refrigeration used in the UK food industry. International Journal of Refrigeration.

Fraunhofer. Propane-based Refrigeration Circuit for Heat Pumps Achieves New Efficiency Record PRESS RELEASE. (2022.). Available at: https://www.ise.fraunhofer.de/content/dam/ise/en/documents/press-releases/2022/1922_ISE_e%20PR_%20efficiency%20record%20refrigerant%20cycle.pdf [Accessed 22 Jun. 2023].

Gouliaev, A.H., Senning, A. (1995). Synthesis: Carbon with Three or Four Attached Heteroatoms. Comprehensive Organic Functional Group Transformations. Volume. pp. 211 – 247

GVR (Grand View Research). (2016). Transcritical CO2 Systems Market Size & Share Report, 2027. [online] Available at: https://www.grandviewresearch.com/industry-analysis/transcritical-co2-systems-market [Accessed 23 May 2023].

Harby, K. (2017) “Hydrocarbons and their mixtures as alternatives to environmental unfriendly halogenated refrigerants: An updated overview,” Renewable and Sustainable Energy Reviews. Volume 73

Harvey, C. (2021). ‘Ozone Hole Would Have Killed Plants and Raised Global Temperatures’. Scientific American. August 20th

Heredia-Aricapa, Y., Belman-Flores, J.M., Mota-Babiloni, A., Serrano-Arellano, J. and García-Pabón, J.J. (2020). Overview of low GWP mixtures for the replacement of HFC refrigerants: R134a, R404A and R410A. International Journal of Refrigeration, 111, pp.113–123. Doi: https://doi.org/10.1016/j.ijrefrig.2019.11.012.

Honeywell. (2016). " SOLSTICE® ze -THE LOW CARBON, HIGH EFFICIENT COOLING SYSTEM SOLUTION FOR A LEADING RETAILER. [online] Available at: https://nationalref.com/wp-content/uploads/2019/09/FPR020-2016-10-EN_Honeywell-Solstice-ze-Sinop.pdf [Accessed 22 Jun. 2023].

IEA (2018), The Future of Cooling, International Energy Agency, Paris. Available at: https://www.iea.org/reports/the-future-of-cooling. License: CC BY 4.0

IEA. (2021). Executive Summary – Ammonia Technology Roadmap – Analysis. [online] Available at: https://www.iea.org/reports/ammonia-technology-roadmap/executive-summary.

IEA. (2022). World Energy Outlook. The Future of Heat Pumps. [online] Available at: https://iea.blob.core.windows.net/assets/4713780d-c0ae-4686-8c9b-29e782452695/TheFutureofHeatPumps.pdf

IPCC. (2005). Safeguarding the Ozone Layer and the Global Climate System — IPCC. [online] Available at: https://www.ipcc.ch/report/safeguarding-the-ozone-layer-and-the-global-climate-system/ [Accessed 18 Mar. 2021].

IPCC. (2014). Climate Change 2014: Mitigation of Climate Change, Contribution of Working Group III to the Fifth Assessment Report of the Intergovernmental Panel on Climate Change (IPCC), Cambridge University Press.

IPCC. (2021). Climate change 2021: The physical science basis. Working Group I contribution to theIPCC Sixth Assessment Report. Cambridge University Press.

IIR. (2015). International Institute of Refrigeration. Guideline for Life Cycle Climate Performance

Jackson, S. and Brodal, E. (2018). A comparison of the energy consumption for CO2 compression process alternatives. IOP Conference Series: Earth and Environmental Science, 167, p.012031. doi: https://doi.org/10.1088/1755-1315/167/1/012031.

Jain, N. and Alleyne, A.G. (2011). Thermodynamics-Based Optimization and Control of Vapor-Compression Cycle Operation: Control Synthesis. doi: https://doi.org/10.1115/dscc2011-6088.

Jin, W., Wang, Y., Jia, L., Liu, S., Moon, D. and Song, S. (2023). Influence of refrigerant charge volume on the flammability risk of an R32 rotary compressor. 29(5), pp.533–544. doi: https://doi.org/10.1080/23744731.2023.2197813.

Jones, A., Wolf, A. and Kwark, S.M. (2022). Refrigeration system development with limited charge of flammable Refrigerant, R-290. Thermal Science and Engineering Progress, [online] 34, p.101392. doi: https://doi.org/10.1016/j.tsep.2022.101392.

Kaan Suerdem, Taner, T., Ozgen Acikgoz, Ahmet Selim Dalkilic and Panchal, H. (2023). Performance of refrigerants employed in rooftop air-conditioners. 70, pp.106301–106301. doi: https://doi.org/10.1016/j.jobe.2023.106301.

Kalla, S. (2018). ALTERNATIVE REFRIGERANTS FOR HCFC 22—A REVIEW. Journal of Thermal Engineering, pp.1998–2017. doi: https://doi.org/10.18186/journal-of-thermal-engineering.410435.

Keller, F., Lee, R.P. and Meyer, B. (2020). Life cycle assessment of global warming potential, resource depletion and acidification potential of fossil, renewable and secondary feedstock for olefin production in Germany. Journal of Cleaner Production, 250, p.119484. doi: https://doi.org/10.1016/j.jclepro.2019.119484.

Kim, M. (2004). Fundamental process and system design issues in CO2 vapor compression systems. Progress in Energy and Combustion Science, 30(2), pp.119–174. doi: https://doi.org/10.1016/j.pecs.2003.09.002.

Kim, M. H., Lim, B. H., Chu, E. S. (1998) The performance analysis of a hydrocarbon refrigerant R-600a in a household refrigerator/freezer. Journal of Mechanical Science and Technology.

Lamb, R. (2016). Engage Network Discuss Learn. [online] Available at: http://cold.org.gr/library/downloads/Docs/Refrigerant%20choices%20for%20the%20future_Small%20industrial%20refrigeration%20applications.pdf [Accessed 26 Jun. 2023].

Lee, K., Liu, X., Vyawahare, P., Sun, P., ELGOWAINY, A. and Wang, M. (2022). Techno-economic performances and life cycle greenhouse gas emissions of various ammonia production pathways including conventional, carbon-capturing, nuclear-powered, and renewable production. Green Chemistry. doi: https://doi.org/10.1039/d2gc00843b.

Lee, Lee, M.J. and Jeon, S. (2018). Performance evaluation of HFO-1234yf as a substitute for R-134a in a household freezer/refrigerator. doi: https://doi.org/10.18462/iir.hfo.2018.1127.

Li, G., Tang, Z., Zou, H. and Zhang, R. (2023). Experimental investigation of cooling performance of a CO2 heat pump system with an integrated accumulator heat exchanger for electric vehicles: Impact of refrigerant charge and valve opening. Applied Thermal Engineering, [online] 224, p.120077. doi: https://doi.org/10.1016/j.applthermaleng.2023.120077.

Liang, X. and Wu, L. (2022). A brief review: The mechanism; simulation and retardation of frost on the cold plane and evaporator surface. Energy and Buildings, [online] 272, p.112366. doi: https://doi.org/10.1016/j.enbuild.2022.112366.

Liu, L., Dou, Y., Yao, B, et al. (2019). Historical and Projected HFC-410A emission from room air conditioning sector in China. Atmospheric Environment. Volume 212. pp. 194-200

Liu, X., Elgowainy, A. and Wang, M. (2020). Life cycle energy use and greenhouse gas emissions of ammonia production from renewable resources and industrial by-products. Green Chemistry, 22(17), pp. 5751–5761. doi: https://doi.org/10.1039/d0gc02301a

Luyben, W.L. (2017). Estimating refrigeration costs at cryogenic temperatures. Computers & Chemical Engineering, 103, pp.144–150. doi: https://doi.org/10.1016/j.compchemeng.2017.03.013.

Mateu-Royo, C., Sawalha, S., Mota-Babiloni, A. and Navarro-Esbrí, J. (2020). High temperature heat pump integration into district heating network. Energy Conversion and Management, 210, p.112719. doi: https://doi.org/10.1016/j.enconman.2020.112719.

McLinden, M.O. and Huber, M.L. (2020). (R)Evolution of Refrigerants. Journal of Chemical & Engineering Data, 65(9), pp.4176–4193. doi: https://doi.org/10.1021/acs.jced.0c00338.

McLinden, M.O., Brown, J.S., Brignoli, R., Kazakov, A.F. and Domanski, P.A. (2017). Limited options for low-global-warming-potential refrigerants. Nature Communications, [online] 8(1). doi: https://doi.org/10.1038/ncomms14476.

Morales-Fuentes, A., Ramírez-Hernández, H.G., Méndez-Díaz, S., Martínez-Martínez, S., Sánchez-Cruz, F.A., Silva-Romero, J.C. and García-Lara, H.D. (2021). Experimental study on the operating characteristics of a display refrigerator phasing out R134a to R1234yf. International Journal of Refrigeration, 130, pp.317–329. doi: https://doi.org/10.1016/j.ijrefrig.2021.05.032.

Mota-Babiloni, A., Makhnatch, P. and Khodabandeh, R. (2017). Recent investigations in HFCs substitution with lower GWP synthetic alternatives: Focus on energetic performance and environmental impact. International Journal of Refrigeration, [online] 82, pp.288–301. doi: https://doi.org/10.1016/j.ijrefrig.2017.06.026.

Myers, M., Kourtza, E., Kane, D. and Harkin, S. (2018). The Cost of Installing Heating Measures in Domestic Properties the Delta-ee Team. [online] Available at: https://assets.publishing.service.gov.uk/government/uploads/system/uploads/attachment_data/file/913508/cost-of-installing-heating-measures-in-domestic-properties.pdf.

Nair, V. (2021). HFO refrigerants: A review of present status and future prospects. International Journal of Refrigeration, [online] 122, pp.156–170. doi: https://doi.org/10.1016/j.ijrefrig.2020.10.039.

NASA (2023). Vital Signs. Carbon Dioxide. Available at: https://climate.nasa.gov/vital-signs/carbon-dioxide/

NIC. (2018). National Infrastructure Commission. Energy and Fuel Bills today and in 2050. Available at:https://nic.org.uk/studies-reports/national-infrastructure-assessment/national-infrastructure-assessment-1/energy-and-fuel-bills/

NOAA. (2023). NASA Ozone Watch. Available at: https://ozonewatch.gsfc.nasa.gov/

Nouvel, R., Cotrado Sehgelmeble, M. and Pietruschka, D., (2015). European mapping of seasonal performances of air-source and geothermal heat pumps for residential applications. In Proceedings of International Conference CISBAT 2015 Future Buildings and Districts Sustainability from Nano to Urban Scale (No. CONF, pp. 543-548). LESO-PB, EPFL.

NRC (National Research Council) (US) Committee on Acute Exposure Guideline Levels. Acute Exposure Guideline Levels for Selected Airborne Chemicals: Volume 6. Washington (DC): National Academies Press (US); 2008. 2, Ammonia Acute Exposure Guideline Levels. Available from: https://www.ncbi.nlm.nih.gov/books/NBK207883/

Oram, D.E. (2005). Chlorofluorocarbons And Other Halocarbons. Encyclopaedia of Analytical Science. pp. 80-89.

Pabon, J.J.G., Khosravi, A., Belman-Flores, J.M., Machado, L. and Revellin, R. (2020). Applications of refrigerant R1234yf in heating, air conditioning and refrigeration systems: A decade of researches. International Journal of Refrigeration, [online] 118, pp.104–113. doi: https://doi.org/10.1016/j.ijrefrig.2020.06.014.

Panagiotopoulos, A.Z. (2011). Essential Thermodynamics. CreateSpace.

Papasavva, S., Hill, W.R. and Andersen, S.O. (2010). GREEN-MAC-LCCP: A Tool for Assessing the Life Cycle Climate Performance of MAC Systems. Environmental Science & Technology, 44(19), pp.7666–7672. doi: https://doi.org/10.1021/es100849g.

Pardo, P. and Mondot, M. (2018). Purdue e-Pubs Experimental evaluation of R410A, R407C and R134a alternative refrigerants in residential heat pumps Experimental evaluation of R410A, R407C and R134a alternative refrigerants in residential heat pumps. [online] Available at: https://docs.lib.purdue.edu/cgi/viewcontent.cgi?article=2990&context=iracc.

Park, K. J., Jung, D., (2008) Performance of R290 and R1270 for R22 applications with evaporator and condenser temperature variation. Journal of Mechanical Science and Technology. pp. 532-537

Payne, W. and Domanski, P. (n.d.). A Comparison of an R22 and an R410A Air Conditioner Operating at High Ambient Temperatures. [online] Available at: https://tsapps.nist.gov/publication/get_pdf.cfm?pub_id=860880.

Pettinger, T. (2019). Environmental Kuzents Curve. Economics Help.

Piddington J, Garrett H, Nowak, T (2013). FB62 Housing in the UK: National comparisons in typology, condition and cost of poor housing. IHS BRE Press, Bracknell.

Qi, Z. (2015). Performance improvement potentials of R1234yf mobile air conditioning system. International Journal of Refrigeration, 58, pp.35–40. doi: https://doi.org/10.1016/j.ijrefrig.2015.03.019.

Rai, A. and Tassou, S.A. (2017). Environmental impacts of vapour compression and cryogenic transport refrigeration technologies for temperature controlled food distribution. Energy Conversion and Management, 150, pp.914–923. doi: https://doi.org/10.1016/j.enconman.2017.05.024.

Rajendran, R. (2011). Refrigerants Update. [online] Available at: https://www.epa.gov/sites/default/files/documents/RefrigerantUpdates.pdf [Accessed 22 Jun. 2023].

Renz, S. (2020) HPT Magazine Vol. 38 No 2/2020 - Heat pumps for the retrofit and renovation market

Rogala, Z. and Kwiatkowski, A. (2022). Modeling of a Three-Stage Cascaded Refrigeration System Based on Standard Refrigeration Compressors in Cryogenic Applications above 110 K. Modelling, 3(2), pp.255–271. doi: https://doi.org/10.3390/modelling3020017.

Rossi di Schio, E., Ballerini, V., Dongellini, M. and Valdiserri, P. (2021). Defrosting of Air-Source Heat Pumps: Effect of Real Temperature Data on Seasonal Energy Performance for Different Locations in Italy. Applied Sciences, 11(17), p.8003. doi: https://doi.org/10.3390/app11178003.

Samsung. (2023). Samsung Series 5 Fridge-Freezer. Technical Specifications. (Subject to market availability)

Shahbaz, M., Ozturk, I., Afza, T., Ali, A. (2013). Revisiting the environmental Kuznets curve in a global economy. Renewable and Sustainable Energy Reviews. Volume 25. Sep 2013. pp. 494 – 502

Shanmugam, S.K.G. and Mital, M. (2019). An ultra-low ammonia charge system for industrial refrigeration. International Journal of Refrigeration, 107, pp.344–354. doi: https://doi.org/10.1016/j.ijrefrig.2019.07.006.

Shen, B., Li, Z. and Gluesenkamp, K.R. (2022). Experimental study of R452B and R454B as drop-in replacement for R410A in split heat pumps having tube-fin and microchannel heat exchangers. Applied Thermal Engineering, 204, p.117930. doi: https://doi.org/10.1016/j.applthermaleng.2021.117930.

Sherman, P., Lin, H., McElroy, M. (2022). Projected global demand for air conditioning associated with extreme heat and implications for electricity grids in poorer countries. Energy and Buildings. Volume 268

Sholahudin, S., Ohno, K., Yamaguchi, S. and Saito, K. (2019). Multi-step ahead prediction of vapor compression air conditioning system behaviour using neural networks. IOP Conference Series: Materials Science and Engineering, 539, p.012003. doi: https://doi.org/10.1088/1757-899x/539/1/012003.

Sieres, J., Ortega, I., Cerdeira, F. and Álvarez, E. (2020). Influence of the refrigerant charge in an R407C liquid-to-water heat pump for space heating and domestic hot water production. International Journal of Refrigeration, [online] 110, pp.28–37. doi: https://doi.org/10.1016/j.ijrefrig.2019.10.021.

Sieres, J., Ortega, I., Cerdeira, F. and Álvarez, E. (2021). Drop-in performance of the low-GWP alternative refrigerants R452B and R454B in an R410A liquid-to-water heat pump. Applied Thermal Engineering, 182, p.116049. doi: https://doi.org/10.1016/j.applthermaleng.2020.116049.

SKM Enviros. (2011). Examination of the Global Warming Potential of Refrigeration in the Food Chain

Song, M., Deng, S., Dang, C., Mao, N. and Wang, Z. (2018). Review on improvement for air source heat pump units during frosting and defrosting. Applied Energy, 211, pp.1150–1170. doi: https://doi.org/10.1016/j.apenergy.2017.12.022.

Sonne, J. and Barkaszi, S. (n.d.). Measured Impacts of Air Conditioner Condenser Shading. [online] Available at: https://www.aceee.org/files/proceedings/2002/data/papers/SS02_Panel1_Paper24.pdf.

Spatz, M. W. and Minor, B. H. (2007). HFO-1234yf: A low GWP refrigerant for MAC. Review of Automotive Air Conditioning (JSAE), Tokyo, Japan,

Spatz, M., Minor, B. and Dupont, H. (2008). HFO-1234yf Low GWP Refrigerant Update Honeywell / DuPont Joint Collaboration International Refrigeration and Air Conditioning Conference at Purdue

Spatz, M.W. and Yana, S.F. (2004). An evaluation of options for replacing HCFC-22 in medium temperature refrigeration systems. 27(5), pp.475–483. doi: https://doi.org/10.1016/j.ijrefrig.2004.02.009.

Tan, W., Du, H., Liu, L., Su, T., Liu, X. (2017). Experimental and numerical study of ammonia leakage and dispersion in a food factory. Journal of Loss Prevention in the Process Industries. Volume 47. pp. 129-139

The Building Regulations 2010. Part 6. No 2214. Available at: https://www.legislation.gov.uk/uksi/2010/2214/contents/made

The Fluorinated Greenhouse Gases (Amendment) Regulations 2018.98 [online] Available at: https://www.legislation.gov.uk/uksi/2018/98/made.

The James Hutton Institute. (2022). Climate Trends and Future Predictions in Scotland. D5-2 Climate Change Impacts on Natural Capital.

Tierney, J. E., Haywood, A. M., Feng, R., Bhattacharya, T., & Otto-Bliesner, B. L. (2019). Pliocene warmth consistent with greenhouse gas forcing. Geophysical Research Letters, 46, 9136 – 9144. https://doi.org/10.1029/2019GL083802

UK DECC. (2020). Department of Energy & Climate Change. 2050 Carbon Calculator Tool. Available at: http://2050-calculator-tool.decc.gov.uk/#/guide

UK Government. (2008). Climate Change Act 2008

UK Government. (2012). Department for Environment, Food and Rural Affairs Guidance on Minimising Greenhouse Gas Emissions from Refrigeration, Air- conditioning and Heat Pump Systems Guidance: F Gas and Ozone Regulations Information Sheet RAC 7: Alternatives. Available at: https://assets.publishing.service.gov.uk/government/uploads/system/uploads/attachment_data/file/394851/fgas-rac7-alternatives.pdf

UK Government. (2014). Impacts of Leakage from Refrigerants in Heat Pumps. Available at: https://assets.publishing.service.gov.uk/government/uploads/system/uploads/attachment_data/file/303689/Eunomia_-_DECC_Refrigerants_in_Heat_Pumps_Final_Report.pdf.

UK Government. (2018). Heatwaves: Adapting to climate change. Commons Select Committee. Environmental Audit. July 26.

UK Government. (2020a). Updated energy and emissions projections 2019. Department for Business, Energy & Industrial Strategy. Available at: https://assets.publishing.service.gov.uk/government/uploads/system/uploads/attachment_data/file/931323/updated-energy-and-emissions-projections-2019.pdf

UK Government. (2020b). MODELLING 2050: ELECTRICITY SYSTEM ANALYSIS. Available at: https://assets.publishing.service.gov.uk/government/uploads/system/uploads/attachment_data/file/943714/Modelling-2050-Electricity-System-Analysis.pdf.

UK Government. (2022). Department for Business, Energy & Industrial Strategy. 2022 Government Greenhouse Gas Conversion Factors for Company Reporting.

UK Government. (2023). Heat Pump Investment Roadmap Leading the way to net zero. (2023). Available at: https://assets.publishing.service.gov.uk/government/uploads/system/uploads/attachment_data/file/1148930/heat-pumps-net-zero-investment-roadmap.pdf.

UNCC (2023). The Paris Agreement. Available at: https://unfccc.int/process-and-meetings/the-paris-agreement

UNDP. (2022). Montreal Protocol and Chemicals and Waste Management Unit and Greening Moonshot GUIDANCE NOTE. Available at: https://www.undp.org/sites/g/files/zskgke326/files/2022-07/Refrigerants%20methodology%20version%20July%202022.pdf?trk=organization_guest_main-feed-card_feed-article-content [Accessed 22 Jun. 2023].

UNEP. (2018). Technology and Economic Assessment Panel. Assessment Report. Montreal Protocol on Substances that Deplete the Ozone Layer

United Nations (UN). (2016). Chapter XXVII Environment. 2. f Amendment to the Montreal Protocol on Substances that Deplete the Ozone Layer. Kilgali.15 Oct

United Nations (UN). (2021). Climate Change 'Biggest Threat Modern Humans Have Ever Faced', World-Renowned Naturalist Tells Security Council, Calls for Greater Global Cooperation. Security Council. Press Release.

US Government, (2021). Climate Change Regulatory Actions and Initiatives. EPA. Executive Order 13990

Varrasi, J. (2011). Global Cooling: The History of Air Conditioning. The American Society of Mechanical Engineers

Venkatarathnam, G. and Srinivasa Murthy, S. (2012). Refrigerants for vapour compression refrigeration systems. Resonance, [online] 17(2), pp.139–162. doi: https://doi.org/10.1007/s12045-012-0015-x.

Venkataiah, S. and Rao, G. (2014). Analysis of Alternative Refrigerants to R22 for Air-Conditioning Applications at Various Evaporating Temperatures. Journal of Engineering Research and Applications www.ijera.com, [online] 4(3), pp.39–46. Available at: https://www.ijera.com/papers/Vol4_issue3/Version%202/H43023946.pdf [Accessed 17 Jul. 2023].

Wang, J., Belusko, M., Evans, M., Liu, M., Zhao, C. and Bruno, F. (2022). A comprehensive review and analysis on CO2 heat pump water heaters. Energy Conversion and Management: X, 15, p.100277. doi: https://doi.org/10.1016/j.ecmx.2022.100277.

Wang, L., Dang, C., Hihara, E,. Dai, B. (2022). HFC-410A emission from room air conditioning sector in China. International Journal of Thermal Sciences. Volume 191

Watson, S.D., Lomas, K.J. and Buswell, R.A. (2021). How will heat pumps alter national half-hourly heat demands? Empirical modelling based on GB field trials. Energy and Buildings, 238, p.110777. doi:https://doi.org/10.1016/j.enbuild.2021.110777.

Wernke, M.J.(2014). Encyclopedia of Toxicology (Third Edition). Academic Press. pp. 664-666. ISBN 9780123864550

Widodo, W., et al. (2021). IOP Conf. Ser.: Mater. Sci. Eng. 1098 062109

Wu, D., Hu, B. and Wang, R.Z. (2021). Vapor compression heat pumps with pure Low-GWP refrigerants. Renewable and Sustainable Energy Reviews, 138, p.110571. doi: https://doi.org/10.1016/j.rser.2020.110571.

Wygonik, E. and Goodchild, A. (2011). Evaluating CO 2 emissions, cost, and service quality trade-offs in an urban delivery system case study. IATSS Research, 35(1), pp.7–15. doi: https://doi.org/10.1016/j.iatssr.2011.05.001.

Xu, W., Zhao, R., Deng, S., et al. (2021). Is zeotropic working fluid a promising option for organic Rankinecycle: A quantitative evaluation based on literature data. Renewable and Sustainable Energy Reviews. Volume 148.

Yang, C., Seo, S., Takata, N., Thu, K. and Miyazaki, T. (2021). The life cycle climate performance evaluation of low-GWP refrigerants for domestic heat pumps. International Journal of Refrigeration, 121, pp.33–42. doi: https://doi.org/10.1016/j.ijrefrig.2020.09.020.

Yelishala, S.C, Kannaiyan, K., Sadr, R., Wang, Z., Levendis, Y., Metghalchi, H., (2020). Performancemaximization by temperature glide matching in energy exchangers of cooling systems operating with natural hydrocarbon/CO2 refrigerants. International Journal of Refrigeration. Volume 119. pp. 294 – 304

Yoro, K., Daramola, M.O. (2020). Chapter 1 - CO2 emission sources, greenhouse gases, and the global warming effect. Advances in Carbon Capture. pp. 3 – 28.

Zhang, Y., Yang, Z., Lv, Z., Chen, Y., He, H., Chen, S. and Liu, B. (2022). Research on the effect of flame retardants on the mildly flammable refrigerant ammonia. Journal of Loss Prevention in the Process Industries, 77, p.104787. doi: https://doi.org/10.1016/j.jlp.2022.104787.

Zhang, Z.-P., Wang, Y., Wu, X., Pan, X. and Xing, Z. (2020). Theoretical and experimental research on the performance of twin screw compressor using R513A as R134a replacement. 235(2), pp.170–177. doi: https://doi.org/10.1177/0954408920951141.

Zhao, Y. et al. (2019). Azeotropic refrigerants and its application in vapor compression refrigeration cycle. International Journal of Refrigeration. Volume 108. pp. 1 – 13.

Zhu, Z., Liang, K., Li, Z., Jiang, H. and Meng, Z. (2021). Thermal-economic-environmental analysis on household refrigerator using a variable displacement compressor and low-GWP refrigerants. International Journal of Refrigeration, 123, pp.189–197. doi: https://doi.org/10.1016/j.ijrefrig.2020.12.009.

Zogg M. (2008), History of Heat Pumps - Swiss Contributions and International Milestones, Swiss Federal Office of Energy, Berne

7. Appendices

7.1 Data Tables

7.1.1 Case 1: Cryogenic

		Stage 2							Stage 1	
		HFC Blend	HFC		Natural		HFO		HFC	Natural
		R404A	R134a	R600a	R717	R290	R1234yf	R1234ze(E)	R23	R1150
GWP	(-)	3922	1300	3	0	3	0.501	1.37	14600	4
Compressor Eff.	(%)	82%	82%	84%	78%	84%	70%	70%	70%	70%
Cooling Capacity	(kW)	1	1	1	1	1	1	1	1	1
Charge per kW	(kg/kW)	0.50	0.67	0.03	0.26	0.06	0.38	0.55	0.41	0.03
Charge	(kg)	0.500	0.667	0.033	0.260	0.060	0.377	0.545	0.409	0.033
COPc	(-)	2.373	2.596	2.593	2.570	2.556	2.164	2.255	1.058	1.007
Compressor Work	(kW)	0.421	0.385	0.386	0.389	0.391	0.462	0.443	0.9703	0.9926
Refrigerant Flowrate	(kg/s)	2.44E-02	1.92E-02	1.11E-02	2.56E-03	1.01E-02	9.71E-03	8.16E-03	6.18E-03	3.47E-03
Cond. Pressure	(bar)	14.25	7.75	4.06	11.77	10.86	9.86	7.38	12.02	22.30
Cond. Temperature	(°C)	46.3	51.1	39.1	159	48.8	57.8	64.3	113.7	100.9
Evap. Pressure	(bar)	2.028	0.839	3.884	3.01	1.668	9.04	5.53	0.316	1.26
Evap. Temperature	(°C)	-30.4	-30	-30	-30	-30	-27.1	-27	-100	-100

7.1.2 Case 2: Fridge – Freezer

		HFC Blend		HFC		Natural		HFO	
		R404A	R407C	R134a	R600a	R717	R290	R1234yf	R1234ze(E)
GWP	(-)	3922	1624.21	1300	3	0	3	0.501	1.37
Compressor Eff.	(%)	82%	82%	82%	84%	78%	84%	70%	70%
Cooling Capacity	(kW)	1	1	1	1	1	1	1	1
Charge per kW	(kg/kW)	0.50	0.389	0.667	0.030	0.260	0.060	0.377	0.545
Charge	(kg)	0.50	0.389	0.667	0.033	0.260	0.060	0.377	0.545
COPc	(-)	2.627	2.861	2.886	2.985	2.694	2.91	2.178	2.294
COP_HS		4.06	4.374	4.434	4.611	4.219	4.478	2.692	2.833
COP_LS		1.754	1.978	1.99	2.039	1.911	2.004	1.664	1.755
Compressor Work	(kW)	0.761	0.699	0.693	0.670	0.742	0.687	0.918	0.872

		HFC Blend		HFC	Natural			HFO	
		R404A	R407C	R134a	R600a	R717	R290	R1234yf	R1234ze(E)
Refrigerant Flowrate	(kg/s)	1.90E-02	1.30E-02	1.40E-02	8.00E-03	2.00E-03	7.00E-03	1.902E-02	1.60E-02
m_hs		1.10E-02	7.00E-03	8.00E-03	4.00E-03	1.00E-03	4.00E-03	9.31E-03	7.81E-03
m_ls		8.00E-03	6.00E-03	6.00E-03	4.00E-03	1.00E-03	3.00E-03	9.71E-03	8.16E-03
Cond. Pressure	(bar)	18.261	15.266	10.224	5.313	15.672	13.739	12.712	9.692
Cond. Temperature	(°C)	57	69.7	60.2	47.8	161.7	56.8	60.1	63.8
Evap. Pressure	(bar)	2.045	1.39	0.847	0.461	1.193	1.682	9.04	5.53
Evap. Temperature	(°C)	-30.5	-35.2	-30	-30	-30	-30	-30	30

7.1.3 Case 3: Air Conditioning

		HFC Blend		HFC	HCFC	Natural			HFO	
		R410A	R454B	R32	R22	R600a	R717	R290	R1234yf	R1234ze(E)
GWP	(-)	2088	466	771	1960	3	0	3	0.501	1.37
Compressor Eff.	(%)	82%	76%	70%	70%	84%	78%	84%	70%	70%
Cooling Capacity	(kW)	1	1	1	1	1	1	1	1	1
Charge per kW	(kg/kW)	0.474	0.296	0.183	0.409	0.033	0.260	0.060	0.377	0.545
Charge	(kg)	0.474	0.296	0.183	0.409	0.280	0.260	0.060	0.377	0.545
COPc	(-)	2.698	2.602	2.864	3.006	3.09	3.04	2.941	2.325	2.493
Compressor Work	(kW)	0.371	0.384	0.349	0.333	0.324	0.329	0.340	0.430	0.401
Refrigerant Flowrate	(kg/s)	0.0071	0.0057	0.0045	0.0063	0.0042	0.0010	0.0041	0.0010	0.0086
Cond. Pressure	(bar)	36.67	32.84	37.28	23.347	8.526	24.675	20.659	16.055	12.433
Cond. Temperature	(°C)	93.5	104.8	115.7	96.5	62.8	166.3	74.4	69.6	73
Evap. Pressure	(bar)	8.234	7.658	8.388	5.141	1.624	4.458	4.885	3.259	2.242
Evap. Temperature	(°C)	6	6.5	6	6	6	6	6	5.9	5.9

7.1.4 Case 4: ASHP Air-Air

		HFC Blend		HFC	Natural				HFO	
		R410A	R407C	R32	R600a	R717	R744	R290	R1234yf	R1234ze(E)
GWP	(-)	2,088.00	1624.21	771	3	0	1.00	3	0.501	1.37
Compressor Eff.	(%)	82%	82%	70%	84%	78%	78%	84%	70%	70%

		HFC Blend		HFC	Natural				HFO	
		R410A	R407C	R32	R600a	R717	R744	R290	R1234yf	R1234ze(E)
Cooling Capacity	(kW)	8	8	8	8	8	8	8	8	8
Charge per kW	(kg/kW)	0.474	0.389	0.183	0.033	0.260	0.157	0.060	0.377	0.545
Charge	(kg)	3.79	3.11	1.46	0.27	2.08	1.26	0.48	3.02	4.36
COPh	(-)	4.708	4.631	4.772	4.993	4.729	4.498	4.902	4.173	4.278
Compressor Work	(kW)	0.27	0.275	0.265	0.25	0.268	0.286	0.256	0.315	0.305
Refrigerant Flowrate	(kg/s)	0.0444	0.0467	0.0296	0.0285	0.0070	0.0465	0.0268	0.0651	0.0560
Cond. Pressure	(bar)	20.528	14.408	20.808	4.52	12.704	73.783	11.841	8.707	6.461
Cond. Temperature	(°C)	67.4	65.1	88.6	42	135.7	83	50.8	46.6	50.4
Evap. Pressure	(bar)	5.158	3.097	5.242	0.964	2.57	2.5674	3.12	1.98	1.303
Evap. Temperature	(°C)	-8	-5.8	-8	-8	-8	-6.1	-8	-8	-8

7.1.5 Case 5: ASHP Space

		HFC Blend		HFC	Natural				HFO	
		R410A	R407C	R32	R600a	R717	R744	R290	R1234yf	R1234ze(E)
GWP	(-)	2,088.00	1,624.21	771.00	3.00	0	1.00	3.00	0.50	1.37
Compressor Eff.	(%)	82%	82%	70%	84%	78%	78%	84%	70%	70%
Cooling Capacity	(kW)	8	8	8	8	8	8	8	8	8
Charge per kW	(kg/kW)	0.474	0.389	0.183	0.033	0.260	0.157	0.060	0.377	0.545
Charge	(kg)	3.79	3.11	1.46	0.27	2.08	1.26	0.48	3.02	4.36
COPh	(-)	3.196	3.205	3.317	3.445	3.409	3.498	3.354	2.84	2.971
Compressor Work	(kW)	0.455	0.454	0.432	0.409	0.415	0.400	0.425	0.545	0.507
Refrigerant Flowrate	(kg/s)	0.0551	0.0574	0.03464	0.0348	0.07678	0.0465	0.0331	0.0851	0.06988
Cond. Pressure	(bar)	32.70	23.35	33.20	7.57	21.63	73.78	18.56	14.28	10.97
Cond. Temperature	(°C)	96.2	90.6	125.5	60.2	192.8	83	73	67.1	71.8
Evap. Pressure	(bar)	5.154	3.049	5.24	0.963	2.57	2.5674	3.118	1.978	1.302
Evap. Temperature	(°C)	-8	-8	-8	-8	-8	-6.1	-8	-8	-8

7.1.6 Case 6: ASHP Domestic Hot Water

		HFC Blend	HFC	Natural				HFO	
		R407C	R32	R600a	R717	R744	R290	R1234yf	R1234ze(E)
GWP	(-)	1,624.21	771.00	3.00	0	1.00	3.00	0.50	1.37
Compressor Eff.	(%)	82%	70%	84%	78%	78%	84%	70%	70%
Cooling Capacity	(kW)	2	2	2	2	2	2	2	2
Charge per kW	(kg/kW)	0.389	0.183	0.033	0.260	0.157	0.060	0.377	0.545
Charge	(kg)	0.78	0.37	0.07	0.52	0.31	0.12	0.75	1.09
COPh	(-)	2.245	2.458	2.539	2.686	2.998	2.429	2.017	2.196
Compressor Work	(kW)	0.803	0.686	0.65	0.593	0.501	0.7	0.983	0.836
Refrigerant Flowrate	(kg/s)	0.0202	0.0108	0.0113	0.0021	0.0116	0.0111	0.0319	0.0238
Cond. Pressure	(bar)	37.72	50.80	11.90	34.72	73.78	27.70	22.18	17.50
Cond. Temperature	(°C)	118	160.9	77.8	247.2	83	94.5	87.4	92.3
Evap. Pressure	(bar)	2.982	5.238	0.962	2.57	2.567.4	3.116	1.974	1.301
Evap. Temperature	(°C)	-6.8	-8	-8.1	-8	-6.1	-8.1	-8.1	-8.1

7.1.7 Case 7: GSHP Space

		HFC Blend		HFC	Natural				HFO	
		R410A	R407C	R32	R600a	R717	R744	R290	R1234yf	R1234ze(E)
GWP	(-)	2,088.00	1,624.21	771.00	3.00	0	1	3.00	0.50	1.37
Compressor Eff.	(%)	82%	82%	70%	84%	78%	78%	84%	70%	70%
Cooling Capacity	(kW)	8	8	8	8	8	8	8	8	8
Charge per kW	(kg/kW)	0.474	0.389	0.183	0.033	0.260	0.157	0.060	0.377	0.545
Charge	(kg)	3.79	3.11	1.46	0.27	2.08	1.26	0.48	3.02	4.36
COPh	(-)	4.034	4.056	3.726	4.415	4.31	4.488	4.274	3.61	3.771
Compressor Work	(kW)	2.637	2.618	2.935	2.343	2.417	2.904	2.294	2.443	3.060
Refrigerant Flowrate	(kg/s)	0.0535	0.0548	0.0341	0.0323	0.0076	0.0312	0.0473	0.0312	0.0779
Cond. Pressure	(bar)	32.89	23.41	33.30	7.57	17.75	73.78	18.61	14.31	11.00
Cond. Temperature	(°C)	87.1	83.6	117.6	58.4	155.7	67.5	69.2	64.6	68
Evap. Pressure	(bar)	7.978	4.911	8.126	1.567	4.295	34.899	4.739	3.151	2.162
Evap. Temperature	(°C)	5	6.8	5	5	5	5.1	5	4.9	5

7.1.8 Case 8: GSHP Domestic Hot Water

		HFC Blend	HFC	Natural				HFO	
		R407C	R32	R600a	R717	R744	R290	R1234yf	R1234ze(E)
GWP	(-)	1,624.21	771.00	3.00	-	1	3.00	0.50	1.37
Compressor Eff.	(%)	82%	70%	84%	78%	78%	84%	70%	70%
Cooling Capacity	(kW)	2	2	2	2	2	2	2	2
Charge per kW	(kg/kW)	0.389	0.183	0.033	0.260	0.157	0.060	0.377	0.545
Charge	(kg)	0.78	0.37	0.07	0.52	0.31	0.12	0.75	1.09
COPh	(-)	2.702	2.635	3.087	3.205	3.488	2.926	2.436	2.641
Compressor Work	(kW)	1.175	1.223	0.958	0.907	2.308	1.192	0.804	1.038
Refrigerant Flowrate	(kg/s)	0.0183	0.0106	0.0103	0.0021	0.0230	0.0174	0.0118	0.0103
Cond. Pressure	(bar)	36.01	50.80	11.92	34.88	73.78	27.79	22.24	17.56
Cond. Temperature	(°C)	109.4	155.1	76.2	207.6	67.5	91.1	85.3	88.9
Evap. Pressure	(bar)	2.68	8.122	1.566	4.295	34.899	4.735	3.146	2.16
Evap. Temperature	(°C)	4.3	5	4.9	5	5.1	4.9	4.9	4.9